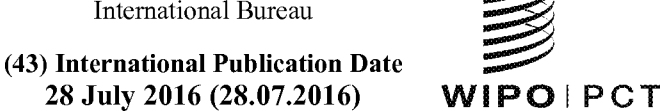
(12) INTERNATIONAL APPLICATION PUBLISHED UNDER THE PATENT COOPERATION TREATY (PCT)

(19) World Intellectual Property Organization

International Bureau





(10) International Publication Number WO 2016/118536 A2

(51) International Patent Classification: Not classified

(21) International Application Number:

PCT/US2016/013974

(22) International Filing Date:

19 January 2016 (19.01.2016)

(25) Filing Language:

English

(26) Publication Language:

English

(30) Priority Data:

20 January 2015 (20.01.2015) 62/105,559

US

- (71) Applicant: THE JOHNS HOPKINS UNIVERSITY [US/US]; 3400 N. Charles Street, Baltimore, MD 21218
- (72) Inventors: KATZ, Howard, E.; C/o The Johns Hopkins University, 3400 N. Charles Street, Baltimore, MD 21218 (US). HUANG, Weiguo; C/o The Johns Hopkins University, 3400 N. Charles Street, Baltimore, MD 21218 (US).
- (74) Agent: HSIEH, Timothy, M.; MH2 Technology Law Group, 1951 Kidwell Drive, Suite 550, Tysons Corner, VA 22182 (US).

- (81) Designated States (unless otherwise indicated, for every kind of national protection available): AE, AG, AL, AM, AO, AT, AU, AZ, BA, BB, BG, BH, BN, BR, BW, BY, BZ, CA, CH, CL, CN, CO, CR, CU, CZ, DE, DK, DM, DO, DZ, EC, EE, EG, ES, FI, GB, GD, GE, GH, GM, GT, HN, HR, HU, ID, IL, IN, IR, IS, JP, KE, KG, KN, KP, KR, KZ, LA, LC, LK, LR, LS, LU, LY, MA, MD, ME, MG, MK, MN, MW, MX, MY, MZ, NA, NG, NI, NO, NZ, OM, PA, PE, PG, PH, PL, PT, QA, RO, RS, RU, RW, SA, SC, SD, SE, SG, SK, SL, SM, ST, SV, SY, TH, TJ, TM, TN, TR, TT, TZ, UA, UG, US, UZ, VC, VN, ZA, ZM, ZW.
- (84) Designated States (unless otherwise indicated, for every kind of regional protection available): ARIPO (BW, GH, GM, KE, LR, LS, MW, MZ, NA, RW, SD, SL, ST, SZ, TZ, UG, ZM, ZW), Eurasian (AM, AZ, BY, KG, KZ, RU, TJ, TM), European (AL, AT, BE, BG, CH, CY, CZ, DE, DK, EE, ES, FI, FR, GB, GR, HR, HU, IE, IS, IT, LT, LU, LV, MC, MK, MT, NL, NO, PL, PT, RO, RS, SE, SI, SK, SM, TR), OAPI (BF, BJ, CF, CG, CI, CM, GA, GN, GQ, GW, KM, ML, MR, NE, SN, TD, TG).

Published:

without international search report and to be republished upon receipt of that report (Rule 48.2(g))



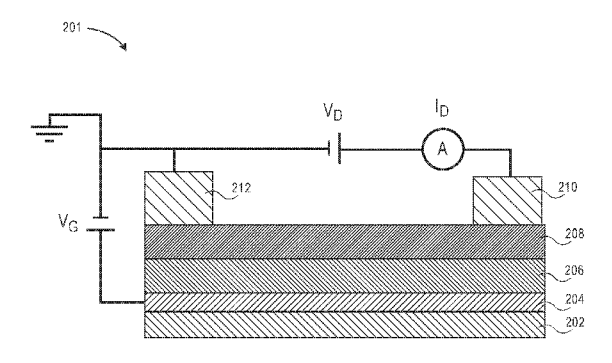


FIG. 2A

(57) Abstract: Provided is a method for making a self-healing polymer-based organic field-effect transistor (SHP-OFET). The method includes a method for making a self-healing polymer- based organic field-effect transistor (SHP-OFET). The method includes depositing a first metal and a second metal over a flexible substrate, patterning the first metal and the second metal to form a source electrode and a drain electrode, respectively, depositing a solution comprising an organic semiconductor over the substrate to form an organic semiconductor channel, depositing a solution including a first polymer and a second polymer over the substrate to form a self-healing polymer blend dielectric layer,, and depositing a conductor over the substrate to form a gate. The first polymer includes at least one of a hydroxyalkyl methacrylate, an acrylate, methacrylamide, acrylamides, or mixtures thereof, and the second polymer includes a polyimine additive.





PRINTABLE HIGH DIELECTRIC CONSTANT AND SELF-HEALABLE DIELECTRIC POLYMER COMPOSITION

Cross-Reference To Related Applications

[0001] This application claims priority to U.S. Provisional Patent Application Ser. No. 62/105,559, filed on January 20, 2015, the entirety of which is incorporated herein by reference.

Government Support Statement

[0002] This invention was made with government support under Grant No. 1005398 awarded by the National Science Foundation, Division of Materials Research. The government has certain rights in the invention.

Field of the Invention

[0003] This disclosure is generally directed to electronic devices, in particular electronic devices that incorporate self-healing dielectric compositions (i.e., self-healable electronics), including organic field effect transistors with self-healing dielectric layers.

Background of the Invention

[0004] Printable and flexible electronics attract sustained attention for their low cost, easy scale up and potential application in wearable and implantable sensors. However, they are susceptible to scratching, rupture, or other damage from bending or stretching due to their "soft" nature compared to their rigid counterparts (Si based electronics), leading to loss of functionality. Self-healing capability is highly desirable for these "soft" electronic devices.

[0005] Self-healable high performance electronic materials have been intensively investigated in recent years. Early studies on self-healing materials were mainly focused on creation of self-repairable coatings and restoration of mechanical properties. For example, self-healing coatings based on halloysite clay polymer composites for protection of copper

alloys have previously been developed. Bioinspired self-healing superhydrophobic coatings also exist by covalently attaching a fluoroalkylsilane layer. There is also a transparent organic polymeric material that can mechanically mend and "re-mend" itself under mild conditions as well as a bio-based furan polymer with self-healing ability via reversible Diels-Alder reaction. A self-healing system based on covalent dynamic gels and a self-healing polymer (SHP) based on siloxane equilibration have also been prepared.

[0006] More recently, healable electronic properties have been considered simultaneously with healable mechanical properties. For example, a repeatable, room-temperature self-healing electronic sensor skin has been developed followed by a drastic increase in the cycling lifetime of silicon microparticle anodes using self-healing chemistry. Additionally, film conductivity has been restored in other systems by embedding microcapsules filled with conductive agents in the materials. Film conductivity has also been restored just by applying a water drop to a damaged area, and a class of organometallic polymers comprising N-heterocyclic carbenes and transition metals which can be electrically healed have been developed.

There are many other examples of electrically healable materials. However, most research in healable electronics has been limited to conductive media, such as conductive wire, film and bulk materials; there has been very little work on integrating self-healing materials into organic field effect transistors (OFETs), and especially not as gate insulators. Additionally, prior attempts at introducing self-healing dielectric layers into organic field effect transistors have demonstrated only the healing behavior following dielectric breakdown, rather than after both mechanical and electrical breakdown, and the electrical self-healing process was relatively slow in those systems. Furthermore, these were not based on a potentially printable technology. Accordingly, what is needed in the art,

therefore, is a material which simultaneously exhibits excellent dielectric properties for OFETs, especially printable OFETs, and autonomic mechanical self-healing behavior.

SUMMARY

In an embodiment, there is a method for making a self-healing polymer-based organic field-effect transistor (SHP-OFET). The method includes depositing a first metal and a second metal over a flexible substrate, patterning the first metal and the second metal to form a source electrode and a drain electrode, respectively, depositing a solution comprising an organic semiconductor over the substrate to form an organic semiconductor channel, depositing a solution comprising a first polymer and a second polymer over the substrate to form a self-healing polymer blend dielectric layer, wherein the first polymer comprises at least one of a hydroxyalkyl methacrylate, an acrylate, methacrylamide, acrylamides, or mixtures thereof, and wherein the second polymer comprises a polyimine additive, and depositing a conductor over the substrate to form a gate.

In an embodiment, there is an alternative method for making a SHP-OFET. The method includes depositing a first metal and a second metal on a flexible substrate, and patterning the first metal and the second metal to form a source electrode and a drain electrode, respectively. The method further includes depositing a solution comprising an organic semiconductor over the source and drain electrodes to form an organic-semiconductor channel, depositing a solution comprising a first polymer and a second polymer over the substrate to form a self-healing polymer blend dielectric layer, wherein the first polymer comprises at least one of a hydroxyalkyl methacrylate, an acrylate, methacrylamide, acrylamides, or mixtures thereof, and wherein the second polymer comprises a polyimine additive, and depositing a conductor over the self-healing polymer blend dielectric layer to form a gate.

[0010] In an embodiment, there is another alternative method for making a SHP-

OFET. In the method, a substrate is provided. A gate conductor is deposited on the substrate, a self-healing polymer blend dielectric layer is coated over the gate conductor, and an organic semiconductor is deposited from solution over the dielectric. The method further includes depositing a first metal and a second metal on the organic semiconductor, and patterning the first metal and the second metal to form a source electrode and a drain electrode, respectively.

In another embodiment, there is a self-healing polymer-based organic field-effect transistor (SHP-OFET) that includes a substrate, a source electrode and a drain electrode disposed over the substrate, an organic semiconductor channel disposed between the source and the drain electrodes, a self-healing dielectric layer disposed over the organic semiconductor channel, and a gate disposed over the dielectric layer. The dielectric layer may include a first polymer and a second polymer, wherein wherein the first polymer comprises at least one of a hydroxyalkyl methacrylate, an acrylate, methacrylamide, acrylamides, or mixtures thereof, and wherein the second polymer comprises a polyimine additive.

[0012] In another embodiment there is a chemical sensor comprising an SHP-OFET.

[0013] In yet another embodiment, there is a solution-processable composition. The composition can include a poly(methyl methacrylate) derivative comprising a hydroxyl group, a polyimine, and a solvent. A weight ratio of poly(methyl methacrylate) derivative to polyimine is from about 2:1 to about 1:1.

[0014] In even still another embodiment, there is a self-healing polymer-based capacitor. The capacitor includes a self-healing dielectric layer disposed between a first electrode and a second electrode, wherein the self-healing dielectric layer comprises a nonionic polymer blend comprising a first polymer and a second polymer.

[0015] Advantages of at least one embodiment include a dielectric layer formed of a

print-deposited nonionic polymer blend composition that shows surprisingly high capacitance (e.g., up to 1,400 nF/cm2 at 120 nm thickness), which is much higher than previously reported polymer dielectrics, and much higher than expected from the bulk dielectric constant of the individual components of the blend. Furthermore, this blend polymer system exhibits excellent self-healing behavior, which can automatically heal itself upon both mechanical and electrical breakdown.

[0016] An additional advantage of at least one embodiment provides a dielectric layer formed of self healing polymer blend dielectric, for example a nonionic polymer blend, that can even restore the conductivity of a gate electrode material coated above it simultaneously with the process of healing itself, without need of any added healing agent, which represents a significant step forward for development of fully healable electronics. Based on these attractive properties, a self-healable, low-voltage operable, printed and flexible OFET may be formed and may include the self healing polymer blend described herein as a dielectric layer. Additionally, this dielectric layer shows promising application in improving the sensitivity of a gas sensor, such as for NH₃. The thin dielectric layer comprising a self healing polymer blend of the embodiments also shows promising application for decreasing the voltage at which sensors of either small molecules or biomolecules, more specifically biomacromolecules, can be operated. Accordingly, additional advantages of the embodiments include highly sensitive, wearable, implantable and low-voltage operable selfhealable polymer-based OFET chemical sensors.

[0017] Additional advantages of the embodiments will be set forth in part in the description which follows, and in part will be understood from the description, or may be learned by practice of the invention. The advantages will be realized and attained by means of the elements and combinations particularly pointed out in the appended claims.

[0018] It is to be understood that both the foregoing general description and the

following detailed description are exemplary and explanatory only and are not restrictive of the invention, as claimed.

[0019] The accompanying drawings, which are incorporated in and constitute a part of this specification, illustrate embodiments of the invention and together with the description, serve to explain the principles of the invention.

BRIEF DESCRIPTION OF THE DRAWINGS

[0020] FIG. 1A shows chemical structures of polymers that may be used in a self-healing polymer blend, for example: the chemical structure of formula (I): poly (2-hydroxypropyl methacrylate) (PHPMA); and the chemical structure of formula (II): poly (ethyleneimine) (PEI).

[0021] FIGS. 1B-1D are graphs showing supporting measurements for different polymer blend dielectric compositions, including DSC curves of PHPMA (FIG. 1B), PEI (FIG. 1C), and the self-healing polymer blend of an embodiment comprising PHPMA/PEI at a 1:1 weight ratio.

[0022] FIG. 1E illustrates a self-healing process for a self-healing polymer blend of an embodiment.

[0023] FIG. 2A is a cross-sectional view of an organic field effect transistor (OFET), for example, a self-healing OFET having a dielectric layer comprising a self-healing polymer blend of the embodiments.

[0024] FIG. 2B shows chemical structures of four organic semiconductors that can be used as the organic semiconductor active layer of the OFET of FIG. 2A.

[0025] FIG. 2C illustrates a method for forming a non-printed device, for example a non-printed OFET, such as the OFET of FIG. 2A.

[0026] FIG. 3 illustrates a method for forming an all printed device, for example an all printed OFET.

[0027] FIG. 4A is a perspective view of a top-gate self-healing organic field effect transistor (SHP-OFET) according to an embodiment.

[0028] FIG. 4B illustrates a method for forming a self-healing device, for example, a top-gate SHP-OFET, such as the SHP-OFET of FIG. 4A.

[0029] FIG. 5A are images of a self-healing polymer blend of an embodiment shown during a mechanical self-healing test.

[0030] FIGS. 5B-5C are images of the self-healing polymer blend specimen of FIG. 5A during the testing of mechanical self-healing test as it is reassembled (FIG. 5B) and as it is elongated (FIG. 5C) after severing.

FIG. 5D is a graph showing tensile measurement results taken during the mechanical self-healing test of the self-healing polymer blend of the original, unsevered self-healing polymer blend specimen (PHPMA/PEI 1:1) of FIG. 5A, and of the severed specimen after it has undergone 3 minutes of healing at room temperature and at an extension ratio 0.5mm/min, Load was measured with a resolution of 0.01 N and used to calculate the stress in the specimen. The specimens were about 1.5 cm in length, 0.3 cm in width and 0.3 cm in thickness. While not limited to any particular theory, it is believed that the fluctuation of both curves may be caused by instant polymer chain relaxation in the specimens.

FIG. 6A-6D include images of scratch tests performed on films of a self-healing polymer blend of an embodiment comprising PHPMA and PEI (FIG. 6A), poly(methyl methacrylate) (PMMA) (FIG. 6B), polystyrene (PS) (FIG. 6C) and PHPMA alone (i.e., no PEI) (FIG. 6D).

FIGS. 7A-7B are graphs showing the result of a carbon paint conductivity healing test for a test structures comprising carbon paint coated on a self-healing polymer layer comprising a self-healing polymer blend of an embodiment. Data points in each graph represent means \pm s.d. of at least 5 independent experiments.

[0034] FIG. 8 illustrates a self healing test at different stages indicated by schematic diagrams of a SHP-OFET of an embodiment such as that shown in FIG. 4A and formed according to the method illustrated in FIG. 4B.

[0035] FIG. 9 is a graph showing respective transistor behavior (I-V characteristics) at the different stages of the self-healing process of FIG. 8.

[0036] FIG. 10 is an illustration of a metal-isolator-metal (MIM) device architecture used for devices on which capacitance measurements, impedance tests, leakage current measurements and electrical break down tests were performed.

[0037] FIGS. 11A-11B are graphs showing capacitance of a PHPMA film (FIG. 11A) and capacitance of a self-healing polymer blend of an embodiment comprising PHPMA/PEI vs. PEI weight ratio (FIG. 11B). The capacitance values were obtained from a MIM device configuration using an Agilent 4284A Precision LCR meter. Data points represent means ± s.d. of at least 15 independent experiments.

[0038] FIGS. 11C-11E are graphs showing experimental capacitance values of different polymer films, including for films comprising self healing polymer blends of the embodiments at different ratios of poly(2-hydroxypropyl methacrylate) (PHPMA) to poly(ethyleneimine) (PEI) and for comparative films.

[0039] FIGS. 11F-11I are graphs showing results of impedance measurements, including | Z | value over frequency (FIGS. 11F-11G), and Nyquist plots (FIGS. 11H-11I).

[0040] FIG. 11J is an illustration of an equivalent circuit based on the results of impedance measurements of a PHPMA/PEI (1:1) metal-isolator-metal (MIM) capacitor such as that shown in FIG. 10.

[0041] FIGS. 12A-12D are graphs showing leakage current densities of different polymers blends at various thicknesses between +/- 5V in MIM architecture devices.

FIGS. 13A-13I are graphs showing results of an electrical breakdown test for four different polymer films with the same thickness range.

FIGS. 14A-14E are output curves (FIGS. 14A-14D) and transfer curves (FIGs. 14E-14H) for OFET devices comprising a polymer blend dielectric film of the embodiments, here a blend comprising PHPMA and PEI in a 1:1 ratio, and including an organic semiconductor active layer comprising pentacene (FIG. 14B), 5FPE-NTCDI (FIG. 14C), P3HT (FIG. 14D), and quinacridone (FIG. 14E). The devices have a channel length of 250 μm and channel widths of 8000 μm. The gate voltage was swept at a rate of 50mVs⁻¹.

FIGS. 15A-15C are comparative transfer curves for OFET devices comprising 150 nm PMMA as the dielectric layer and including organic semiconductor active layers comprising pentacene (FIG. 15A), 5FPE-NTCDI (FIG. 15B) and quinacridone (FIG. 15C), The devices have channel lengths of 250 μ m and channel widths of 8000 μ m. The gate voltage was swept at a rate of 50mVs⁻¹.

FIGS. 16A-16C are comparative transfer curves for OFET devices comprising 100 nm polystyrene (PS) as the dielectric layer and including organic semiconductor active layers comprising pentacene (FIG. 16A), 5FPE-NTCDI (FIG. 16B) and (c) quinacridone (FIG. 16C), The devices had channel lengths of 250 μm and channel widths of 8000 μm. The gate voltage was swept at a rate of 50mVs⁻¹.

FIGS. 17A-17D are comparative transfer curves for OFET devices comprising 300 nm SiO₂ as the dielectric layer and including organic semiconductor active layers comprising pentacene (FIG. 17A), 5FPE-NTCDI (FIG. 17B), P3HT (FIG. 17C) and quinacridone (FIG. 17D) –based OFETs. The devices had channel lengths of 250 μ m and channel widths of 8000 μ m. The gate voltage was swept at a rate of 50 mVs⁻¹.

[0047] FIGS. 18A-18C are comparative transfer curves for OFET devices comprising 120 nm PHPMA as the dielectric layer and including organic semiconductor active layers

comprising pentacene (FIG. 18A), 5FPE-NTCDI (FIG. 18B), P3HT (FIG. 18C) and quinacridone (FIG. 18D).. The devices had channel lengths of 250 μ m and channel widths of 8000 μ m. The gate voltage was swept at a rate of 50 mVs⁻¹.

FIG. 19 is a graph that shows stability of OFET device of an embodiment comprising pentacene as the organic semiconductor active layer and a self healing polymer blend dielectric layer (i.e., pentacene/SHP-OFET) during storage at ambient condition (R.H = 20%, 25 °C), specifically shown are a source-drain current change of the pentacene/SHP-OFET over storage time. The result shows that pentacene/SHP OFET device was as stable as a comparative OFET device comprising pentacene as the organic semiconductor active layer and SiO₂ as the dielectric layer.

[0049] FIGS. 20A-20D show hysteresis behavior of OFET devices that include a self healing polymer (SHP) blend dielectric layer, and an organic semiconductor active layer comprising pentacence (FIG. 20A), 5FPE- NTCDI (FIG. 20B), P3HT (FIG. 20C), and quinacridone (FIG. 20D).

FIGS. 21A-21C show electrical behavior of printed P3HT OFET devices assembled according to a model printing study using syringe delivery for which resulting devices had channel lengths of $600 \mu m$ and channel widths of $18,000 \mu m$, and for which the gate voltage was swept at a rate of 50mVs^{-1} ; and (c) electrical behavior output curves for P3HT OFET with gold bottom contacts (W/L = 30) and with 750 nm-thick dielectric inkjet-printed from ethanol solution; and (d) a photograph of the dielectric printed over the gold electrodes.

[0051] FIG. 21D is a photograph showing self-healing polymer blend of an embodiment formed as a dielectric layer over gold electrodes.

[0052] FIG. 23 shows optical image of a carbon painting layer healing process. It is noted that resistance decreased as the healing process continued as evidence by the resistivity change shown in FIG. 7.

FIGS. 24A-24C are graphs showing the sensing behavior of OFET devices having organic semiconductor active layers formed of 5FPE-NTCDI. The OFET device from which the data of FIG. 24A was measured included a self-healing polymer blend dielectric layer comprising PHPMA/PEI (1:1). The OFET device from which the data of FIG. 24B was measured included PMMA as the dielectric layer. FIG. 24C shows the average responses of P3HT/SHP-OFET and 5FPE-NTCDI/SHP-OFET devices to 0.5 ppm NH₃ with error bars.

DESCRIPTION OF THE EMBODIMENTS

[0054] Reference will now be made in detail to the present embodiments, examples of which are illustrated in the accompanying drawings. Wherever possible, the same reference numbers will be used throughout the drawings to refer to the same or like parts.

Notwithstanding that the numerical ranges and parameters setting forth the broad scope of the invention are approximations, the numerical values set forth in the specific examples are reported as precisely as possible. Any numerical value, however, inherently contains certain errors necessarily resulting from the standard deviation found in their respective testing measurements. Moreover, all ranges disclosed herein are to be understood to encompass any and all sub-ranges subsumed therein. For example, a range of "less than 10" can include any and all sub-ranges between (and including) the minimum value of zero and the maximum value of 10, that is, any and all sub-ranges having a minimum value of equal to or greater than zero and a maximum value of equal to or less than 10, e.g., 1 to 5. In certain cases, the numerical values as stated for the parameter can take on negative values. In this case, the example value of range stated as "less that 10" can assume negative values, e.g. -1, -2, -3, -10, -20, -30, etc.

The following embodiments are described for illustrative purposes only with reference to the Figures. Those of skill in the art will appreciate that the following description is exemplary in nature, and that various modifications to the parameters set forth herein could be made without departing from the scope of the present invention. It is intended that the specification and examples be considered as examples only. The various embodiments are not necessarily mutually exclusive, as some embodiments can be combined with one or more other embodiments to form new embodiments.

[0057] Printable and flexible, low-voltage operating, self-healable electronics are a highly desirable suite of technologies proposed for future intelligent electronic devices such as body monitors and window displays. Embodiments described herein comprise a key material used in printed logic circuits--the "gate dielectric" insulator—demonstrates various attributes described, but not limited, to those in the descriptions and examples below.

Accordingly, in an embodiment there is a self-healing polymer blend which shows excellent electrical and mechanical self-healing ability and may be used for forming the dielectric layer of an electronic device, such as an organic field effect transistor (OFET). In order to obtain a high performance self-healable material as the dielectric layer for printable and flexible OFETs, the polymer blend material of the embodiments should be readily soluble in common solvents, thus allowing solution processability. More importantly, high capacitance is desirable, as well as capability for repeated self-healing. Furthermore, it is noted that a high dielectric capacitance value is required to achieve low-voltage OFET operation. This is obtainable for H-bonded materials from a small degree of proton transport. Poly (methyl methacrylate) (PMMA) is a commonly used solution processable dielectric. Yet, acting alone it has no self-healing ability under mild conditions due to lack of dynamic bonding and reversible reaction sites. However, because hydrogen bonding groups also yield a highly polar surface that can trap charge carriers, a balance between the H-bond density and

nonpolar groups (here, the methacrylate backbone) should be realized. Therefore, a poly(methyl methacrylate) derivative such as poly (2-hydroxypropyl methacrylate) (PHPMA) as represented, for example, by chemical structure (I) in FIG. 1A, may alternatively be used in a self-healing polymer blend of an embodiment. While not limited to any particular theory, it is believed that the introduction of a hydroxyl group in the derivative significantly strengthens interactions between polymer chains via numerous dynamic hydrogen bonds.

PHPMA shows a high glass transition temperature, above 100 °C, as shown by differential scanning calorimetry (DSC) (FIG. 1B), indicating that the polymer chains have limited mobility at room temperature. In order to overcome this obstacle, a more flexible polymer additive, poly (ethyleneimine) (PEI), as represented, for example, by chemical structure (II) in FIG. 1A, may be employed, and may interact with PHPMA through dynamic hydrogen bonds. The glass transition temperature of PEI is shown by the DSC measurement in FIG. 1C. Accordingly, in an embodiment a polymer blend system comprises PHPMA and PEI and shows an amorphous structure with a much lower glass transition temperature (below 40 °C) (as shown by DSC in FIG. 1D). As a result, the polymer chains of the blend system have much higher freedom of motion at room temperature than PHPMA alone, which may significantly improve self-healing ability. DSC measurements were conducted on DSC Q20 V24.9 Build 121 equipment, OrgMethod 1: Ramp 5.00 °C/min to 200.00 °C; 2: Isothermal for 2.00 min; 3: Ramp 2.00 °C/min to 30.00 °C.

As shown in FIG. 1E, the self-healing polymer blend of the embodiments may undergo a self-healing process 100. FIG. 1E shows a film comprised of a self-healable polymer blend of an embodiment, for example a self-healable polymer blend comprising PHPMA and PEI when it is cut 103 along 103', when it is healing 105, and when it has healed 107. The healing step 107 is illustrated in the inset of FIG. 1E as formed robust hydrogen bonds between the severed surfaces.

[0061] In an embodiment there is a self-healing polymer blend composition comprising a first polymer, for example, PHPMA, and a second polymer, for example, PEI, which may be used as a self-healing dielectric layer in various electronic devices, such as organic field effect transistors. In an example, the self-healing polymer blend may comprise no added salts, and in such a case is referred to as a "nonionic polymer blend".

While in at least one embodiment, the polymer blend usable for a self-healing [0062] dielectric material may be described as including a first polymer such as PHPMA and a second polymer such as PEI, other embodiments may not be so limited. For example, various blends that include at least one hydroxylated polymer and at least one amine polymer may be used for the self-healing dielectric compositions. For example, the first polymer may include at least one hydroxylated polymer. The hydroxylated polymer may be selected from, and include combinations of, polymerized hydroxyalkyl methacrylates. acrylates, methacrylamides, and acrylamides, with alkyl chain lengths of about three to about six carbons, and polymerized hydroxyalkylated polystyrenes and poly(hydroxystyrenes), and poly(hydroxystyrene) (poly(vinylphenol)). The second polymer may include at least one amino-substituted polymer. The amino-substituted polymer may be selected from, and include combinations of polymerized aminoalkyl methacrylates, acrylates, methacrylamides, acrylamides, and polymerized vinylamines. Copolymers and blends of more than two polymers are also contemplated for each of the first polymer and the second polymer. A balance among mechanical integrity and molecular motion contributing to high capacitance and self-healing ability is sought in selecting the specific polymers.

[0063] The self-healing polymer blends of the embodiments exhibit pronounced electrical and mechanical self-healing behavior, automatically healing itself upon electrical and/or mechanical breakdown. Importantly, self-healing polymer blends of the embodiments can serve as the gate dielectric for organic semiconductors, and can even restore the

conductivity of a gate electrode material coated above it simultaneously with the process of healing itself, without need for any added healing agent, thereby enabling fully healable electronics. In other words, the self-healing polymer blends of the embodiments.

[0064] Both poly (2-hydroxypropyl methacrylate) and poly (ethyleneimine) are readily soluble in ethanol, an environmentally friendly and inexpensive solvent, and an orthogonal solvent for many organic and polymeric semiconductors. Accordingly, the self-healing polymer blend of the embodiments, for example, comprising PHPMA/PEI, which may be used for forming a dielectric layer, such as a gate dielectric layer in an OFET, may also be easily coated on semiconductor films without causing damage. Also, most solvents for organic semiconductors such as toluene, THF, chloroform, acetone, dichlorobenzene and dichloromethane cannot dissolve the blend dielectric layer, providing a much more convenient and efficient way to manufacture devices with varied architectures.

While not limited to any particular theory, it is believed that materials used in the polymer blend of the embodiments undergo reversible intermolecular interactions (for example, dynamic H-bonding or reversible chemical reaction). Along with low glass transition temperature or some degree of molecule motion at room temperature, the polymer blend of the embodiments can be used as a self-healing gate material, such as a gate dielectric, for electronic devices. Accordingly, a self-healable, flexible, printable and low-voltage operable OFET having a gate dielectric layer comprising a self-healing polymer blend of the embodiments may be utilized for vapor sensing, biomolecule sensing, more specifically biomacromolecule sensing, for example, protein sensing, as well as other conventional OFET applications and in improving the sensitivity of a gas sensor, such as for NH₃.

[0065] As shown in FIG. 2A, a self-healing polymer blend of an embodiment may be integrated as the dielectric layer of an organic field effect transistor (OFET) to form a self-healable polymer-based organic field effect transistor (SHP-OFET) 201. The SHP-OFET

201 of FIG. 2A includes a substrate 202 on which a gate electrode 204 may be disposed. In some examples, the substrate is rigid, in other examples, the substrate if flexible any may comprise a polymer such as a flexible PET substrate. In FIG. 2A, the gate electrode 204 and substrate 202 together comprise indium tin oxide (ITO) coated PET substrates. A gate dielectric layer 206 is disposed over the gate electrode 204, an active layer 208 is formed over the gate dielectric layer 206, along with a source 210 and drain 212 disposed on the active layer 208. The drain 210 and source 212 may each have a thickness of from about 20 nm to about 2000 nm and may comprise patterned gold or aluminum electrodes or patterned polymer conductors such as PEDOT-PSS or silver-based or carbon-based ink. The active layer 208 may have a thickness of from about 20 nm to about 100 nm and may comprise a semiconductor, such as an organic semiconductor as described below. The gate may have a thickness of from about 20 nm to about 5000 nm and may comprise a self-healing polymer blend of an embodiment.

The active layer 208 may comprise an organic semiconductor, for example, a conjugated molecule. The chemical structures of four different conjugated molecules that may be used for forming the active layer 208 are shown in FIG. 2B and include pentacene as represented by chemical structure (III), N, N'-bis(2-(pentafl-uorophenyl)ethyl)-1,4,5,8-naphthalene tetracarboxylic acid diimide (5FPE-NTCDI) as represented by chemical structure (IV), poly(3-hexylthiophene) (P3HT) as represented by chemical structure (V), and quinacridone as represented by chemical structure (VI).

[0067] FIG. 2C illustrates a method for forming a non-printed device, such as the SHP-OFET 201 of FIG. 2A. In an example, a gate 204, such as ITO, is formed (e.g., coated) on a substrate 202, such as a PET sheet. A self healing polymer blend of an embodiment may be deposited on the gate 204 via spin-coating to form gate dielectric 206. An organic

semiconductor is deposited on the gate dielectric 206 to form an active layer 208. Source and drain electrodes 210, 212 are deposited on the active layer 208 in a predetermined pattern.

Alternatively, the various materials may be printed to form an all printed device having a similar configuration as that of OFET 201. For example, FIG. 3 illustrates a method for forming an all printed device such as an all-printed OFET 301. In an example, a conductive ink such as silver ink is printed on a substrate 302, such as a PET sheet, to form a gate 304. A self healing polymer blend of an embodiment is printed on the gate 204 to form gate dielectric 306. An organic semiconductor is printed on the gate dielectric 306 to form an active layer 308. A silver ink is printed on the active layer 308 to form source 310 and drain 312.

The OFET devices of the embodiments are not limited to bottom gate configurations. For example, FIG. 4A includes a perspective view of a top gate SHP-OFET 401 of an embodiment. The top gate SHP-OFET 401 includes a substrate 402, such as a flexible PET substrate, and source 410 and drain 412 electrodes disposed on the substrate and separated by active layer 408 comprising an organic semiconductor. At least a portion of the active layer 408 is disposed on the substrate 402. A dielectric layer 406 comprising a self-healing polymer blend of an embodiment is formed over the active layer 408 and a gate electrode comprising, for example, carbon paint, is formed over the dielectric layer 406.

[0070] In a method of forming a self-healing device of an embodiment, such as a top gate SHP-OFET 401 of FIG. 4A, as shown in FIG. 4B, source 410 and drain 412 electrodes, each comprising gold, are deposited on a substrate 402 comprising a PET sheet. An organic semiconductor is printed such that it is disposed between the source 410 and drain 412 and at least partially on the substrate 402 and forms active layer 408. A self-healing polymer blend of an embodiment is printed on the active layer 408 and forms gate dielectric layer 406. A

gate material such as carbon paint is then printed on the gate dielectric layer 406 to form gate 404.

The self-healing polymer blends of the embodiments exhibit unexpectedly high effective thin film capacitance (e.g., up to 1,400 nF/cm² at thickness of 120 nm and 20-100 Hz) that has negligible dependence on film thickness as described in the examples below. This high capacitance can be useful in energy storage and in switching transistors between on and off states at low voltage. While not limited to any particular theory, it is believed that the unexpectedly high capacitance results from one or two thin interfacial layers, rather than the bulk. This means that on applying a polarizing voltage, charged species migrate towards at least one interface between the dielectric and a more electronically conductive layer, contributing to the selective polarization of a region of the self-healing polymer near the interface; the higher capacitance values result from polarization occurring at this thinner region rather than across a larger portion of the self-healing polymer. For example, this interfacial region may be about one tenth as thick as the thickness of the entire self-healing polymer film.

[0072] EXAMPLES

[0073] EXAMPLE 1 – Mechanical Properties of Blend Polymer System

A mechanical healing test was performed on a coin shaped bulk sample of a self-healing polymer blend of an embodiment comprising PHPMA and PEI in a 1:1 ratio. FIGS. 5A-5C are images of the sample at different stages of the mechanical healing testing. The dimensions of the sample were 1.5 cm in diameter and 0.3 cm thickness. As shown in FIG. 5A, a blade was used to cut the sample 505 approximately through a middle portion into two pieces 503, and then the two pieces were brought into contact along their severed surface with slight pressure and rejoined/allowed to heal at 505. After 3 minutes, the rejoined sample was exposed to a tensile stress in air under room temperature without adding any other

healing agent as shown in FIG. 5B-5C. The grid size (used as scale bar) on the background paper is about 0.6 cm by 0.6 cm, the original diameter of the coin shape polymer is 1.5 cm, after stretch, the diameter along the stretch direction of the polymer is increased to 4.5 cm. As evidenced by the images of FIG. 5B-5C, the healed area still held together without any damage even at a large strain.

FIG. 5D is a graph showing quantitative results from the mechanical tests conducted on the self-healing polymer blend sample as shown in FIG. 5B-5C. The results of the mechanical tests indicate that the self-healing polymer of the embodiments endured tensile stress that reached up to about 0.5 MPa at strain of 300%, a result which is in the range of other self-healing polymers. No immediate fracture was observed after reaching its maximum tensile stress. Instead, the tensile stress remained at 0.5 MPa until the strain reached 750%. After that, the tensile stress started to decrease slowly, finally showing fracture at 950% strain. After 3 minutes of additional healing in air at room temperature, a severed sample was observed to endure comparable tensile stress level (close to 90% of original sample) at the same strain value, and the tensile stress can be continuous held until the strain reaches up to 600%, then starts decreasing slowly and finally breaks at 1000% strain. This repeatable experiment clearly demonstrates that the self-healing polymer of the embodiments exhibits rapid self-healing behavior.

The self healing polymer blend comprising PHPMA and PEI also shows excellent self-healing ability on scratching. FIGS. 6A-6D show the results of self-healing. For example, as shown in FIG. 6A, a PHPMA/PEI (1:1) film with a thickness about 10 to 11 μm was made as shown in panel (a), and a cross scar (having a width about 15 μm and a depth of 10 μm) was formed on the film surface as shown in panel (b). After slightly warming the film at 50 °C for 5 minutes, the cross scar was partially healed as shown in panel (c), and after 10 minutes' healing, the cross scar completely healed as shown in panel (d). It

is noted that the healing process was also observed at room temperature, but over slightly longer time. Meanwhile, films of PS, PMMA and PHPMA did not completely heal, even when heated at much higher temperatures as observed for FIGS. 6B-6D, respectively. For example, FIG. 6B includes images (a) – (d) at different times after scoring a comparative film of poly(methyl methacrylate) (PMMA). The undisturbed film is shown at (a), the film upon scoring/cutting with a blade is shown at (b) (the cross is a crack in the film), the film after 15 min at 80 °C is shown at (c) with no self-healing evident, and the film after an additional 15 min at 150 °C is shown at (d) with no self-healing evident. FIG. 6C includes images (a) – (d) at different times after scoring a comparative film of polystyrene (PS). The undisturbed film is shown at (a), the film upon scoring/cutting with a blade is shown at (b) (the cross is a crack in the film), the film after 15 min at 80 °C is shown at (c) with no self-healing evident, and the film after an additional 15 min at 150 °C is shown at (d) but in not as good of condition as the self-healing film of FIG. 6A. FIG. 6D includes images (a) – (d) at different times after scoring a comparative film of PHPMA. The undisturbed film is shown at (a), the film upon scoring/cutting with a blade is shown at (b) (the cross is a crack in the film), the film after 15 min at 80 °C is shown at (c) with no self-healing evident, and the film after an additional 15 min at 150 °C is shown at (d) but in not as good of condition as the self-healing film of FIG. 6A.

Based on the observed self-healing property of the film formed from a self-healing polymer blend of an embodiment comprising PHPMA and PEI, further investigation was performed to assess its application on restoring conductivity of a conducting layer coated on it. For example, a layer of carbon paint with a thickness of about $18 \pm 5 \, \mu m$ was coated directly on a $18 \pm 2 \, \mu m$ PHPMA/PEI blend polymer film. The bilayer was then dried under vacuum. Carbon paint was chosen because its solvent is isopropanol, which is similar to the solvent (ethanol) used for self-healing polymer deposition, so that during the drying process,

the two layers partially diffuse into each other. Other conducting inks, based on ethanol, isopropanol, or related solvents, and containing carbon or metal particles, are also contemplated for use. While not limited to any particular theory, it is believed that the resulting interlayer is beneficial in healing the carbon paint layer and partially restores its conductivity.

As shown in FIG. 7A-7B, the carbon paint layer showed good conductivity before cutting: the surface resistance was about 2 k Ω (resistivity of about 4.5 Ω -cm) (the distance between two probes was 0.8 cm). Upon cutting of the carbon paint layer, its resistance drastically increased to over 4 M Ω (resistivity of about 9000 Ω -cm). After 120 minutes, healing at room temperature in air, the resistance decreased to about 200 k Ω (resistivity of about 450 Ω -cm). After 600 minutes, the resistance was about 20 k Ω (resistivity of about 45 Ω -cm). The final resistance was about 16 k Ω (resistivity of about 36 Ω -cm), which was much closer to the original value than the value just after the cut.

This feature—that the underlying self-healing polymer assists with restoring conductivity in a conductive film formed above it— is highly promising since film conductivity restoration is much more difficult than for bulk conductors. For example, severed surfaces of bulk materials can easily be contacted while re-connecting a severed film is much more challenging. The method of healing the electrical properties of a film formed above a film of the self-healing polymer of the embodiments overcomes challenges of conventional attempts to heal by avoiding the need to introduce healing agents (solvents) or embed microcapsules filled with conductive liquid into film to restore of conductivity. As demonstrated here, conductivity restoration can be achieved without any added agent, which is preferable for OFETs because the methods of the embodiments avoid delamination and degradation processes that could be associated with such additives.

[0080] EXAMPLE 2 – Self-healing Organic Field Effect Transistor

Based on this conductivity restoration ability conferred by PHPMA/PEI blend self-healing polymer as described, for example, in Example 1, a self-healing polymer layer and a carbon paint layer were integrated into an OFET as dielectric layer and gate electrode, respectively, to form a top gate SHP-OFET, such as SHP-OFET 401 of FIG. 4A such as according to the method illustrated in FIG. 4B.

For example, a top gate 404, dielectric layer 406, active layer 408, and source and drain electrodes 410 and 411 were patterned on a flexible PET substrate 402 as follows: A P3HT (10mg/mL in dichlorobenzene) solution was drop cast on Au electrodes 810, 812 and annealed under low pressure N_2 at 90 °C for 3 hours to form a P3HT film as the semiconductor layer 808. A self-healing polymer blend composition of an embodiment comprising 200 mg/mL PHPMA/PEI (1:1) ethanol solution was drop cast on the P3HT film and dried under vacuum to form a 16 μ m thick dielectric layer 806. Carbon paint suspension was coated on the self-healing dielectric layer as gate electrode 804 with a thickness of 18 \pm 5 μ m.

[0083] A self-healing test 800' as illustrated in FIG. 8 was performed on the SHP-OFET. The SHP-OFET is shown undisturbed 801, damaged 803 and healed 805. The SHP-OFET was damaged by damaging both the self-healing polymer blend dielectric layer 406 and the gate electrode layer (the carbon paint) 404. The gate electrode layer 404 and the dielectric layer 406 are shown as at least partially healed together as the self-healing polymer dielectric 406 undergoes the self-healing process.

As shown in FIG. 9, corresponding I-V measurements were taken for each of the stages shown during the self-healing process illustrated in FIG. 8, including for the undisturbed SHP-OFET before a cut is made, the damaged SHP-OFET on cutting, and again after the SHP-OFET has at least partially self-healed. As shown in the graph of FIG. 9, before cutting the resulting top gate SHP-OFET 801 shows excellent switching behavior at low

operating gate voltage, showing a drain current at -5 V of about -4.56 μ A (or roughly -4.6 μ A). Upon cutting to damage the self-healing polymer blend dielectric layer 806 and the gate 804 (no damage on P3HT organic semiconductor layer 804), drain current decreased to -2.15 μ A (about 2 μ A) due to the damage to the lower conductance of the carbon paint gate layer. After healing at room temperature in air for 10 hours, the carbon paint conductance was partially restored during the process of PHPMA/PEI dielectric healing itself, as discussed before; and transistor drain current was observed to increase to -3.63 μ A. On cutting, the drain current and mobility decreased to 51% and 32%, the mobility decrease is probably due to the decrease of charge carrier density in the other half part of channel that is less connected with the gate probe. The threshold voltage also slightly shifted, and the on/off ratio decreased due to drain current changing to a smaller value. After healing, the drain current increased to 76% of its original value, the mobility also increased to 64% of its original value, threshold voltage changes toward its original value, and the on/off ratio also increased. This is the first report that multiple layers of an organic field effect transistor can automatically self-heal, achieving step toward fully self-healable electronic devices.

[0084] EXAMPLE 3 – Capacitance and Impedance

[0085] Several MIM (metal-isolator-metal) architecture devices having a configuration of MIM device 1000 (as shown in FIG. 10) and comprised of a first metal layer 1002, a second metal layer 1004 and a dielectric layer 1006 disposed between conductive layers 1002 and 1004, were used for capacitance measurements. Different polymer compositions were used for the dielectric layer 1006. The sample MIMs were prepared by spin coating respective ones of the polymer compositions on ITO coated glass and an Au electrode (37 mm*37 mm, 50 nm in thickness) was subsequently deposited on spin-coated polymer layer. The results of the capacitance measurements are shown in Table 1 which includes capacitance values of different polymers with different thickness at 20 Hz. (All

values are the average of at least 10 samples). While 20 Hz capacitance values are listed in the table, the corresponding FIG. 11A shows that 80–90% of the capacitance is retained for thin films beyond 100 Hz.

TABLE 1

Dielectric layer	Thickness [nm]	Capacitance [nF/cm ²] at		
		20Hz		
PS ^{a)} [10 mg/mL]	100 ± 15	26 ± 2		
PMMA ^{b)} [10 mg/mL]	150 ± 20	20 ± 1		
PHPMA ^{c)} [10 mg/mL]	120 ± 20	66 ± 4		
PHPMA [100mg/mL]	1800 ± 200	5 ± 0.25		
$PHPMA + PEI^{d}$ [10mg/mL, 2:1] ^{e)}	120 ± 20	980 ± 160		
PHPMA + PEI [100mg/mL, 2:1]	3200 ± 200	900 ± 120		
PHPMA + PEI [10mg/mL, 1:1]	120 ± 20	1400 ± 250		
PHPMA + PEI [20mg/mL, 1:1]	160 ± 20	1050 ± 160		
PHPMA + PEI [200mg/mL, 1:1]	16000 ± 1000	1060 ± 250		

^{a)}PS: polystyrene; ^{b)}PMMA: poly (methyl methacrylate); ^{c)}PHPMA: poly (2-hydropropyl) methacrylate; ^{d)}PEI: poly (ethyleneimine); ^{e)}weight ratios.

[0086] With reference to the data in Table 1, PS (polystyrene) and PMMA (poly(methyl methacrylate)) show typical capacitance values as previous reports at a thickness around 100 nm. PHPMA shows a higher capacitance value (66 nF/cm²) than PS and PMMA at the same thickness range, and the value decreases proportionally with the increasing of film thickness, which is a typical feature for electron polarized dielectric materials. Surprisingly, after blending with PEI (2:1 weigh ratio) to form a self-healing polymer blend of an embodiment, the capacitance drastically increased up to 980 nF/cm², further increase of the PEI weigh ratio to 50% lead to a higher capacitance value of 1400 nF/cm² (FIG. 11B), which is higher than all the reported polymer dielectrics (except ion-gel dielectrics which contain more than 90% ions in the material).

[0087] While not limited to any particular theory, it is believed that one possible reason for the high capacitance for the self-healing polymer blend is that the lone electron pair on nitrogen atoms in poly(ethyleneimine) may generate large dipoles when interacting with the OH groups on PHPMA. Additionally, the capacitance value has less-than-predicted

dependence on film thickness; even a 16 µm thick film still exhibits a significantly high capacitance value of about 1000 nF/cm²at 20-100 Hz. This is the first report of a neutral polymer maintaining such high effective capacitance at a macroscopic thickness, useful for robustness and printability. The capacitance decreases with increasing of frequency, as shown in FIGS. 11C-11D, similar to what is observed with ion-polarized dielectric materials. The capacitance values were measured for various films at different frequencies and different thicknesses. The capacitance values were obtained by a MIM device configuration on an Agilent 4284A Precision LCR Meter. The frequency ranges from 20 Hz to 10⁶ Hz. FIG. 11C shows the experimental capacitance values for three different 120 nm thick films comprising PHPMA with no PEI, PHOMA and PEI at a ratio of 2:1, PHPMA at a ratio of 1:1, respectively and a 16000 nm thick film comprising PHPMA and PEI at a ratio of 1:1. FIG. 11E shows experimental capacitance values for 120nm, 160nm and 16,000 nm-thick films, each comprising PHPMA and PEI at a ratio of 2:1.

It is noted that that the thickness dependence of capacitance per unit area appears to be related to both PHPMA/PEI ratio and operating frequency. More specifically, at low frequency, <100 Hz, the capacitances of blend polymer film are largely independent of thickness, while films with very wide thickness range (from 120 nm to 16 μm) show a very narrow capacitance value distribution (650–1400 nF/cm²). However, with increasing frequencies, the thickness dependence of film capacitance becomes more and more obvious. While not limited to any particular theory, it is believed that a possible reason for this phenomenon may be that, at low frequency, the proton transport contribution to the polarization can be completed through a macroscopic thickness, so a thicker film can show capacitance comparable to a thinner film. However, at higher frequency, transport-dependent

polarization is incomplete, resulting in a smaller capacitance value compared to thinner films. Furthermore, the PEI ratio also affects this thickness dependence behavior. In the self-healing blend polymer films of embodiments with a higher PEI ratio, capacitance values show less thickness dependence, and in the blend polymer films of embodiments with a higher PHPMA ratio, capacitance values show higher thickness dependence, as would be expected for typical dielectrics where capacitance is inversely proportional to film thickness.

[0089] Complex impedance measurements, as shown in FIGS. 11F-11G, were performed in the frequency range 0.1 Hz to 1 MHz. The | Z | value was observed to increase on decreasing frequency, and the semicircular plots of Z" vs Z' as shown in FIGS. 11H-11I are consistent with parallel capacitor resistors in series with a small DC resistance, as represented by the equivalent circuit shown in FIG. 11J.

[0090] EXAMPLE 4 – Leakage Current Density Comparison

FIGS. 12A-12D are graphs showing shows the leakage current densities measured for five different polymers under bias voltage between ± 5 V in MIM architecture devices of FIG. 10. FIG. 12A shows results for 100 nm polystyrene (PS) samples, 150 nm poly(methyl methacrylate) (PMMA) samples, 120nm samples of poly (2-hydroxypropyl methacrylate) (PHPMA), and 120nm samples of self-healing polymer (SHP) of the embodiments comprising a polymer blend dielectric comprising PHPMA/PEI at weight ratios of 2:1 and 1:1; FIG. 12B shows results for 120nm samples of self-healing polymer (SHP) of the embodiments comprising a polymer blend dielectric comprising PHPMA/PEI at a weight ratios of 1:1, 120 nm PHPMA samples, 150 nm PMMA samples, and 100 nm PS samples; FIG. 12C shows results for 120 nm, 160 nm, 480 nm, 3000 nm, and about 16000 nm samples of self-healing polymer (SHP) of the embodiments comprising a polymer blend dielectric of PHPMA/PEI at weight ratio of 1:1; and FIG. 12D shows results for 120 nm, 160 nnm, 480 nm, 3300 nm, and about 16000 nm samples of self-healing polymer (SHP) of the

embodiments comprising a polymer blend dielectric of PHPMA/PEI at a weight ratio of 2:1. PHPMA/PEI blend polymer films show slightly lower leakage current than PS and PMMA films with the same thickness range; furthermore, adding PEI into PHPMA decreases the leakage current density. These results further demonstrated that PEI greatly eases the chain motion and leads to more uniform films with fewer pinholes through which leakage current could flow. For further tests, the PHPMA/PEI blend having a ratio of 1:1 was chosen because this ratio provided better performance, while higher PEI ratio (>50%) polymer blend lead to viscous gel-like film rather than a solid film, on which it is difficult to build devices.

[0092] EXAMPLE 5 – Electrical Breakdown and Self-Healing Test

The capability of the gate dielectric to recover from electrical breakdown is vitally important to prevent permanent failure of an OFET. To test this capability for the self-healing polymer blends of the embodiments as dielectric layers in OFETs, leakage current density between \pm 20 V bias voltages was measured, followed by application of a higher bias voltage (sweeping from 100 V to -100 V) to cause breakdown. A recheck of the leakage current densities under bias voltage between \pm 100 V were performed after 1 minute to observe whether the films undergo healing or further degradation. Lastly, leakage current densities between \pm 20 V bias voltages are measured and results with the initial values (before electrical breakdown) are compared to evaluate the electrical self-healing properties.

[0094] As shown in FIGS. 13A-13I, leakage current was measured for four polymers, including, including: a 100 nm film of PMMA (FIG. 13A),a 150 nm film of PS (FIG. 13B), a 130 nm film of PHPMA (FIG. 13C), and a 120 nm film of a polymer blend dielectric of an embodiment comprising PHPMA/PEI at a ratio of 1:1 (FIG. 13D), 150 nm PMMA (FIG. 13E), 100 nm PS (FIG. 13F), 120 nm PHPMA (FIG. 13G), 120 nm of a polymer blend dielectric of an embodiment comprising PHPMA/PEI at a ratio of 1:1 (FIG. 13H), and as

shown for consecutive tests for 120nm of a polymer blend dielectric of an embodiment comprising PHPMA/PEI at a ratio of 1:1 (FIG. 13I).

Leakage current density was first measured between ± 20 V bias voltages, [0095] then higher bias voltage (sweeping from 100 V to -100 V) was applied to cause breakdown. After 1 minute the leakage current densities were rechecked under bias voltage between ± 100 V to investigate whether these films are undergoing healing or further degradation; and finally measure leakage current densities between ± 20 V bias voltages and compare the results with the values before electrical breakdown, to evaluate the electrical self-healing properties. Before electrical breakdown (curves labeled "Before breakdown") the PHPMA/PEI film showed the lowest leakage current density among all four polymer films. By sweeping bias voltage between $\pm 100 \text{ V}$ (curves labeled "apply 100V to breakdown"), electrical breakdown occurred in all four polymer films (leakage current density higher than 1 A/cm²), with PHPMA showing the highest leakage current density after applying high voltages compared to other three polymer films. After electrical breakdown for 1 minute (sweeping bias voltage between ± 100 V again; curves labeled "apply 100V after 1 min"), PMMA, PS and PHPMA films were observed undergoing further degradation as evidenced by additional leakage current density increases, while only the PHPMA/PEI blend (1:1) film showed decrease in leakage current density. This indicated that the PHPMA/PEI blend healed itself immediately after electrical breakdown. Finally, by applying bias voltage between ± 20 V (curves labeled "apply 20V after 2 min"), only the PHPMA/PEI blend (1:1) film showed leakage current level comparable with the value before electrical breakdown, while all three other polymer films showed at least one order of magnitude higher leakage current densities than before breakdown. The PHPMA film completely lost its resistance, and no sign of healing could be observed. All these results clearly demonstrate that PEI may

significantly improve resistance restoration in the PHPMA film, accomplishing electrical self-healing.

[0096] EXAMPLE 6 – Performance of Self-Healing Polymer as Dielectric in Organic Field Effect Transistor

[0097] In order to evaluate the performance of the self-healing polymer, a PHPMA/PEI 1:1 blend was incorporated as a gate dielectric in an OFET. Bottom-gated OFETs were fabricated on flexible ITO coated PET substrates. Four conjugated molecules were used as the organic semiconductor channel layer: pentacene, *N*, *N*'-bis(2-(pentafluorophenyl)ethyl)-1,4,5,8-naphthalene tetracarboxylic acid diimide (5FPE-NTCDI), poly(3-hexylthiophene) (P3HT) and quinacridone. These materials cover the range of p and n-type, small molecule and polymer, hydrophilic and hydrophobic semiconductors. The four conjugated materials were employed to comprehensively assess the performance of PHPMA/PEI (1:1) blend self-healing polymer as a dielectric material.

[0098] As a control, OFETs with PS, PMMA, PHPMA and SiO₂ (no surface treatment) as gate dielectrics were also fabricated under exactly the same conditions as for the self-healing polymer, the only difference being that the OFETs with SiO₂ as dielectric were fabricated on rigid silica wafers, and not on flexible PET substrates.

[0099] Hydrophilic (highly polar) surfaces have generally been found to be unfavorable for charge carrier transport in OFETs due to their providing trap sites for electrons and holes, decreasing mobility and increasing the threshold voltage. However, as shown in transfer curves of FIGS. 14E-14H, the self-healing polymer dielectric-based OFETs (SHP-OFETs) of the embodiments still show significantly higher drain current values with lower driving voltages as compared to OFETs using the other four dielectrics due to the much higher capacitance of the blend. Output curves for the OFET utilizing the self-healing polymer blend of the embodiments with different organic semiconductor active layers are

shown in FIGS. 14A-14D and comparative transfer curves for OFETs with each of the other four dielectrics are shown in FIGS. 15A-15D, 16A-16D, 17A-17D and 18A-18D.

[00100] Additionally, the mobility of self healing polymer OFETs (SHP-OFETs) and PHPMA-OFETs are usually higher than for OFETs using the other dielectric layers, as shown in Table 2 below.

TABLE 2 - Characterizations of OFETs based on five different dielectric layers.

dielectrics	OSC	Pentacene	5FPE-NTCDI	P3HT ^{a)}	Quinacridone ^{b)}
PHPMA/PEI	$\mu \text{ [cm}^2\text{V}^{-1}\text{S}^{-1}\text{]}$	2.38E-01	2.17E-02	2.18E-01	1.1E-01
1:1 [120 nm]	$V_{th}[V]$	-2.7	-0.3	-2.128	-6.71
	On/off ratio	10^{3}	10^{2}	10^{3}	10^{3}
PHPMA	$\mu \text{ [cm}^2\text{V}^{-1}\text{S}^{-1}\text{]}$	4.68E-02	1.62E-01	6.5E-04	5.07E-03
[120nm]	$V_{th}[V]$	0.218	0.885	4.35	-3.56
	On/off ratio	10	10^{2}	2	10
PMMA	$\mu \text{ [cm}^2\text{V}^{-1}\text{S}^{-1}\text{]}$	4.1E-02	2.55E-02	N/A	2.94E-03
[150nm]	$V_{th}[V]$	-3.74	0.08	N/A	-8.91
	On/off ratio	10^{2}	10^{2}	N/A	10
PS	$\mu \text{ [cm}^2\text{V}^{-1}\text{S}^{-1}\text{]}$	3.1 E-02	1.16E-02	N/A	N/A
[100nm]	$V_{th}[V]$	-2.36	5.65	N/A	N/A
	On/off ratio	10^{3}	10^{2}	N/A	N/A
SiO ₂	$\mu \text{ [cm}^2\text{V}^{-1}\text{S}^{-1}\text{]}$	1.48E-02	1.45E-03	4.71E-04	6.45E-05
[300 nm]	$V_{th}[V]$	-3.05	-45.9	75.4	24.1
	On/off ratio	10^{3}	10^{0}	10^{0}	10^{0}

^{a)}for PMMA and PS based OFETs, P3HT device cannot be fabricated because P3HT solution destroy PMMA and PS layer, so no data is available for P3HT devices; ^{b)}for PMMA and PS based quinacridone OFET devices, no transistor behavior was detected.

[00101] While not limited to any particular theory, it is believed that larger charge carrier mobilities are observed from high charge density induced in the OFET channel. Large carrier densities result in increased trap-filling and a general smoothing of electrostatic potential variations in the film due to trapped charge, and these combined effects may lead to higher carrier mobilities. Furthermore, SHP based OFETs show excellent stability during storage in ambient conditions (pentacene, for example, see FIG. 19) and negligible hysteresis behavior (FIGS. 20A-20D), and still function well even after many cycles of bending.

[00102] In order to quantitatively analyze the performance of SHP-OFETs under strain/stress, a bending stress was applied to a flexible SHP-OFETs, for example, comprising a self-healing polymer blend of an embodiment. In order to fully load strain/stress on the

active device area, a P3HT based SHP-OFET was located at the center of the fl exible substrate where the strain/stress is maximized. The strain can be calculated by $\varepsilon = t/(2r+t)$ where t is the thickness of the device and r is the bending radius. Here, t is about 150 μ m. In a first stage, no bending stress is applied. The ε value was 0% and the distance between the two ends of the flexible device is 2 cm. Then this distance was reduced to 1.5 cm. By measuring the bending radius (r = 3 mm), the ε is calculated to about 2.5%. Then, the distance was further reduced to 1.0 and 0.5 cm, with the corresponding bending radius of about 1.96 and 1.19 mm, respectively; 3.8% and 6.3% of obtained strain was applied on the center of the device. The results of this test are summarized in Table 3.

TABLE 3

Distance	r	ε	I_{ε}/I_{o}	m_{ϵ}/m_{o}	V_{th}	On/off at -
						5B
2.0 cm	N/A	0%	1	1	-1.46±0.24	15±1
1.5 cm	3.0 mm	2.5	1.1±0.05	1.1±0.123	-1.53±0.09	18±4
1.0 cm	1.96 mm	3.8	1.05±0.057	1.08±0.19	-1.46±0.22	18±1
0.5 cm	1.19 mm	6.3	0.974±0.056	0.897±0.097	-1.27±0.20	12±6
Back to	N/A	0	1.30±0.1	1.34±0.16	-1.36±0.21	15±2
2.0 cm						
After 110	N/A	0	1.056±0.048	1.06±0.08	-1.42±0.16	16±3
bending						
cycles						

[00103] At 2.5% and 3.8% strain, the drain current slightly increased, which is attributed to the increase of mobilities; the possible reason may be that the stress induced a certain degree of alignment of polymer chains in the P3HT film, thus increasing the mobilities. Only at 6.3% strain, the drain current and mobilities slightly decreased; this may be because of that much higher strain stress causes some separation of P3HT chains that would make the P3HT film less continuous, leading to decreased mobility. Also, the threshold voltage at higher strain (6.3%) decreased to -1.27 V, making the device lightly easier to turn on, one possible reason being that at this high strain value, the interface between the dielectric layer and the P3HT layer becomes smoother, which could eliminate

some traps in the channel. After releasing the stress and returning to the original status, the performance of the flexible device shows slightly higher current and mobility, rather than degradation, indicating that the stress-induced P3HT film alignment could be retained after releasing the stress. After repeating this bending cycle 110 times, this P3HT/ SHP-OFET still shows highly stable performance; the drain current mobility, threshold voltage, and on/off ratio are still comparable to the original values. All of the above results show that our flexible device can be stably operated under bending strain/stress.

[00104] By using a manual model and actual inkjet deposition, the PHPMA/PEI blend polymer may be printable on flexible substrates and compatible with other printed OFET materials. The transfer and output curves of an all-manual-printed (using microliter syringes) and pneumatically printed dielectric OFETs with P3HT semiconductor are shown in FIGS. 21A-21C. The OFET shows excellent transistor behavior, with a high hole mobility value of from about 0.16 to about 0.21 cm²V⁻¹s⁻¹, comparable to the value for a non-printed P3HT OFET. Comparable currents at similar voltages were achieved with pneumatic printing as well. The results indicated that the self-healing polymer dielectric is highly suitable for print-based fabrication.

[00105] EXAMPLE 7 – Application in Flexible, Printable and Low Voltage operating OFET chemical Sensors

[00106] Another significant application of the self-healing polymer blends of the embodiments used as a dielectric in an OFET (SHP-OFET), is in flexible, printable and low-voltage operable OFET sensors. A flexible P3HT-based OFET device with PHPMA/PEI (1:1) blend as the dielectric layer was exposed to 0.5 ppm NH₃, with operating voltage of -5 V. The 0.50 ppm NH₃ was obtained from diluting 5.00 ppm NH₃ with dry air; the dry air was purified by standard procedures before mixing with 5.00 ppm NH₃. The concentration was precisely controlled and displayed by an Environics SERIES 4040 gas dilution system. The

total flow rate of gas is 1L/min. The sensor devices were characterized before and after each exposure. After an exposure time of 5 minutes, the drain current was observed to have decreased 23%, showing greater sensitivity than conventional P3HT NH₃ sensors. While not limited to any particular theory, the estimated limit of detection for the SHP-OFET detector of the embodiments is much lower than 0.5 ppm. The possible reason for the higher sensitivity to NH₃ could be that this highly polar self-healing dielectric layer has significant affinity for NH₃, so the uptake of NH₃ by the sensor is increased, and more NH₃ can be adsorbed at the interface between the dielectric layer and semiconductor layer (transistor channel), leading to a higher change of drain current. In order to verify this proposed mechanism, a different semiconductor, 5FPE-NTCDI, was incorporated as the sensing layer into an SHP-OFET, instead of the P3HT. 5FPE-NTCDI is a highly stable semiconductor, and it shows negligible response to NH₃, except at higher concentrations (above 10 ppm). As a control, a 5FPE-NTCDI-based OFET was constructed with PMMA as the dielectric layer, and was also exposed to 0.5 ppm NH₃. As shown in FIGS. 24A-24D, after a 5-minute exposure, the 5FPE-NTCDI/PMMA device only showed a 1% current increase, while the 5FPE-NTCDI-based SHP-OFET device showed a much higher response with a more than 5% current increase. This result clearly demonstrated the SHP-OFET of the embodiments is very promising for highly sensitive, flexible, printable and low-voltage operable OFET sensors.

[00107] An alternative chemical sensor embodiment is a biomolecule sensor, more specifically a biomacromolecule sensor, e.g. a protein sensor. For this embodiment, an OFET employing a self-healing polymer blend of an embodiment as a dielectric, such as described in Example 6, is coated with a capacitive coupling layer. A capacitive coupling layer may comprise nonpolar polymers such as CYTOP, polyethylene oligomers, and styrene-containing polymers, and also functional groups, such as amines and carboxylic acids, for binding receptor moieties. A receptor moiety may comprise an antibody. This elaborated

OFET sensor can detect the biomolecule, such as a protein, to which the antibody had been raised. The methods for constructing such a sensor from an OFET have been published, for example, in Weiguo Huang, Kalpana Besar, Rachel LeCover, Pratima Dulloor, Jasmine Sinha, Josué F. Martínez Hardigree, Christian Pick, Julia Swavola, Allen D. Everett, Joelle Frechette, Michael Bevan and Howard E. Katz, "Label-free Brain Injury Biomarker Detection Based on Highly Sensitive Large Area Organic Thin Film Transistor with Hybrid Coupling Layer" Chemical Science 5, 416-426 DOI: 10.1039/C3SC52638K 2014, the contents of which are incorporated herein by reference in its entirety.

[00108] EXAMPLE 8 – Device Fabrication

[00109] Example 8A - Capacitors

[00110] Capacitors were prepared by spin coating polymers on heavily n^{++} doped silicon wafer; the polymer films were annealed at $100\,^{\circ}$ C for 60 minutes in N_2 , and dried for 1 hour under vacuum. Alternative substrates for capacitors include indium tin oxide- and metal-coated flexible plastic substrates or glass. Alternative processing options for capacitors include annealing only or drying only. Polymers were spincoated from ethanol solutions at total solute concentrations of at least 20 mg/mL, at spin speeds ranging from 1,000 to 3,000 rpm. 100-nm-thick Al top contacts were deposited through a shadow mask to form a 0.35 mm by 0.35 mm square electrode.

[00111] Example 8B – Capacitors

[00112] Capacitors were also prepared by spin coating polymers on ITO-coated glass at 1–2 krpm, with the highest capacitances obtained from 10 mg/mL total solid concentrations. Polymer films for electronic measurements (including capacitance, impedance, leakage current, breakdown, and gate dielectric characterizations) were annealed at 90–100 °C, taking care not to exceed 100 °C, for 60 min under N_2 . Higher temperatures or extended heating in the presence of oxygen led to lower capacitance values, though 90 °C

annealing of the thinnest films for 60 min under vacuum gave similar capacitances to those obtained from N_2 annealing. While the samples were not put into vacuum as a separate step, they were exposed to vacuum when semiconductors or electrodes were vapor-deposited. 50 nm thick Au top contacts were deposited through a shadow mask to form a 37 μ m square electrode.

[00113] Example 8C - OFETs

IO0114] OFETs were prepared on flexible substrates. Polymer dielectric was spincoated on ITO-coated 500 μm thick PET thin sheets, annealed at 100 °C for 1 hour in N_2 , and dried for 1 hour under vacuum. Pentacene and 5FPE-NTCDI were thermally vapor-deposited under high vacuum ($\sim 3 * 10^{-6}$ torr) at 0.3 Å/s with final thickness of 50 nm. During deposition, the substrates were held at 80 °C. The P3HT was spin-coated at 1000 rpm for 90 seconds, then annealed at 80 °C for 15 minutes in N_2 , and dried 1 hour under vacuum. 50 nm Au source drain contacts were thermally vacuum-deposited at $\sim 3 * 10^{-6}$ torr. Quinacridone OFETs were fabricated according to conventional methods, however, it is noted that before quinacridone deposition, 30 nm $C_{44}H_{90}$ was first deposited on all five different dielectric layers because the low surface energy of the aliphatic $C_{44}H_{90}$ is critical for growth orientation of the H-bonded molecules, providing π -stacking parallel to the gate electrode and therefore high mobilities.

[**00115**] Example 8D – OFETs

[00116] OFETs were prepared on flexible substrates. Polymer dielectric was spincoated on ITO-coated 127 μm thick PET thin sheets, then annealed at 90-100 °C for 1 hour in N2, and dried for 1 hour under vacuum. Pentacene and 5FPE-NTCDI were thermally vapor-deposited under high vacuum (~3 * 10^{-6} torr) at 0.3 Å/s with final thickness of 50 nm. During deposition, the substrates were held at 80 °C. The P3HT solution was spin-coated at a speed of 1000 rpm for 90 seconds, then annealed at 80 °C for 15 minutes in N₂, and dried for

1 hour under vacuum. 50 nm Au source drain contacts were thermally vacuum deposited at $\sim 3 * 10^{-6}$ torr. Quinacridone OFETs were fabricated according to conventional methods, however, it is noted that before quinacridone deposition, 30 nm C44H90 was first deposited on all five different dielectric layers because the low surface energy of the aliphatic C₄₄H₉₀ is critical for growth orientation of the H-bonded molecules, providing π -stacking parallel to the gate electrode and therefore high mobilities.

For an all-printed device, such as that described above, Ag nanoparticle ink was first printed (by dropcasting from a syringe, as was done for all the printing steps for this example) on a flexible thin PET sheet to form a 2 cm x 2 mm rectangular Ag gate electrode. The ink was dried at 50 °C for 30 min. PHPMA/PEI (200 mg/mL, 1:1) blend ethanol solution ink was printed on the Ag gate electrode to form an insulating film as dielectric layer (~ 16 μm thickness). The assembly was annealed under vacuum (≈0.05 atm) at 50 °C for 60 min). Subsequently, P3HT (10mg/mL in dichlorobenzene) was printed on the dielectric layer. Finally, Ag nanoparticle ink was printed on the P3HT layer with channel length of 600 μm and channel width of 18,000 μm to form the source and drain electrodes. All the printing steps were carried out by dropcasting from syringes in air and the drying processes were conducted in vacuum (~ 0.05 atm) at 50 °C.

[00118] For self-healing OFETs, 50 nm Au source drain contacts were thermally deposited on flexible PET sheets at ~3 x 10^{-6} torr. P3HT solution (10 mg/mL in dichlorobenzene) was drop cast on Au electrodes and annealed for 3 hours at 90 °C in vacuum. A self-healing polymer (200 mg/mL PHPMA/PEI blend) ethanol solution was drop cast on the P3HT layer to form a $16 \pm 2 \mu m$ thick dielectric layer. Finally $18 \pm 5 \mu m$ carbon paint was coated on the self-healing polymer dielectric layer and dried under vacuum to form a gate electrode.

[00119] Electronic characterization of OFETs was conducted on an Agilent 4155C semiconductor parameter analyzer. Capacitances were measured on an Agilent 4284A Precision LCR Meter; the impedance measurement was performed using a Solartron 1260 impedance analyzer from 0.1 Hz to 106 Hz and Solartron 1287 electrochemical interface controlled by ZPlot and Zview software. Conductivity of carbon paint layers was measured by digital multimeter; thicknesses of films were determined by Dektak | A profilometer, and the film self-healing process was monitored by a REYENCE Laser microscope. Tensilestress tests were performed by using ASTM D638 normalized samples, with a strain rate of 0.5 mm/min at room temperature (25 °C), the dimension of the samples are about 1.5 cm in length, 0.3 cm in width and 0.3 cm in thickness. Load was measured with a resolution of 0.01 N and used to calculate the stress in the specimen. For self-healing experiments, the samples were cut by a blade, and the resulting severed samples were contacted again and pressed by hand to make sure the severed surfaces were well in contact with each other. After 3 minutes' healing at room temperature, the sample was subjected to the tensile-stress experiment. For conductivity healing experiments, the samples were cut by a blade to depth about $26 \pm 3 \mu m$ and a width about 40 ± 5 µm. The resistivity was calculated by $R = \rho L / Wt$, where R is resistance, p is resistivity, L, W and t are the length, width, and thickness of measured area, respectively

[00120] MATERIALS

[00121] P3HT (regioregular, average M_n 54,000-75,000, electronic grade, 99.995% trace metals basis) was purchased from Sigma Aldrich; pentacene with 99.995% purity was purchased from Sigma Aldrich and triple-sublimed before use; tetratetracontane (> 98%) was purchased from Sigma Aldrich; quinacridone with purity of 93% were purchased from TCI and sublimed for 5 times before use; 5FPE-NTCDI was synthesized according known methods. Indium tin oxide coated PET with surface resistivity 60 Ω /sq, poly(2-

hydroxypropyl methacrylate), poly(ethyleneimine) (branched, $M_w \sim 25,000$), poly(methyl methacrylate) ($M_w \sim 120,000$), and polystyrene ($M_n \sim 192,000$) were all purchased from Sigma Aldrich. Conductive carbon paint was purchased from SPI Supplies. For spin-coating, P3HT (10 mg/mL in dichlorobenzene), PMMA (10 mg/mL in chloroform), PS (10 mg/mL in toluene), PHPMA (10 mg/mL in ethanol), PHPMA/PEI (10 mg/mL each or 200 mg/mL in ethanol in total) were prepared in a glove box filled with argon. More specifically, PHPMA and PEI were mixed in the desired ratio, most often 1:1, in ethanol at 10, 20, or 50 mg/mL concentrations of total solids. The mixtures were heated at 50 °C or lower (temperatures between 35 and 50 °C are permissible but temperatures above 50 °C should be avoided) with gentle stirring until a uniform mixture was obtained. The solutions were filtered through 0.2 μ m filters before use.

[00122] While the present teachings have been illustrated with respect to one or more implementations, alterations and/or modifications may be made to the illustrated examples without departing from the spirit and scope of the appended claims. For example, it will be appreciated that while the process is described as a series of acts or events, the present teachings are not limited by the ordering of such acts or events. Some acts may occur in different orders and/or concurrently with other acts or events apart from those described herein. Also, not all process stages may be required to implement a methodology in accordance with one or more aspects or embodiments of the present teachings. It will be appreciated that structural components and/or processing stages may be added or existing structural components and/or processing stages may be removed or modified. Further, one or more of the acts depicted herein may be carried out in one or more separate acts and/or phases.

[00123] Furthermore, to the extent that the terms "including," "includes," "having," "has," "with," or variants thereof are used in either the detailed description and the claims,

such terms are intended to be inclusive in a manner similar to the term "comprising." The term "at least one of" is used to mean one or more of the listed items may be selected. Thus, "at least one of and the phrase "one or more of", for example, A, B, and C, means any of the following: either A, B, or C alone; or combinations of two, such as A and B, B and C, and A and C; or combinations of three A, B and C.

[00124] Further, in the discussion and claims herein, the term "on" used with respect to two materials, one "on" the other, means at least some contact between the materials, while "over" means the materials are in proximity, but possibly with one or more additional intervening materials such that contact is possible but not required. Neither "on" nor "over" implies any directionality as used herein.

[00125] Additionally, the term "about" indicates that the value listed may be somewhat altered, as long as the alteration does not result in nonconformance of the process or structure to the illustrated embodiment. Finally, "exemplary" indicates the description is used as an example, rather than implying that it is an ideal. Other embodiments of the present teachings will be apparent to those skilled in the art from consideration of the specification and practice of the disclosure herein. It is intended that the specification and examples be considered as exemplary only, with a true scope and spirit of the present teachings being indicated by the following claims.

WHAT IS CLAIMED IS:

1. A method for making a self-healing polymer-based organic field-effect transistor (SHP-OFET), comprising:

depositing a first metal and a second metal over a flexible substrate;

patterning the first metal and the second metal to form a source electrode and a drain electrode, respectively;

forming an organic semiconductor channel;

depositing a solution comprising a first polymer and a second polymer over the substrate to form a self-healing polymer blend dielectric layer; and

depositing a conductor over the substrate to form a gate.

- 2. The method of claim 1, wherein the solution comprising a first polymer and a second polymer is a non-ionic solution that is deposited over the gate.
- 3. The method of claim 2, wherein the organic semiconductor channel is deposited over the dielectric layer or over the source and drain electrodes.
- 4. The method of claim 3, wherein the first metal and the second metal are deposited over the organic semiconductor channel.
- 5. The method of claim 1, wherein forming the organic semiconductor channel comprises depositing a solution comprising an organic semiconductor over the substrate to form the organic semiconductor channel.
- 6. The method of claim 5, wherein the non-ionic solution is deposited over the organic-semiconductor channel.
- 7. The method of claim 6, wherein the conductor is deposited over the self-healing polymer blend dielectric layer.
- 8. The method of claim 1, wherein the conductor is deposited in solution with a first solvent, the non-ionic solution comprises a second solvent, and the conductor partially diffuses into the self-healing polymer blend dielectric layer.

9. The method of claim 8, wherein the first solvent and the second solvent are the same solvent.

- 10. The method of claim 8, wherein the first solvent and the second solvent are different solvents, the first solvent comprising isopropanol and the second solvent comprises ethanol.
- 11. The method of claim 1, wherein the first and the second polymers are configured to undergo at least one reversible intermolecular interaction.
- 12. The method of claim 1, wherein first and the second polymers of the dielectric layer comprise chains that interact via a plurality of hydrogen bonds.
- 13. The method of claim 1, wherein the first polymer comprises at least one of a hydroxyalkyl methacrylate, an acrylate, methacrylamide, acrylamides, or mixtures thereof, and wherein the second polymer comprises a polyimine additive.
- 14. The method of claim 1, wherein the first polymer comprises alkyl chain lengths of about three to about six carbons.
- 15. The method of claim 1, wherein the first polymer comprises at least one of a hydroxyalkylated polystyrene, poly(hydroxystyrene), poly(hydroxystyrene) (poly(vinylphenol)), or mixtures therof.
- 16. The method of claim 1, wherein the first polymer comprises a poly(methyl methacrylate) derivative comprising a hydroxyl group.
- 17. The method of claim 16, wherein the poly(methyl methacrylate) derivative comprises poly (2-hydroxypropyl methacrylate) (PHPMA).
- 18. The method of claim 1, wherein the solution comprises a nonionic polymer blend.

19. The method of claim 1, wherein the polyimine additive comprises poly (ethyleneimine) (PEI).

- 20. The method of claim 1, wherein a weight ratio of the first polymer to the second polymer is from about 2:1 to about 1:1.
- 21. The method of claim 1, wherein first polymer and the second polymer comprise a polymer blend, and the polymer blend has a glass transition temperature below about 40°C.
- 22. The method of claim 1, wherein the depositing a non-ionic solution comprises printing the non-ionic solution.
- 23. A self-healing polymer-based organic field-effect transistor (SHP-OFET) comprising: a substrate;
 - a source electrode and a drain electrode each disposed over the substrate;
 - an organic semiconductor channel disposed between the source and the drain;
- a self-healing polymer blend dielectric layer disposed over the organic semiconductor channel, wherein the self-healing polymer blend dielectric layer comprises a first polymer and a second polymer; and
 - a gate disposed over the dielectric layer.
- 24. The SHP-OFET of claim 23, wherein the first polymer comprises a poly(methyl methacrylate) derivative comprising a hydroxyl group.
- 25. The SHP-OFET of claim 24, wherein the polymethacrylate derivative comprises poly (2-hydroxypropyl methacrylate) (PHPMA).
- 26. The SHP-OFET of claim 23, wherein wherein the first polymer comprises at least one of a hydroxyalkyl methacrylate, an acrylate, methacrylamide, acrylamides, or mixtures thereof, and wherein the second polymer comprises a polyimine additive.
- 27. The SHP-OFET of claim 23, wherein the polyimine additive comprises poly (ethyleneimine) (PEI).

28. The SHP-OFET of claim 23, wherein a weight ratio of the first polymer to the second polymer is from about 2:1 to about 1:1.

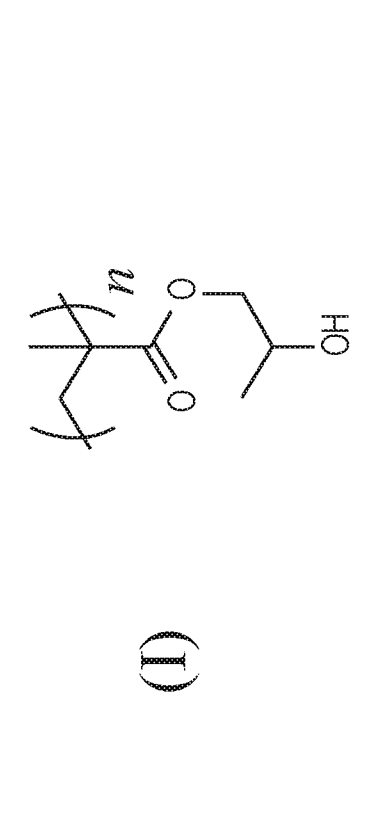
- 29. The SHP-OFET of claim 23, wherein the polymer blend has a glass transition temperature below about 40°C.
- 30. The SHP-OFET of claim 23, wherein the substrate comprises a flexible substrate.
- 31. The SHP-OFET of claim 23, wherein the dielectric layer comprises a thickness in a range of about 120nm to about 16,000 nm.
- 32. The SHP-OFET of claim 23, wherein the dielectric layer exhibits a thin film capacitance of up to 1,400 nF/cm².
- 33. The SHP-OFET of claim 23, wherein the dielectric layer exhibits a thin film capacitance in a range of 980 nF/cm² to about 1400 nF/cm².
- 34. The SFP-OFET of claim 23, wherein the nonionic polymer blend comprises a print-deposited nonionic polymer blend.
- 35. A chemical sensor comprising the SHP-OFET of claim 23.
- 36. The chemical sensor of claim 35, further configured to detect ammonia (NH3).
- 37. The chemical sensor of claim 35, wherein the detector has a detection limit of lower than about 0.5 ppm.
- 38. The chemical sensor of claim 35, further configured to detect at least one biomacromolecule.
- 39. The chemical sensor of claim 35, further configured to detect proteins.

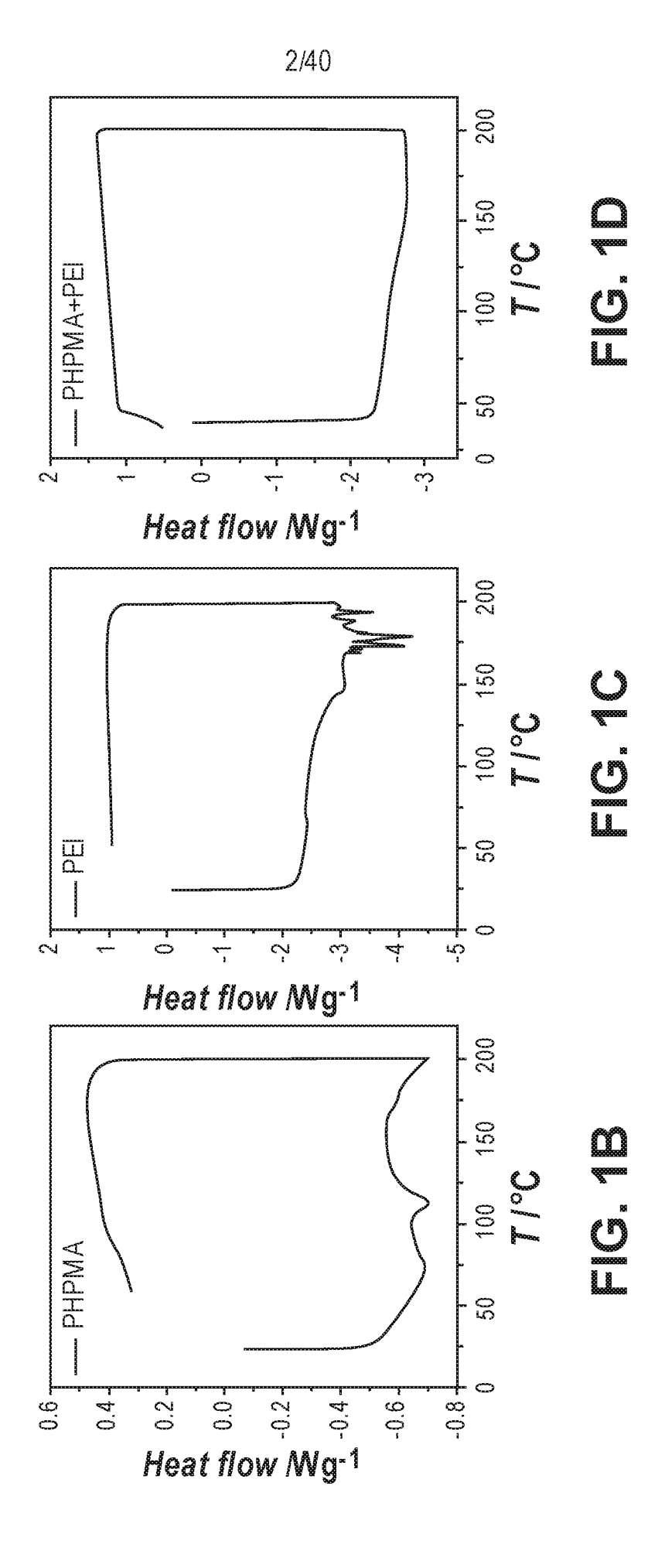
40. The chemical sensor of claim 35, wherein the sensor is configured to be wearable or implantable.

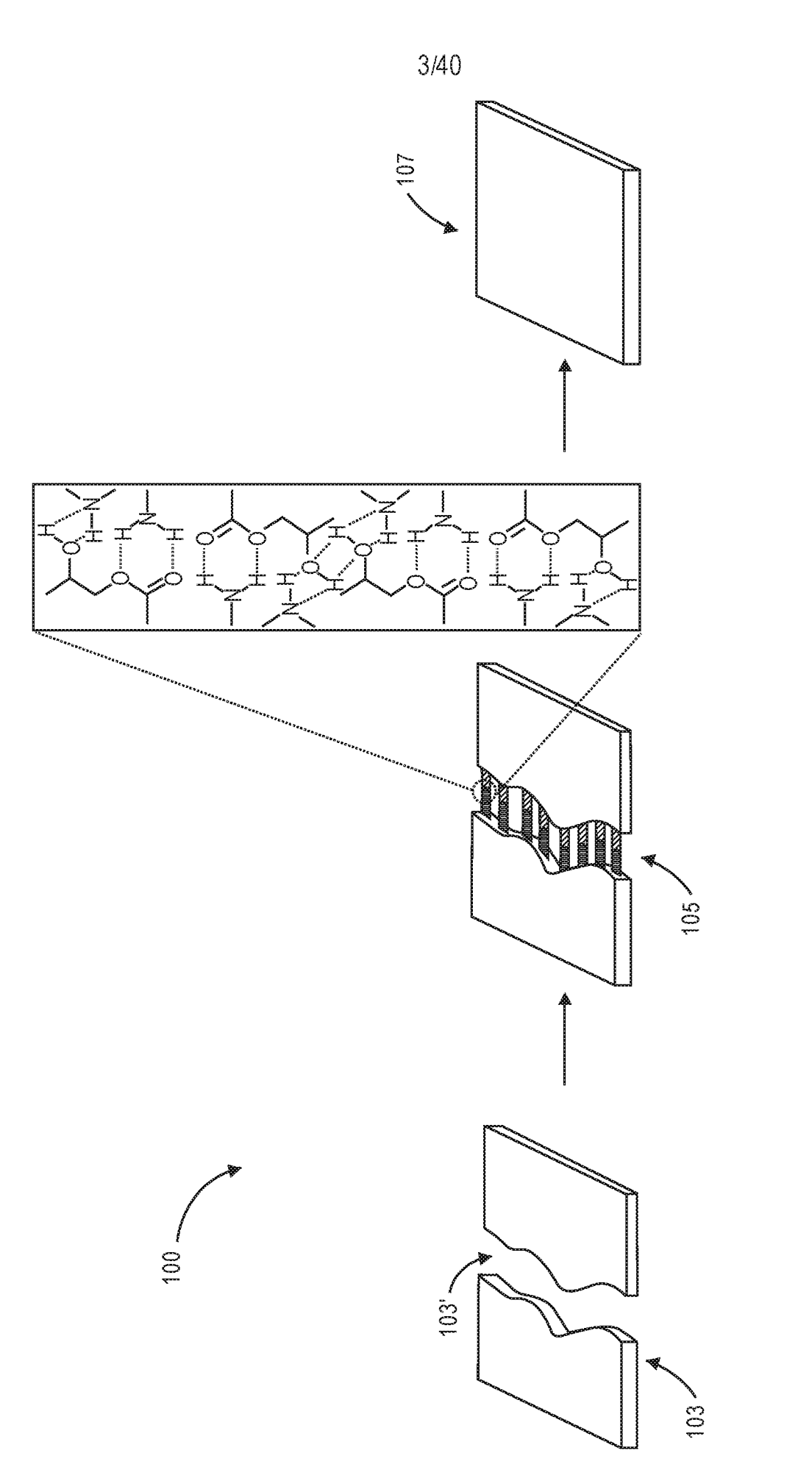
- 41. A polymer blend dielectric composition, comprising:
 - a poly(methacrylate) derivative comprising a hydroxyl group,
 - a polyimine additive, and
 - a solvent,

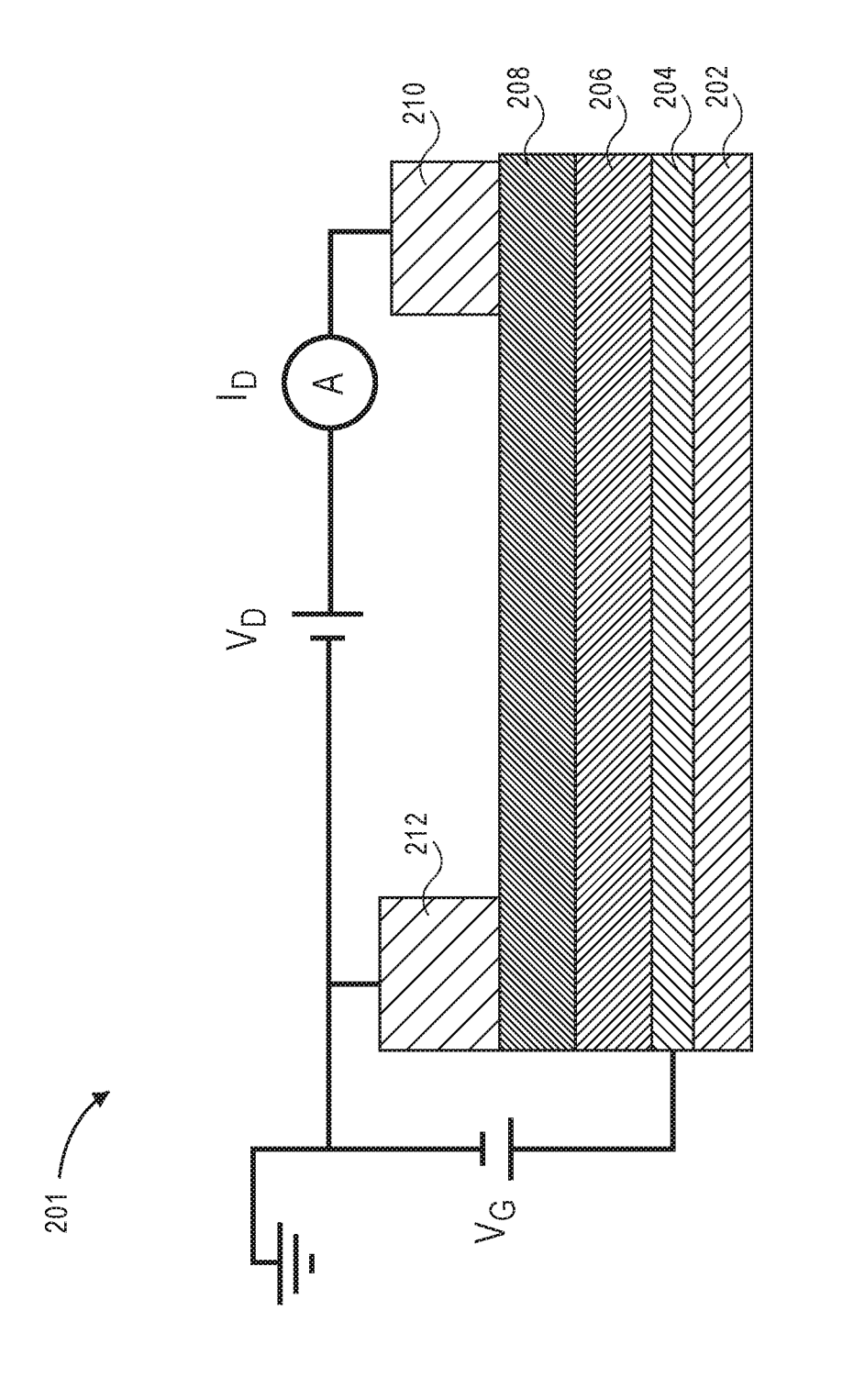
wherein a weight ratio of the poly(methacrylate) derivative to the polyimine is from about 2:1 to about 1:1.

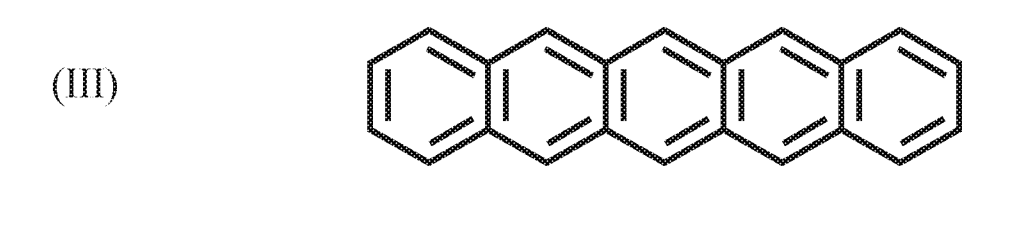
- 42. The composition of claim 41, wherein the poly(methacrylate) derivative comprises poly (2-hydroxypropyl methacrylate) (PHPMA).
- 43. The composition of claim 41, wherein the polyimine comprises poly (ethyleneimine) (PEI).
- 44. The composition of claim 41, wherein the polymer blend is nonionic.
- 45. A self-healing polymer-based capacitor, comprising:
- a self-healing dielectric layer disposed between a first electrode and a second electrode, wherein the self-healing dielectric layer comprises a nonionic polymer blend comprising a first polymer and a second polymer.









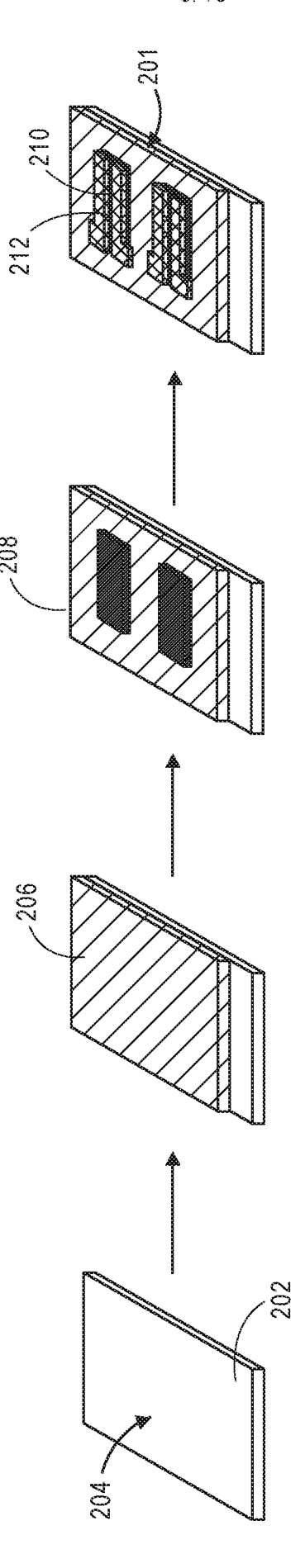


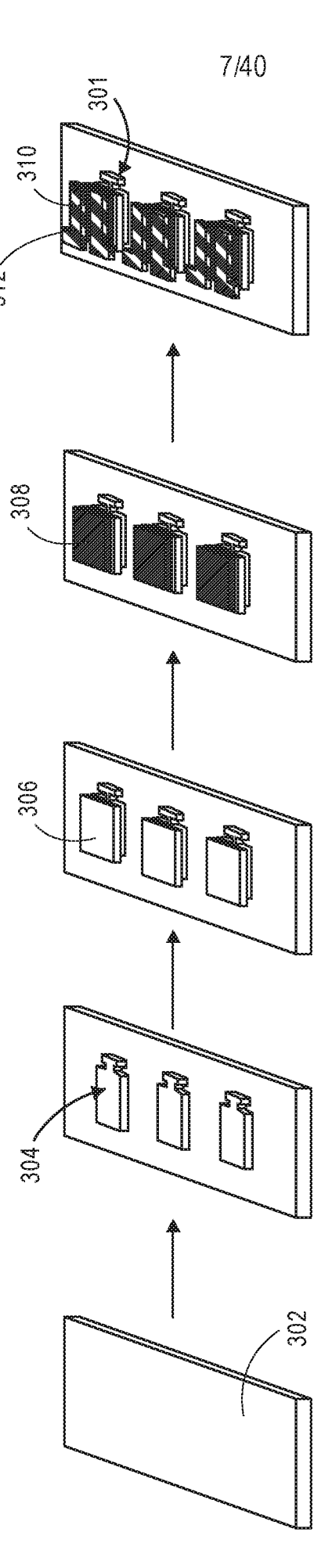
$$(IV) \quad F = \begin{cases} F \\ \\ \\ F \end{cases}$$

$$F = \begin{cases} F \\ \\ \\ F \end{cases}$$

FIG. 2B







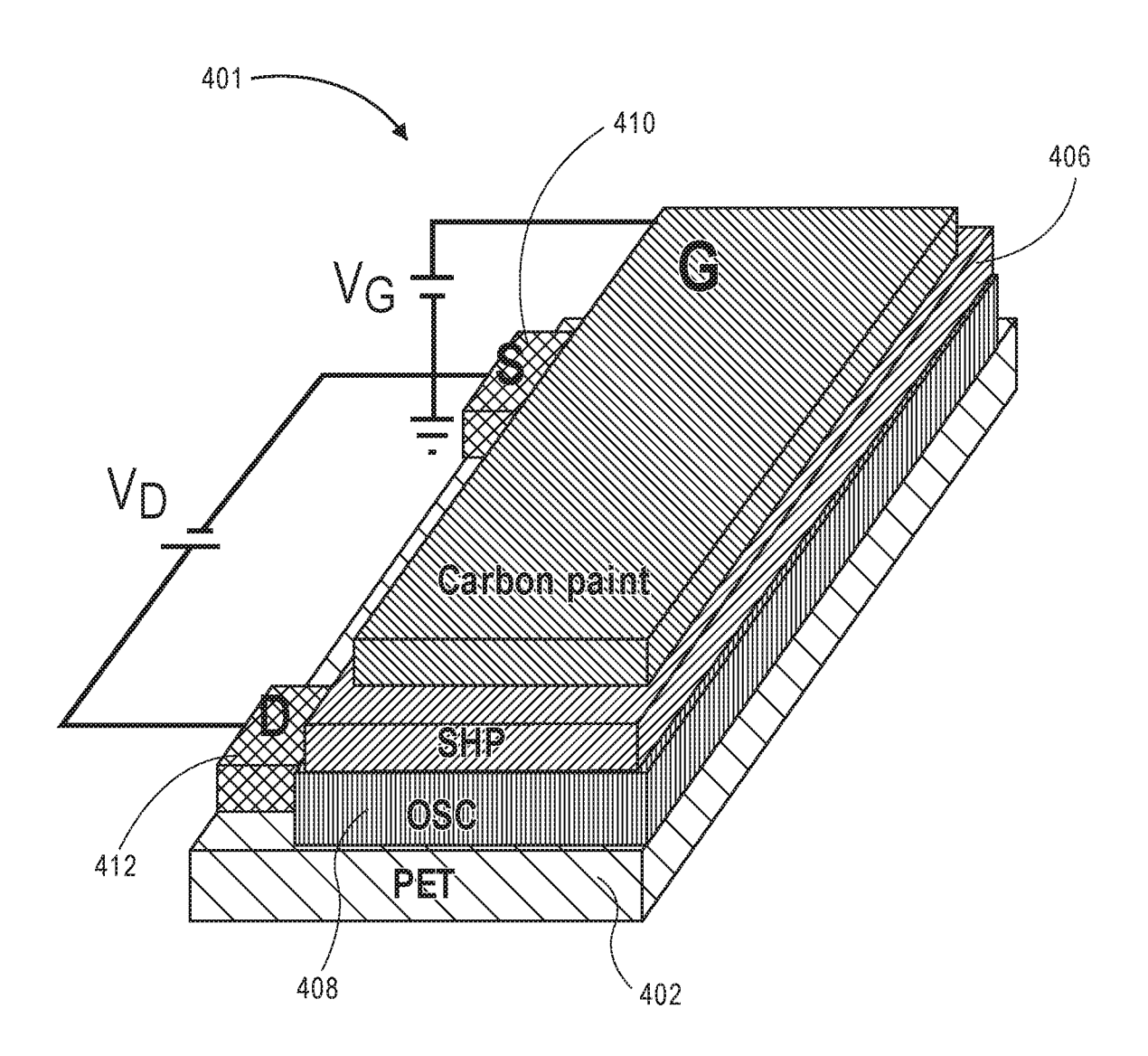
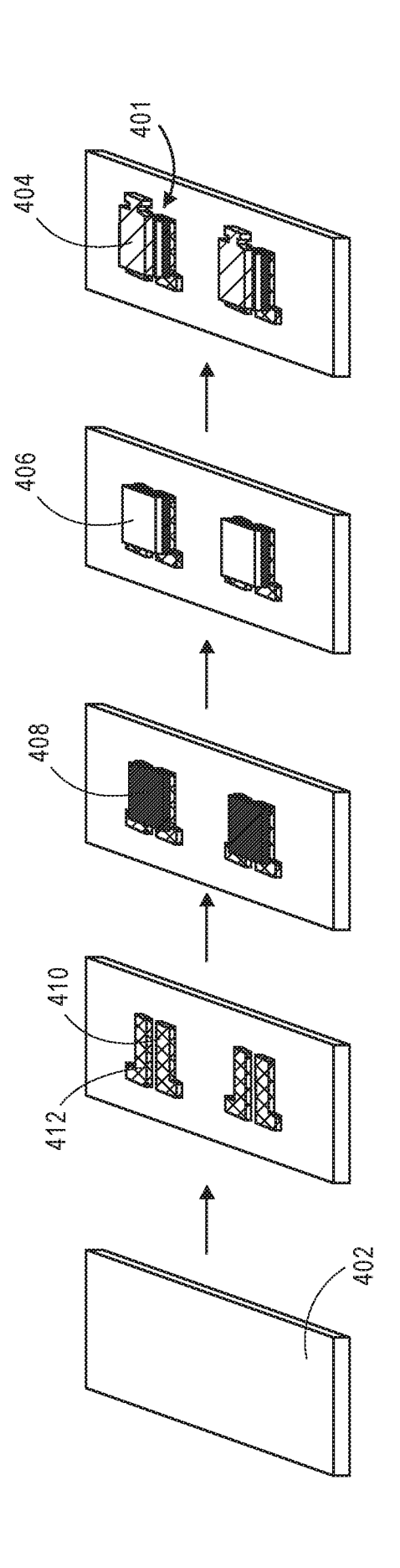
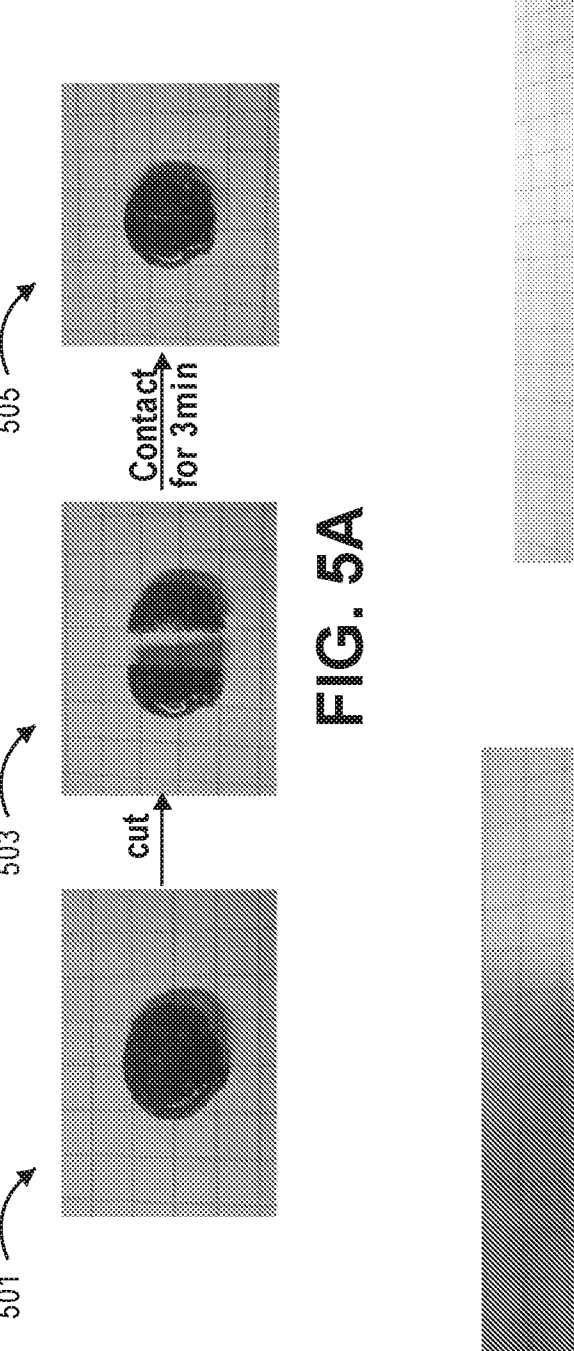
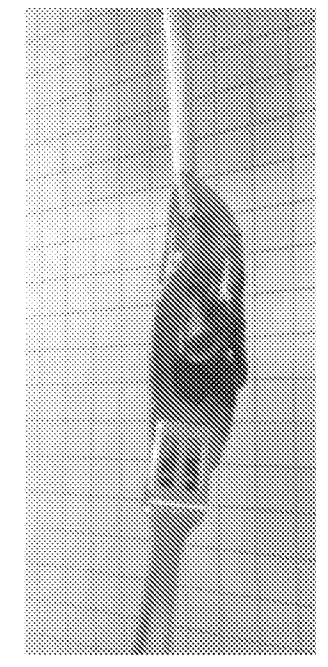


FIG. 4A











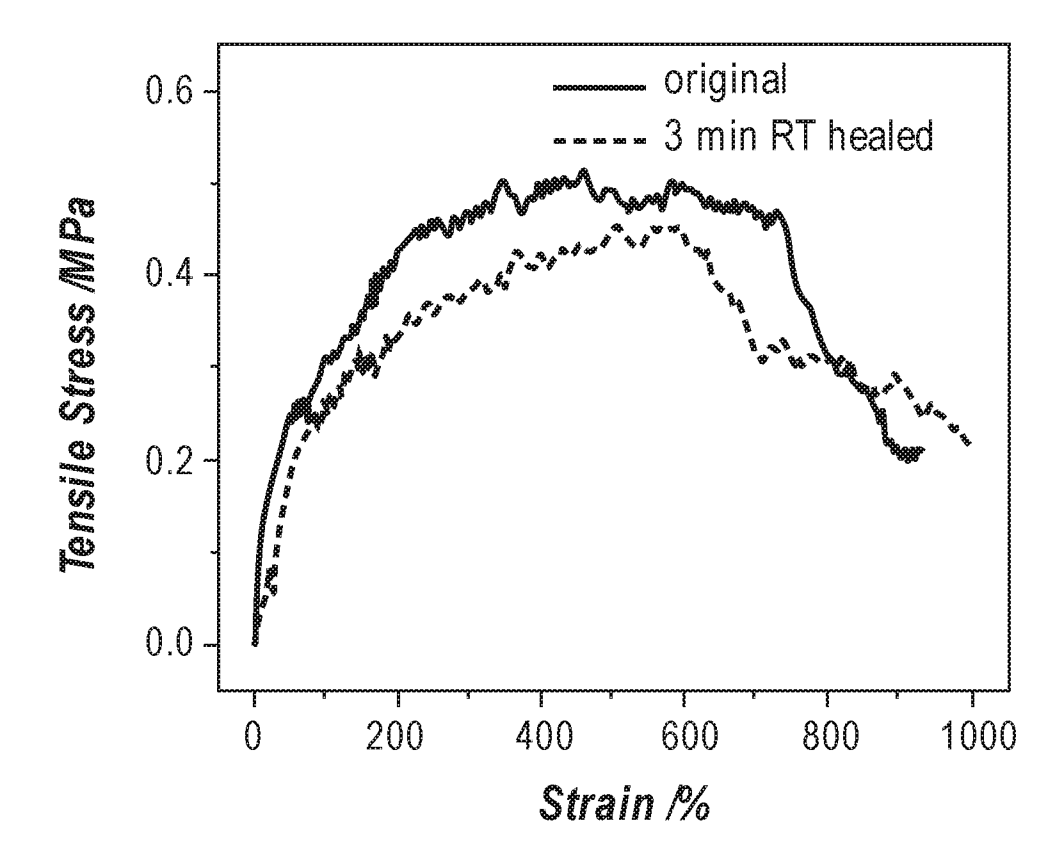


FIG. 5D

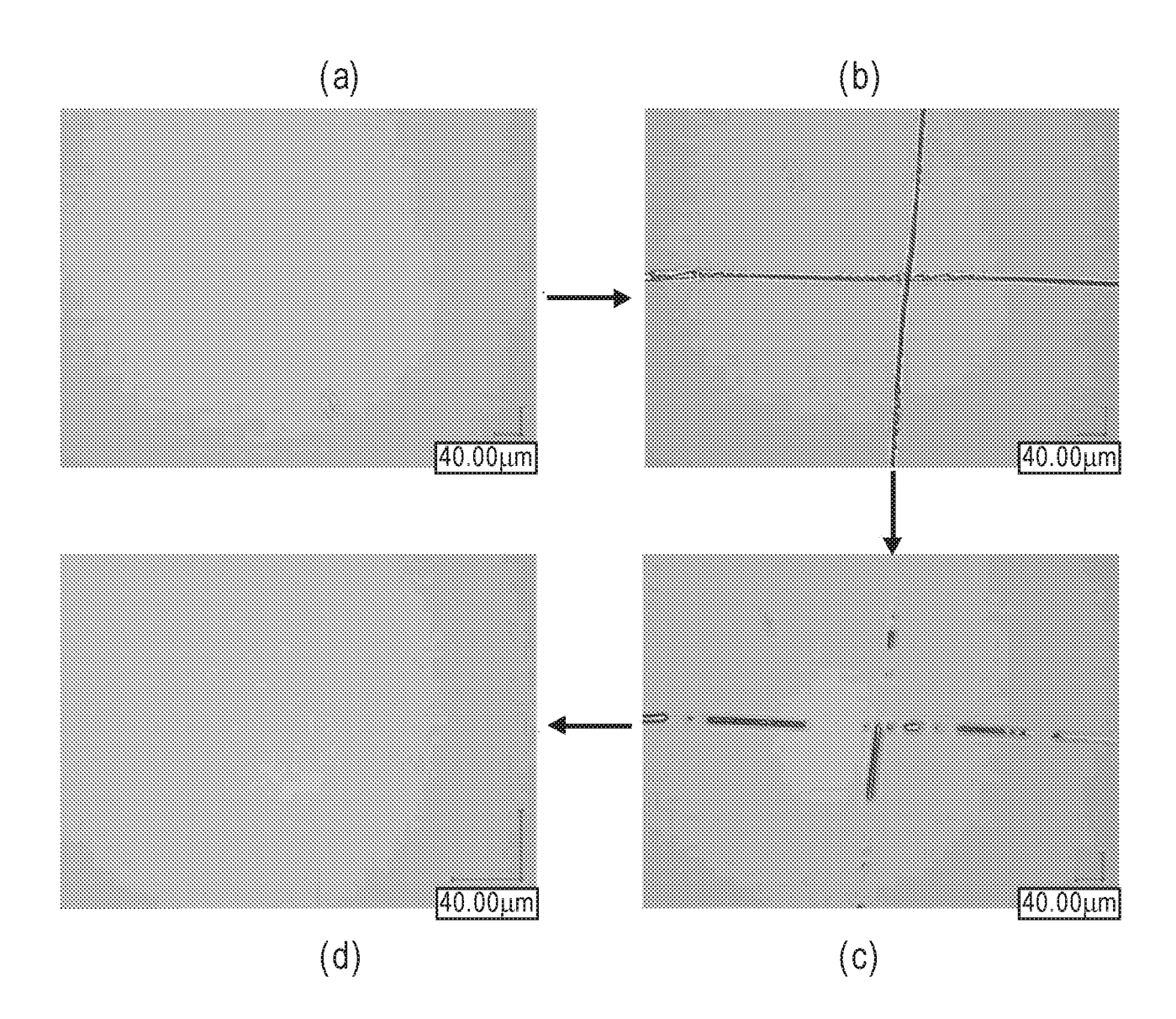


FIG. 6A

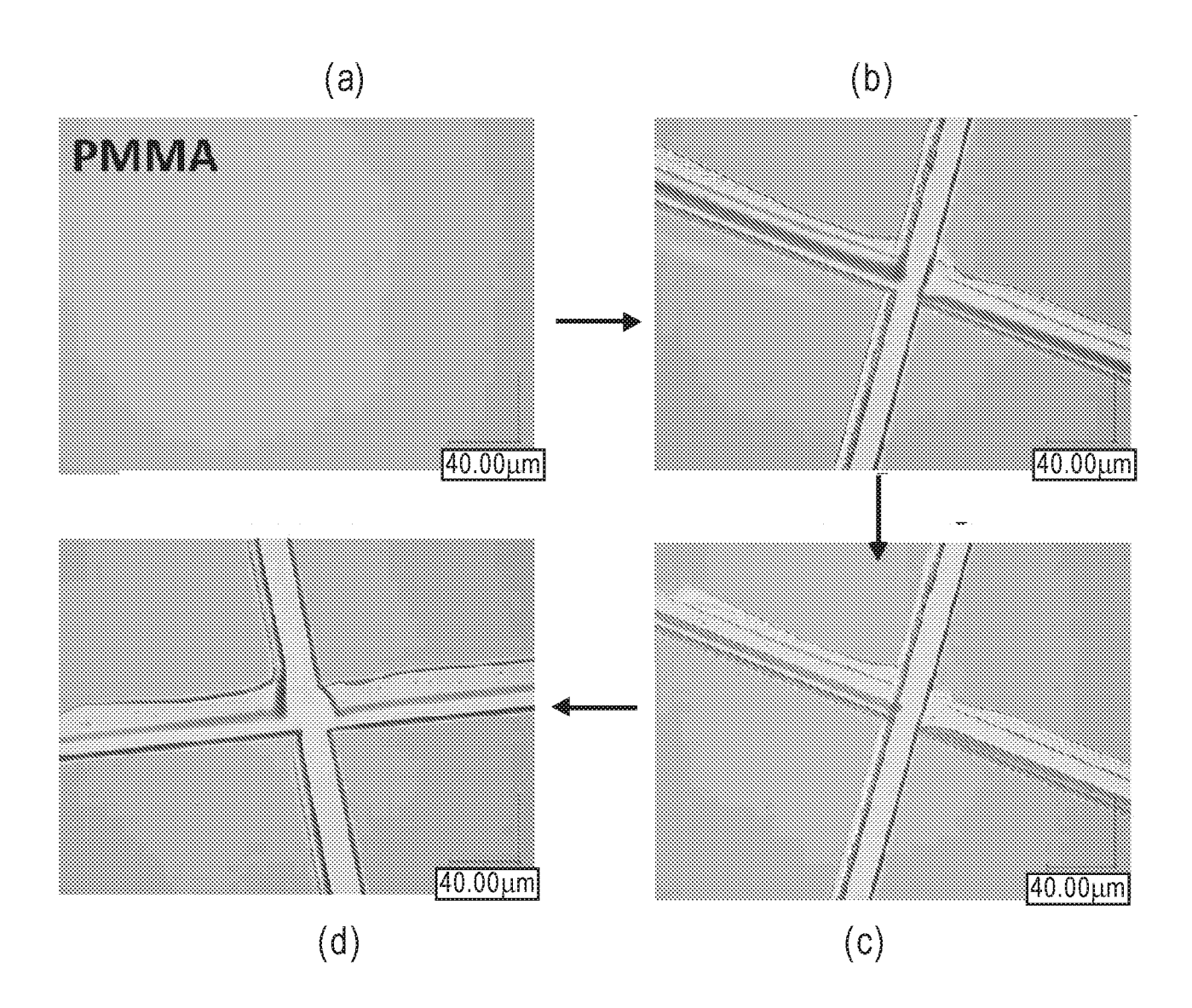


FIG. 6B

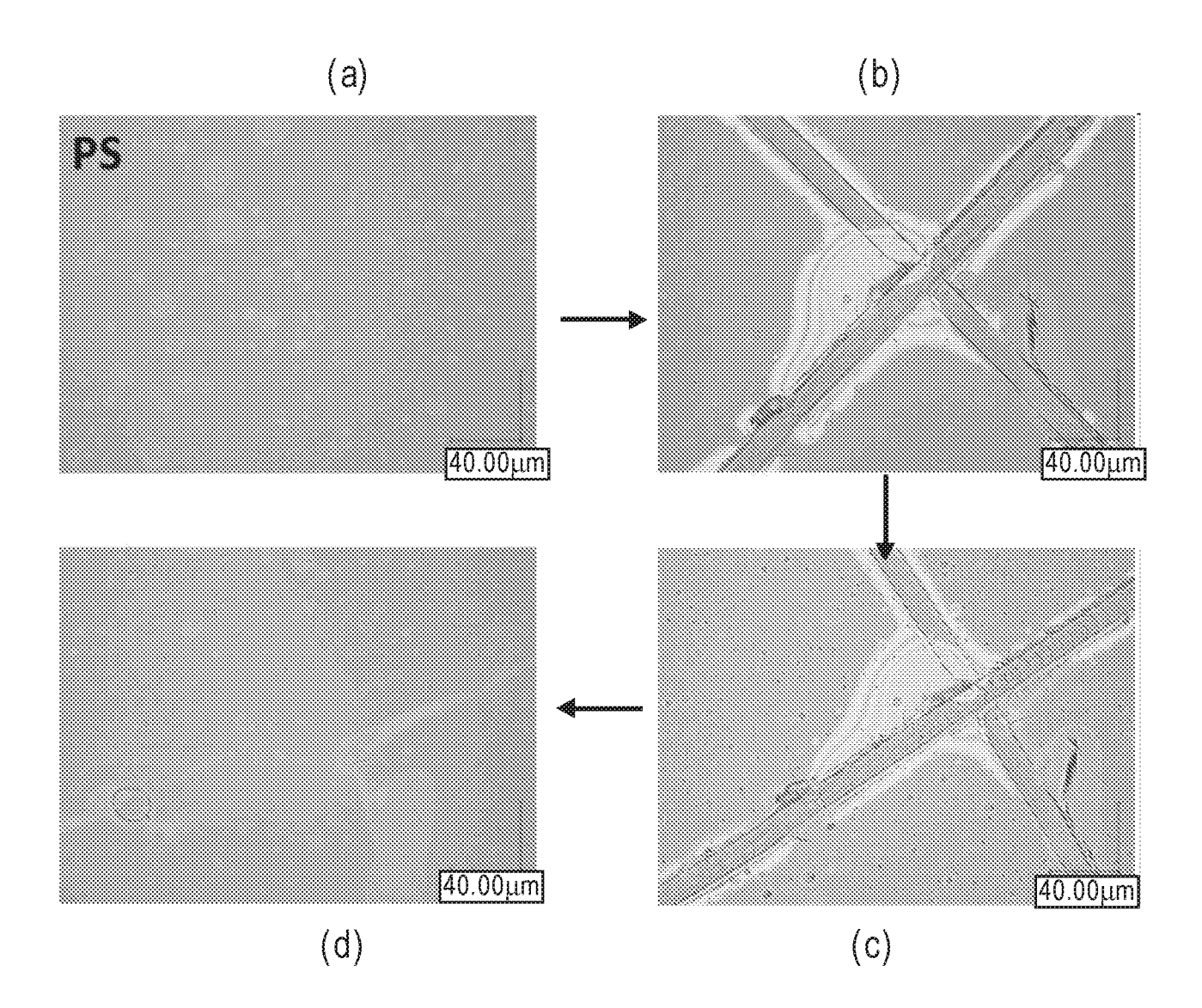


FIG. 6C

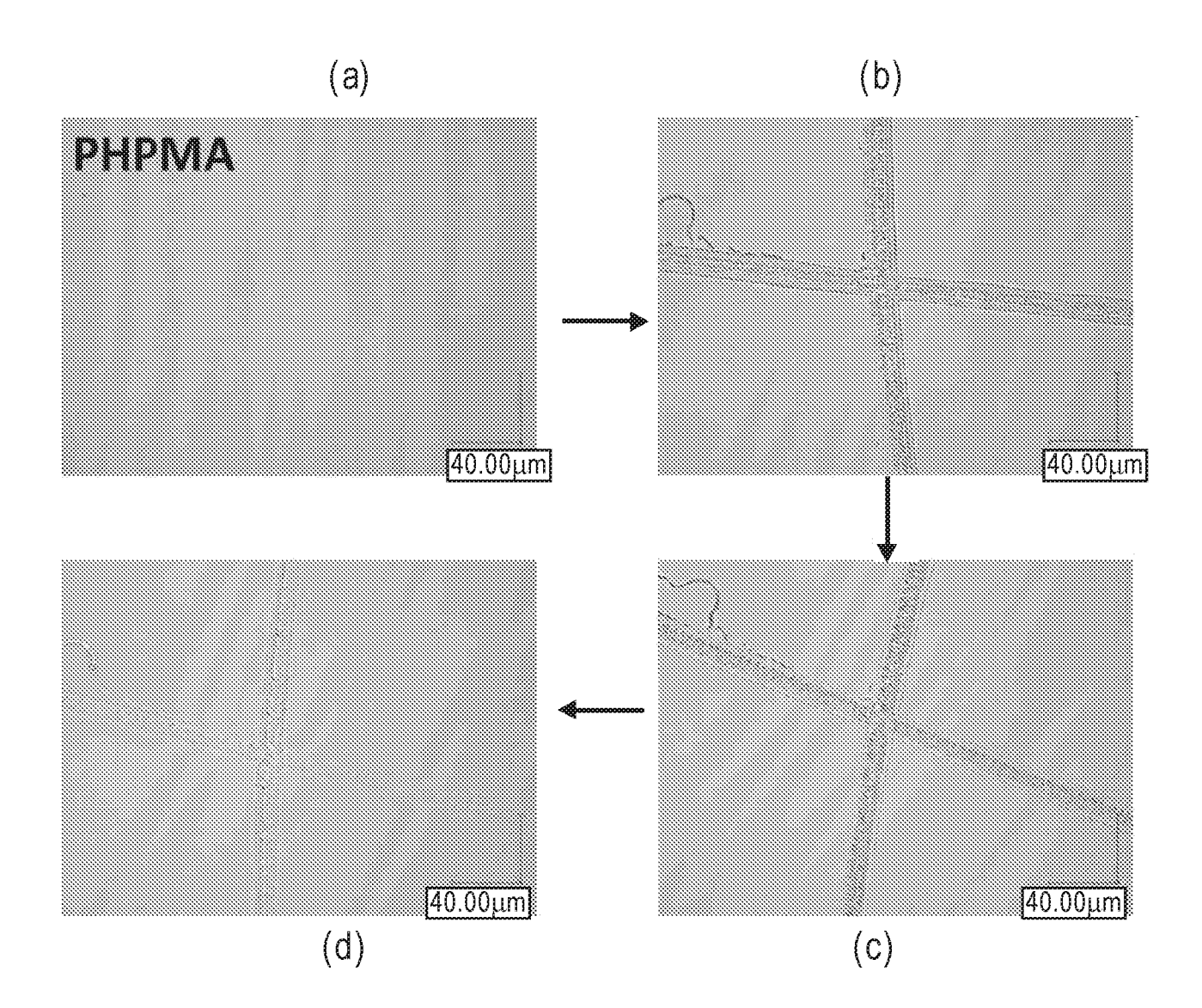
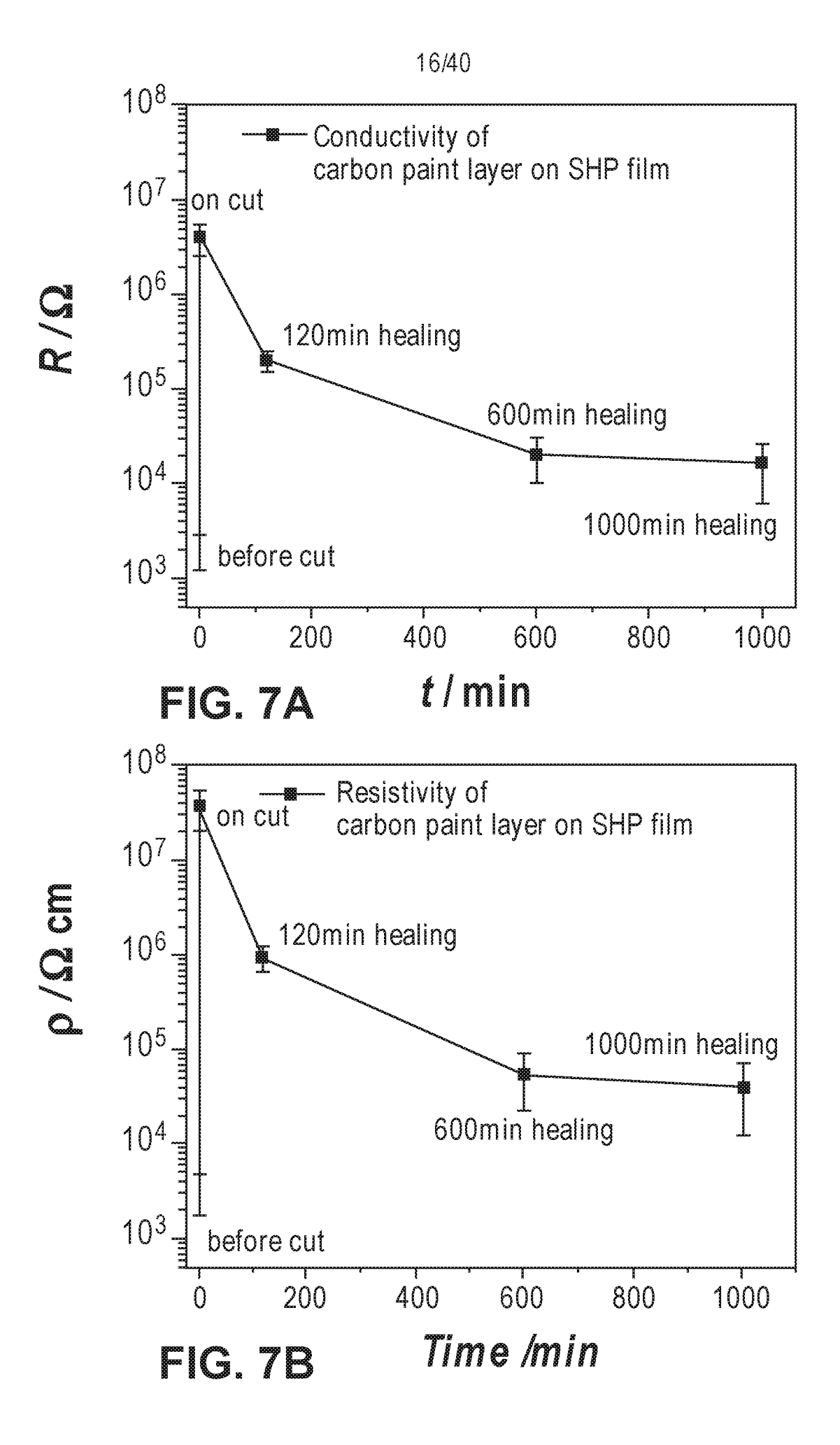
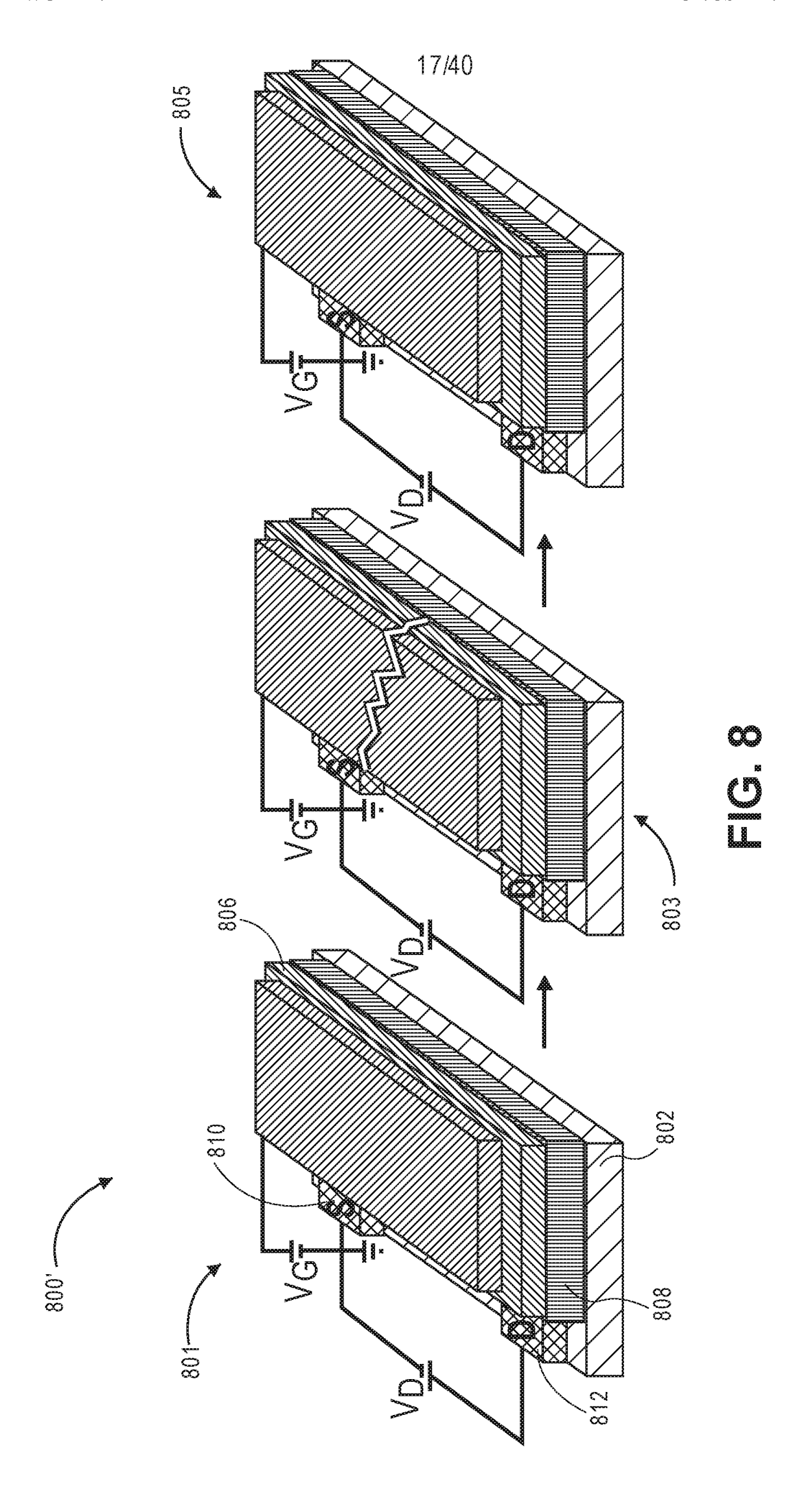


FIG. 6D





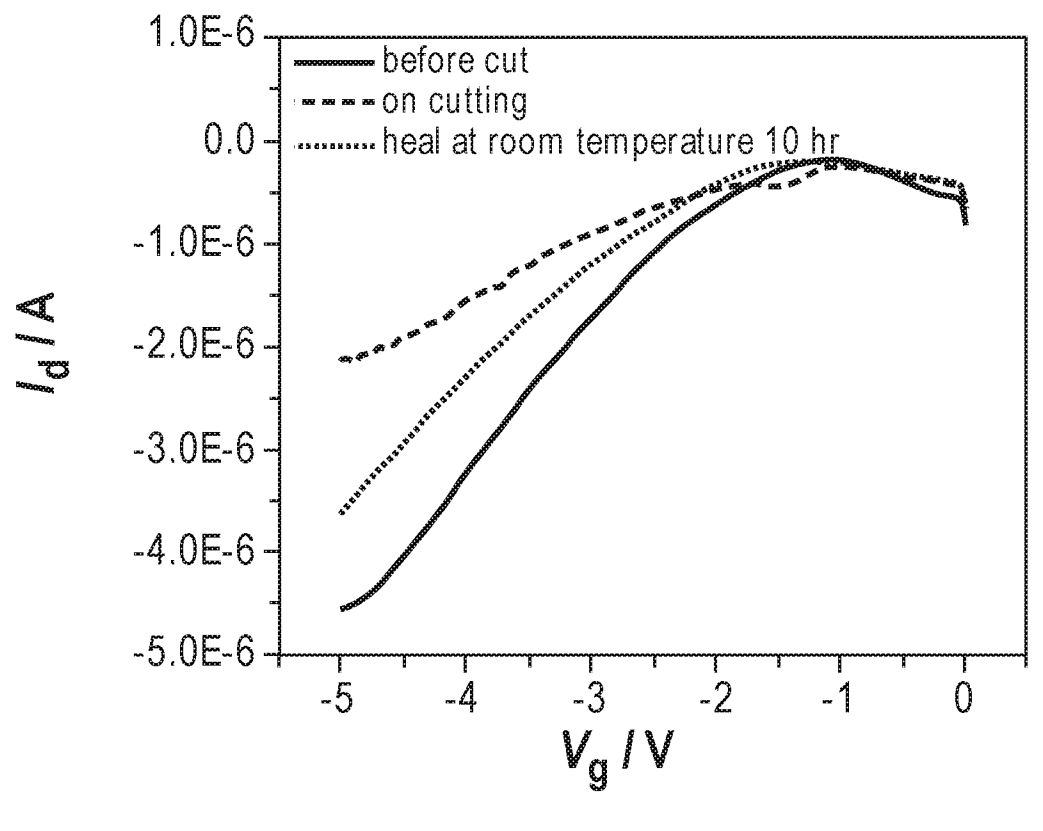


FIG. 9

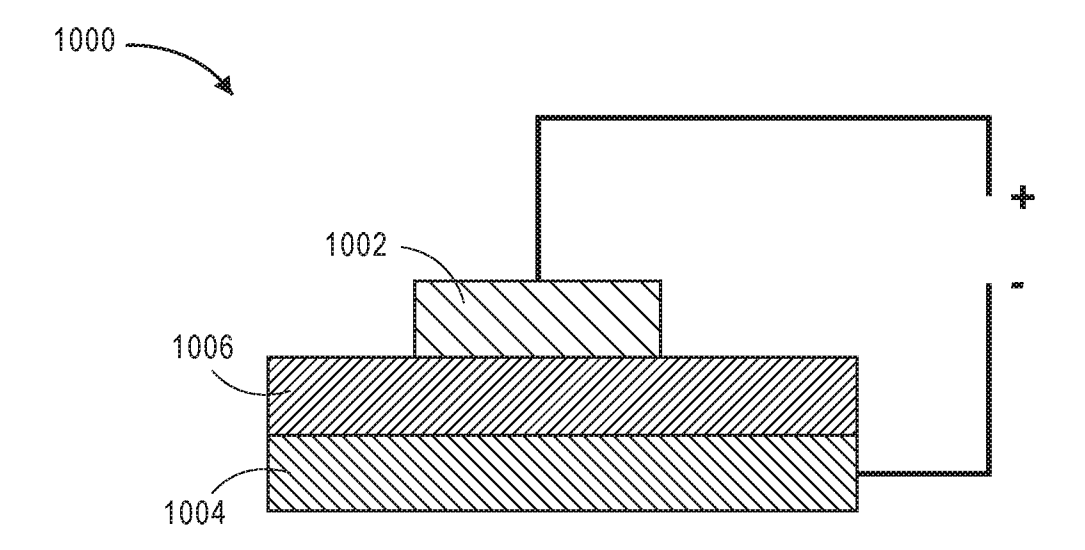
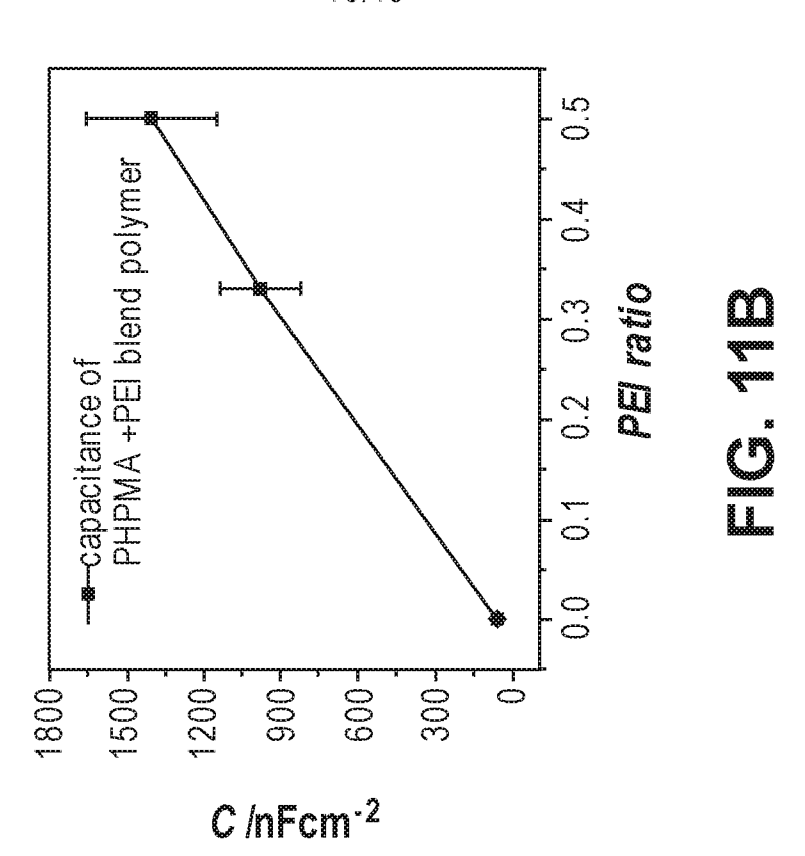
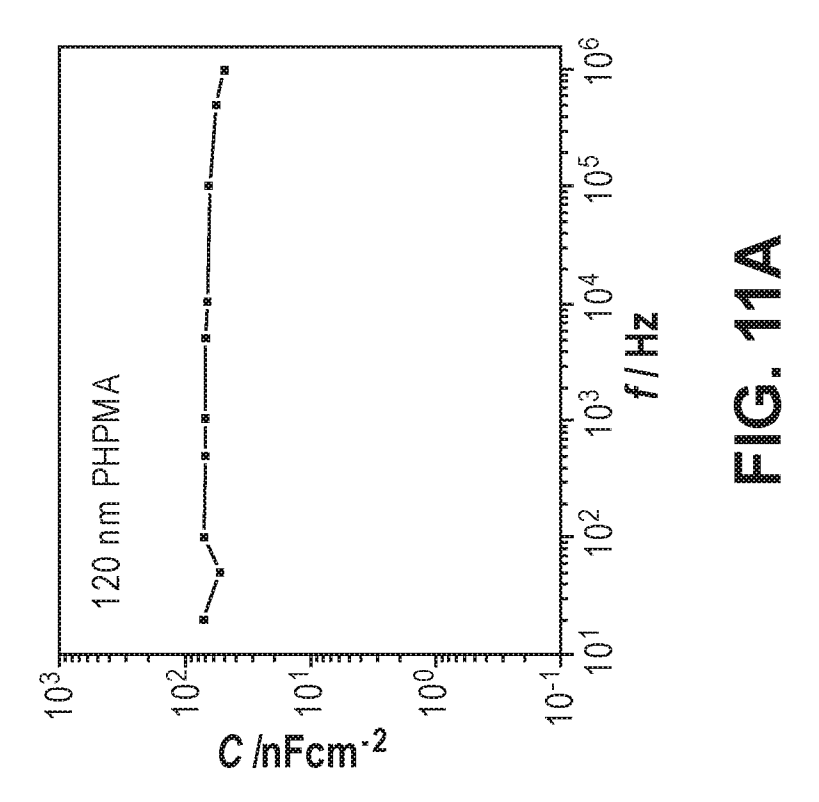
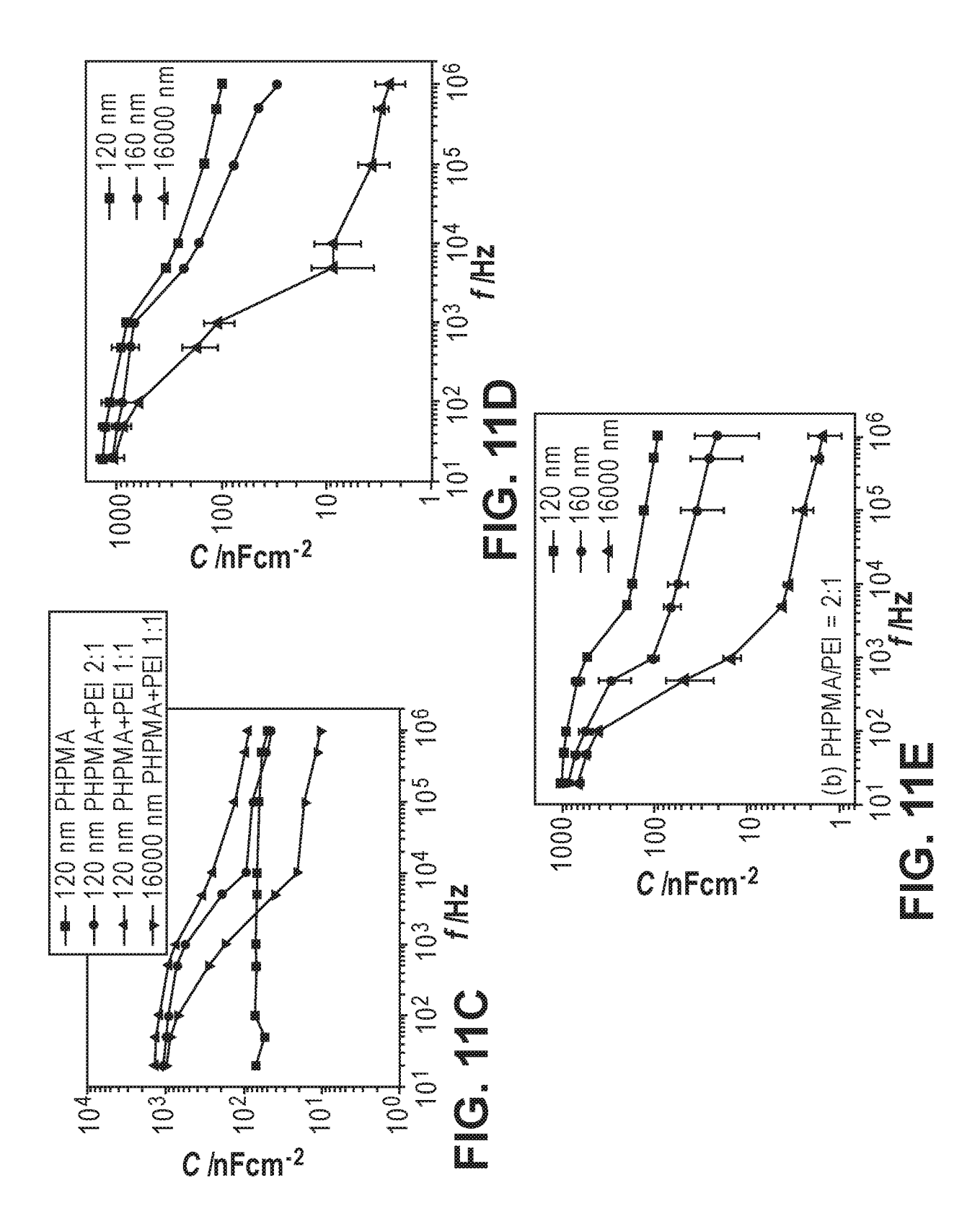


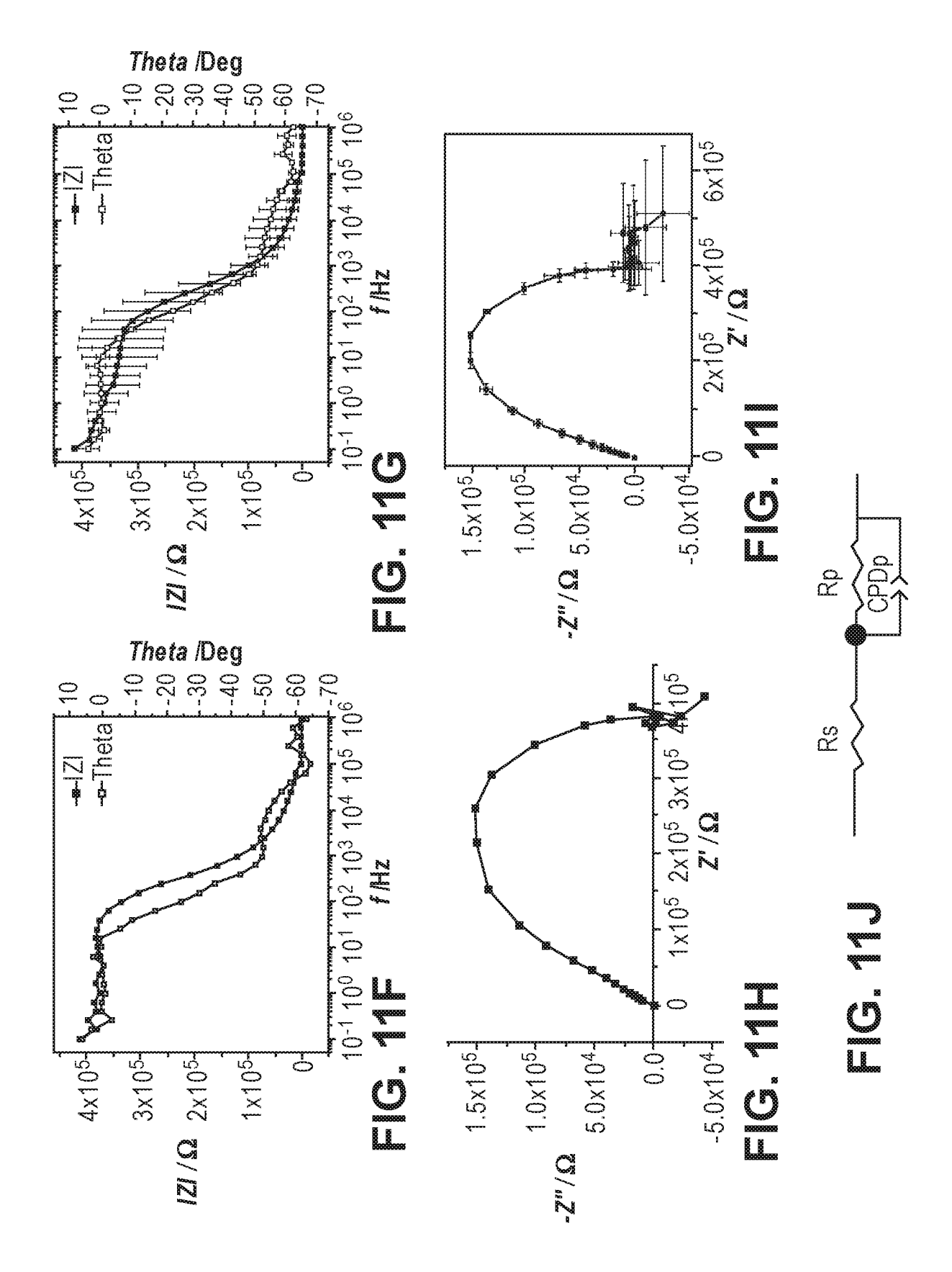
FIG. 10

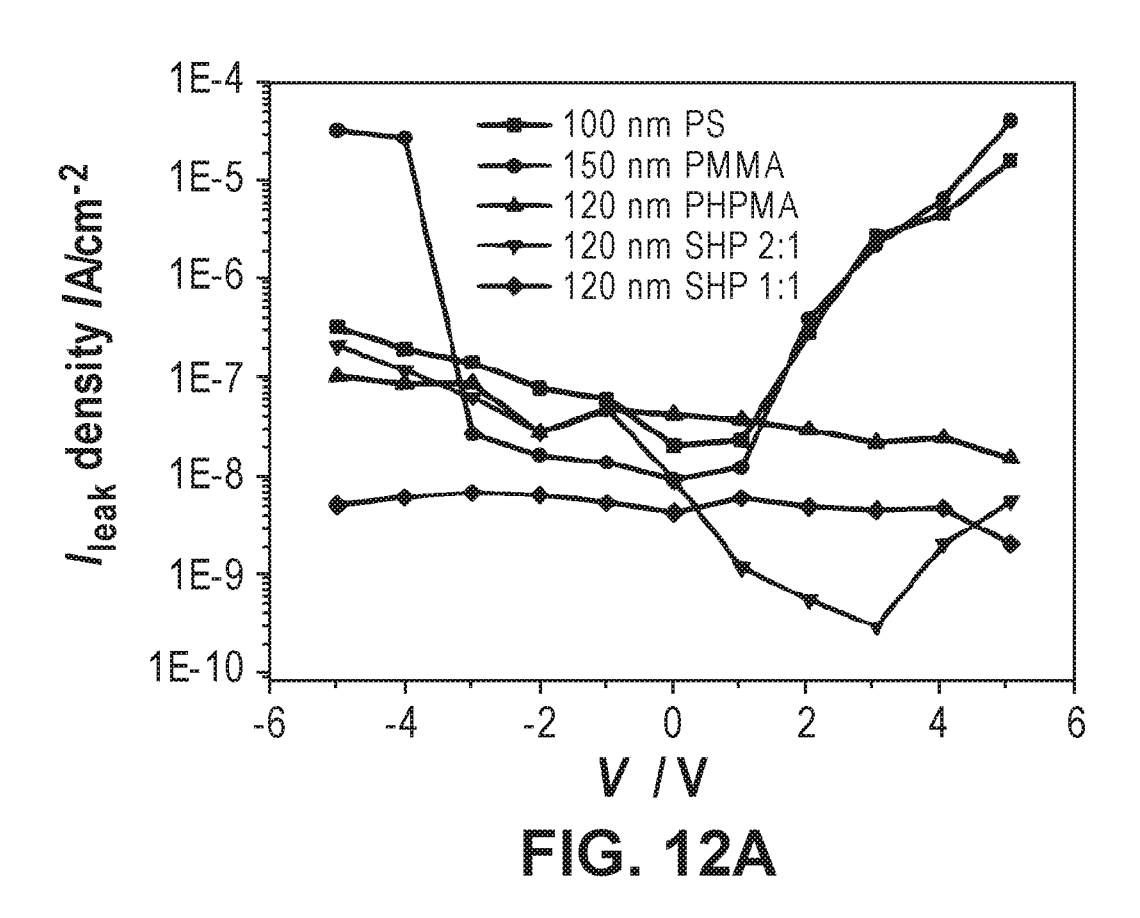


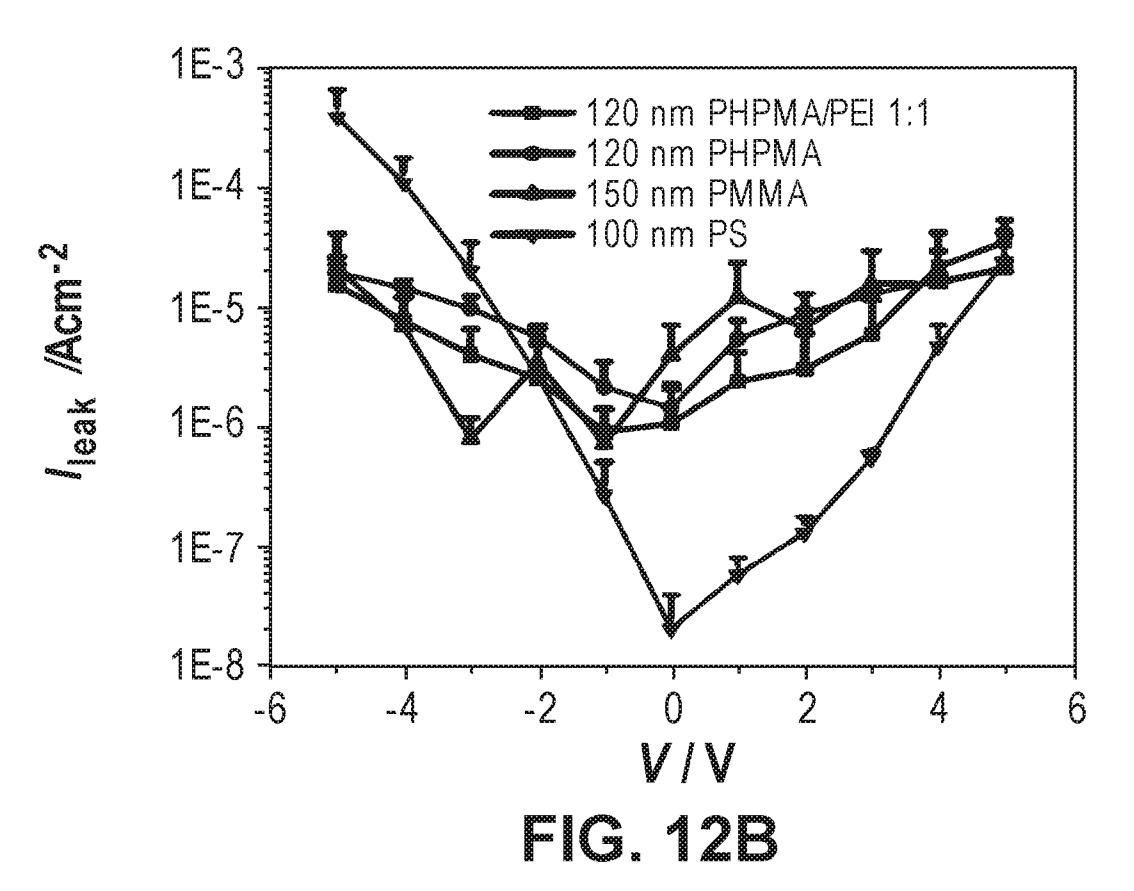


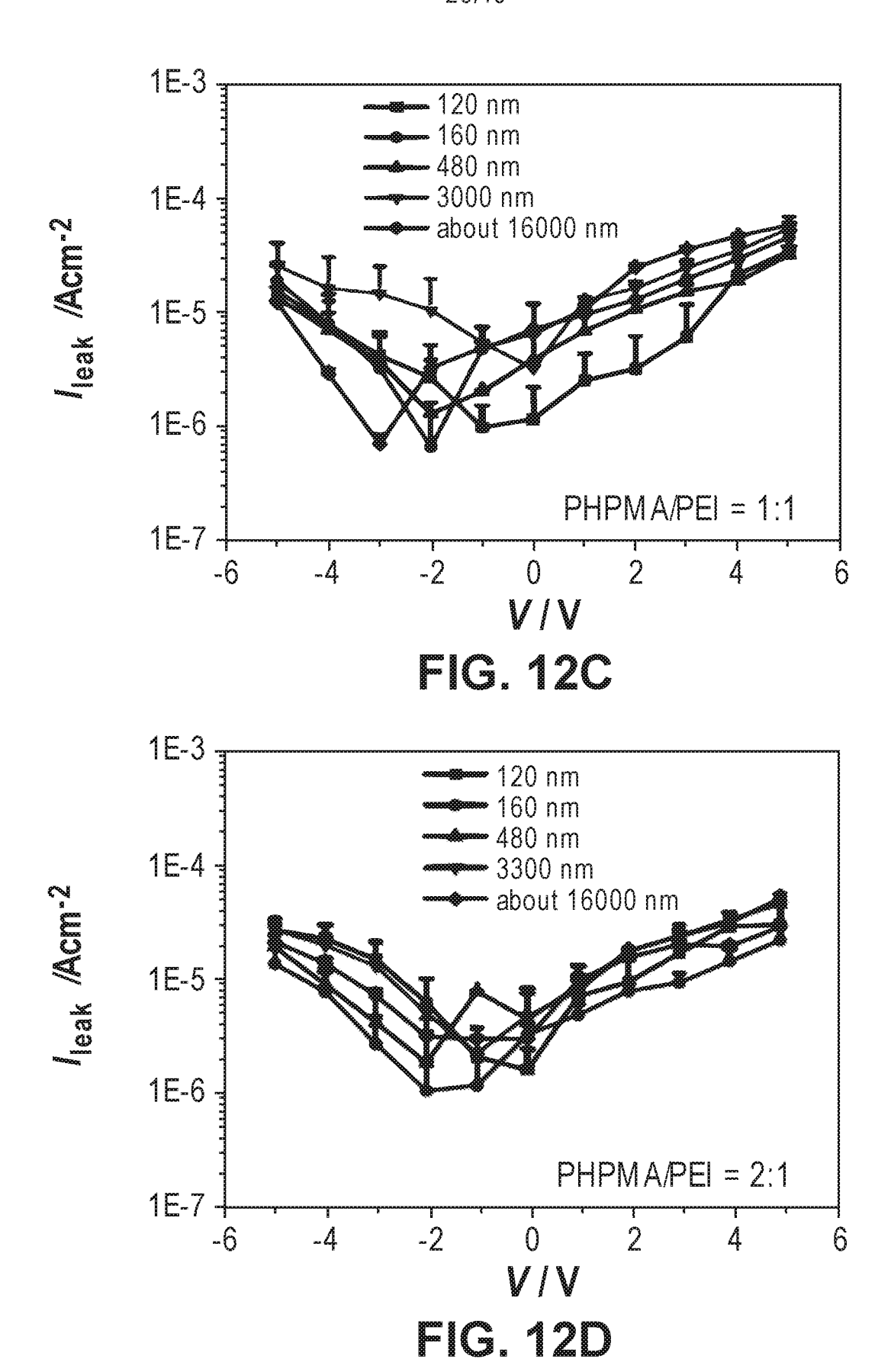


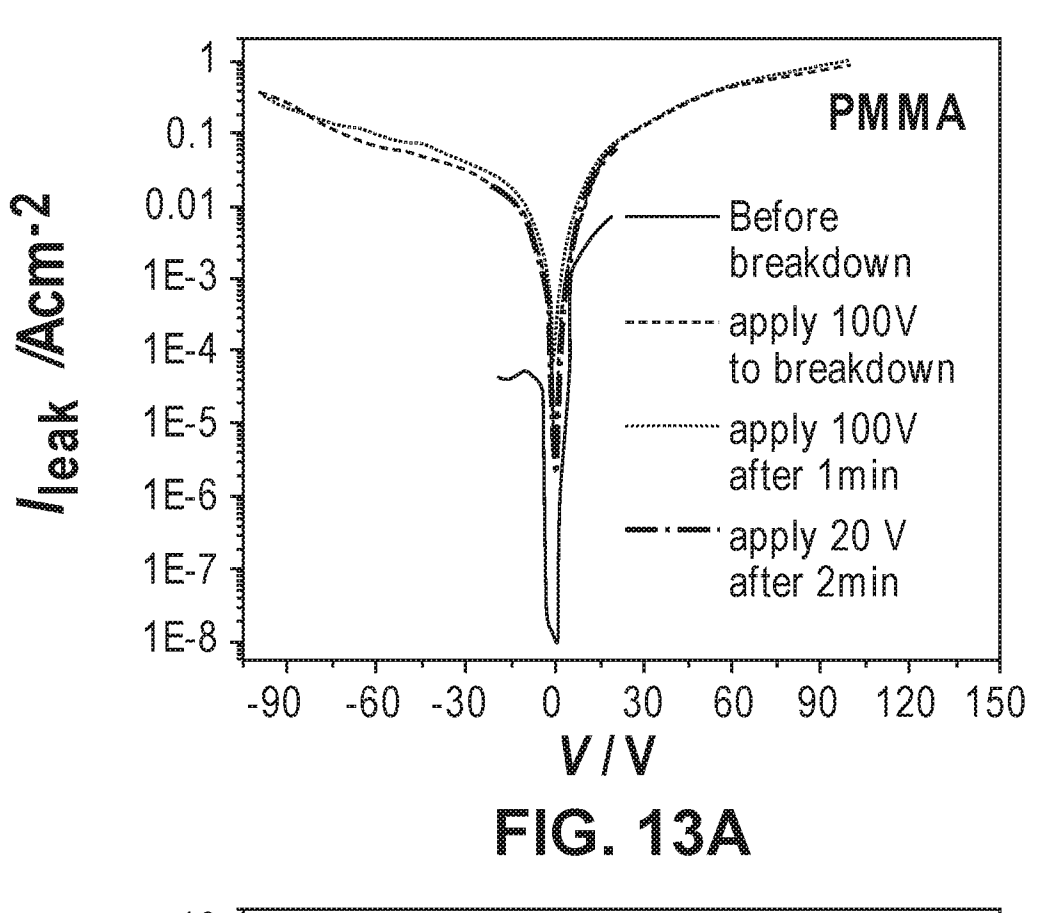


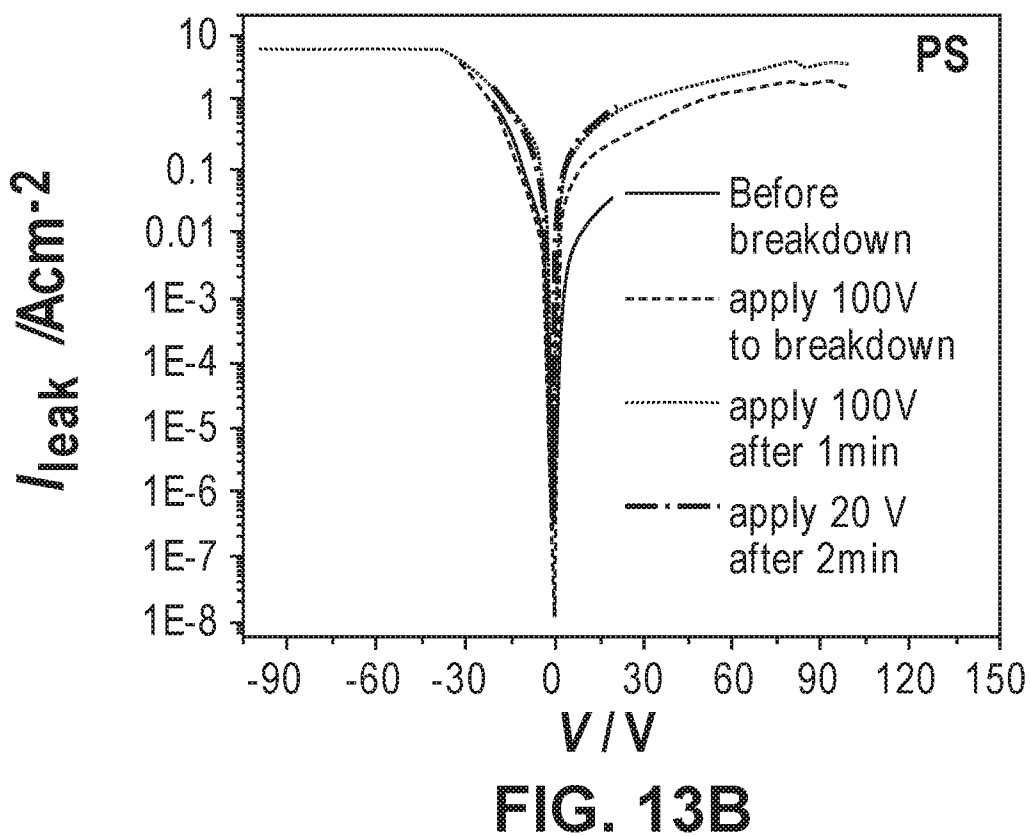


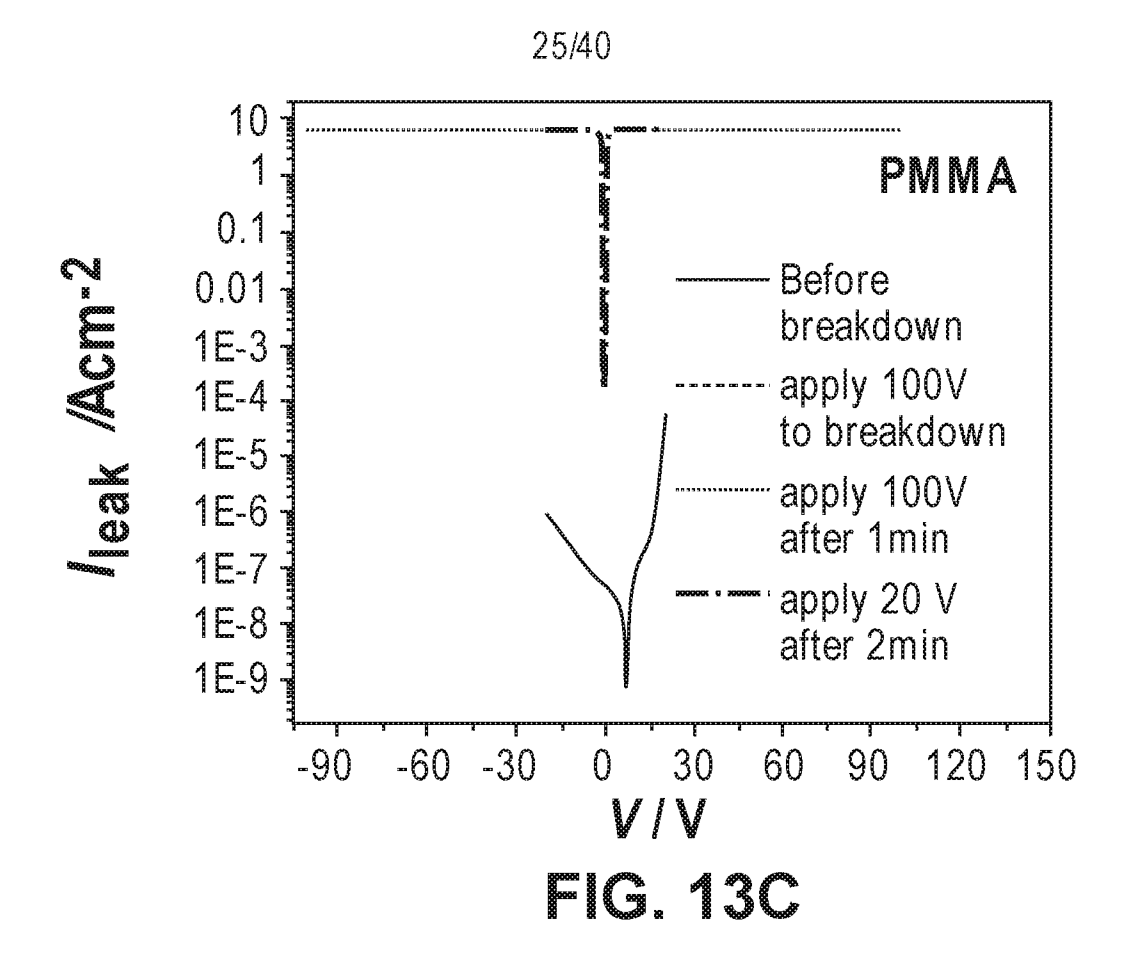


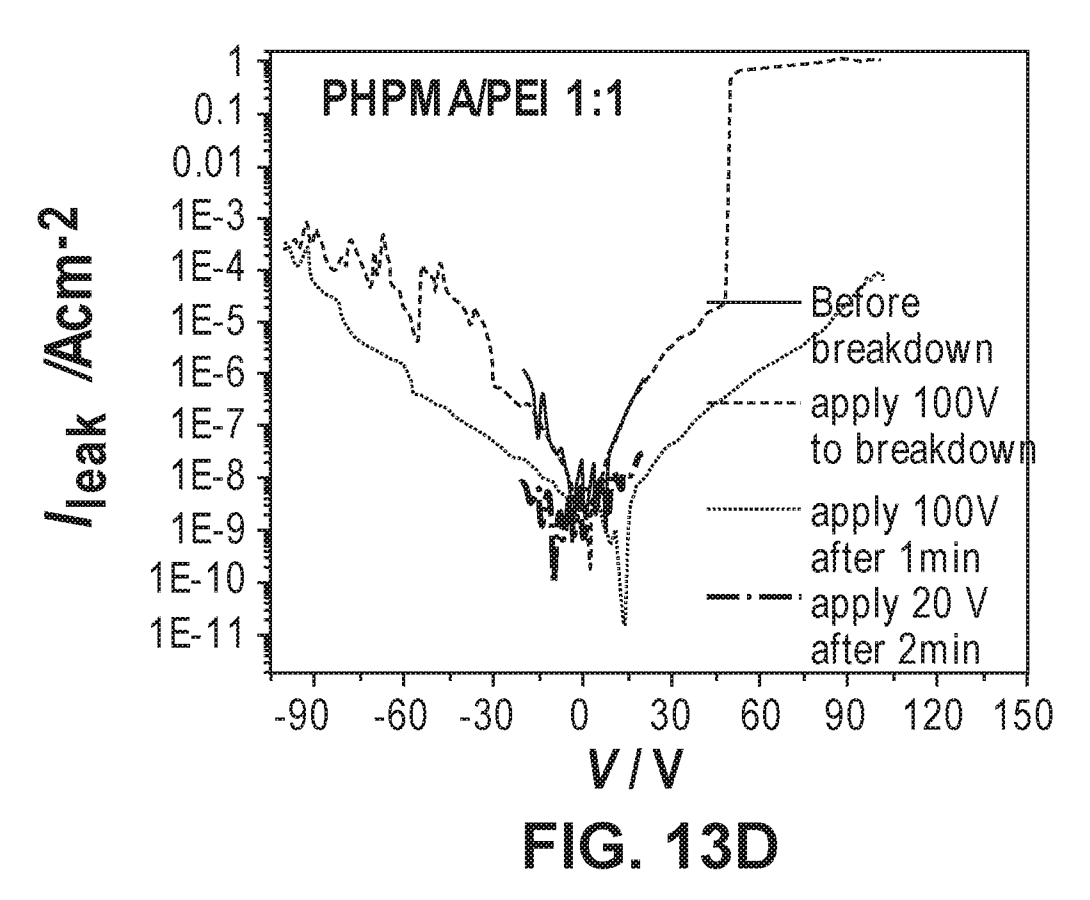


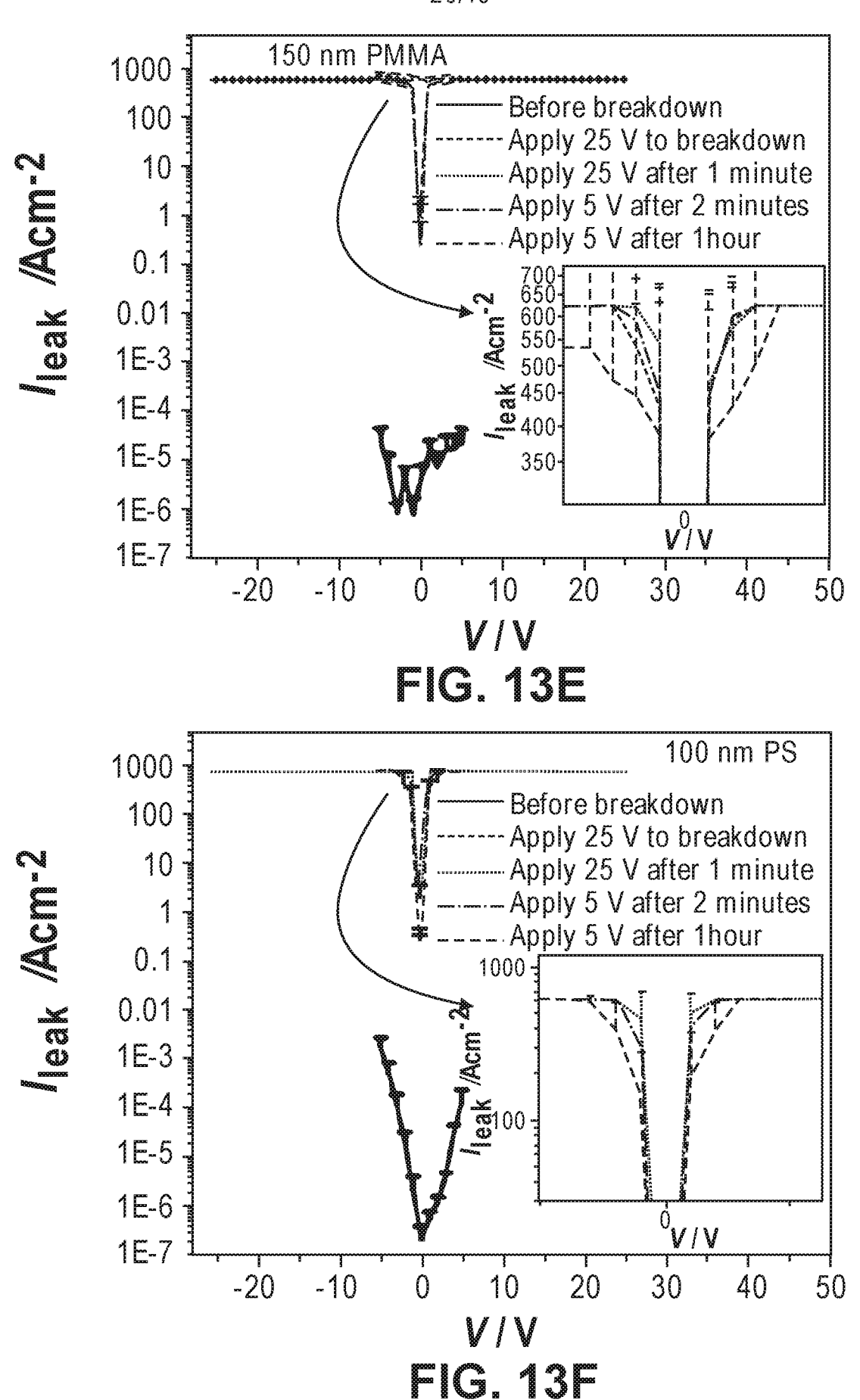


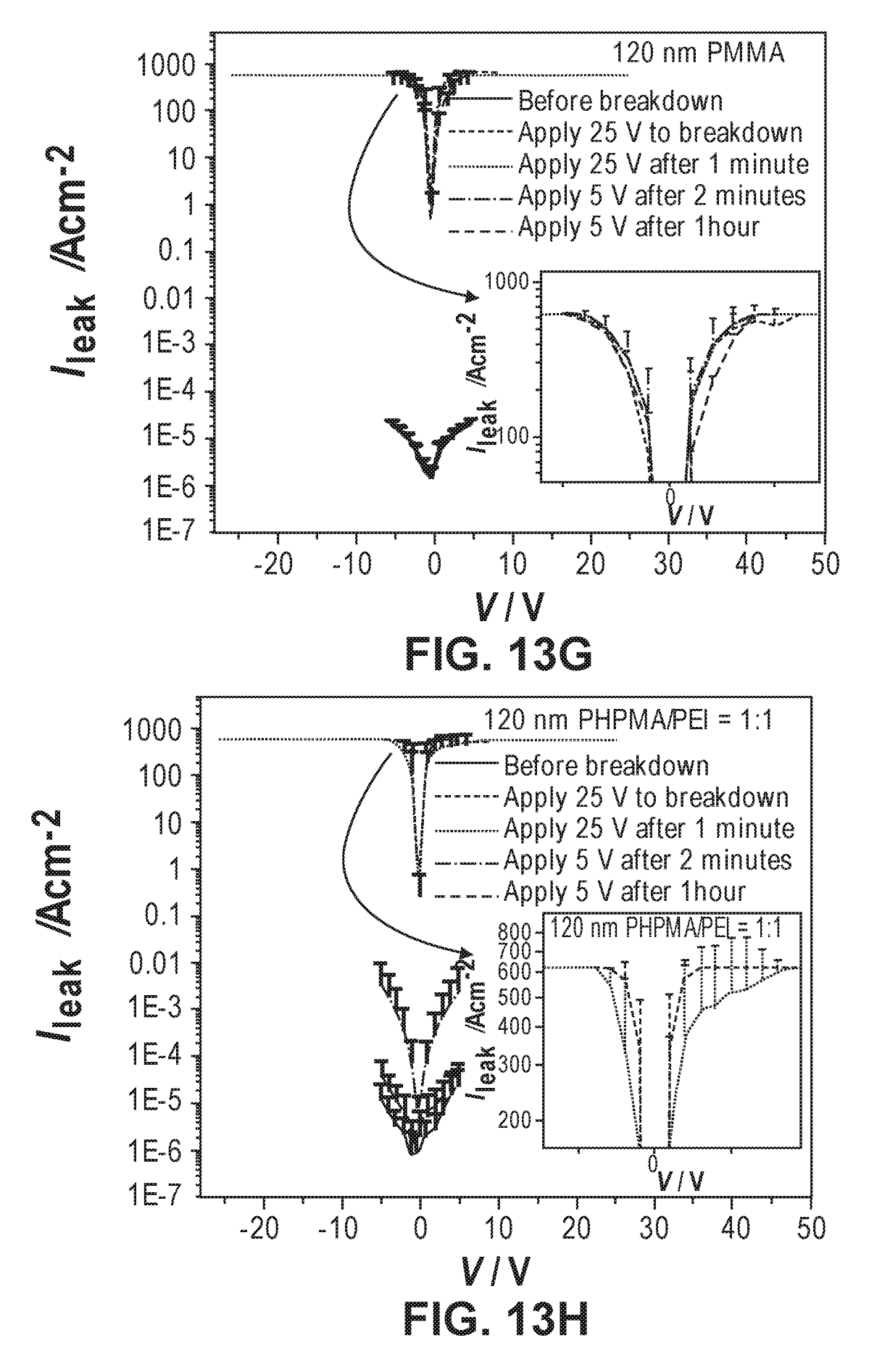












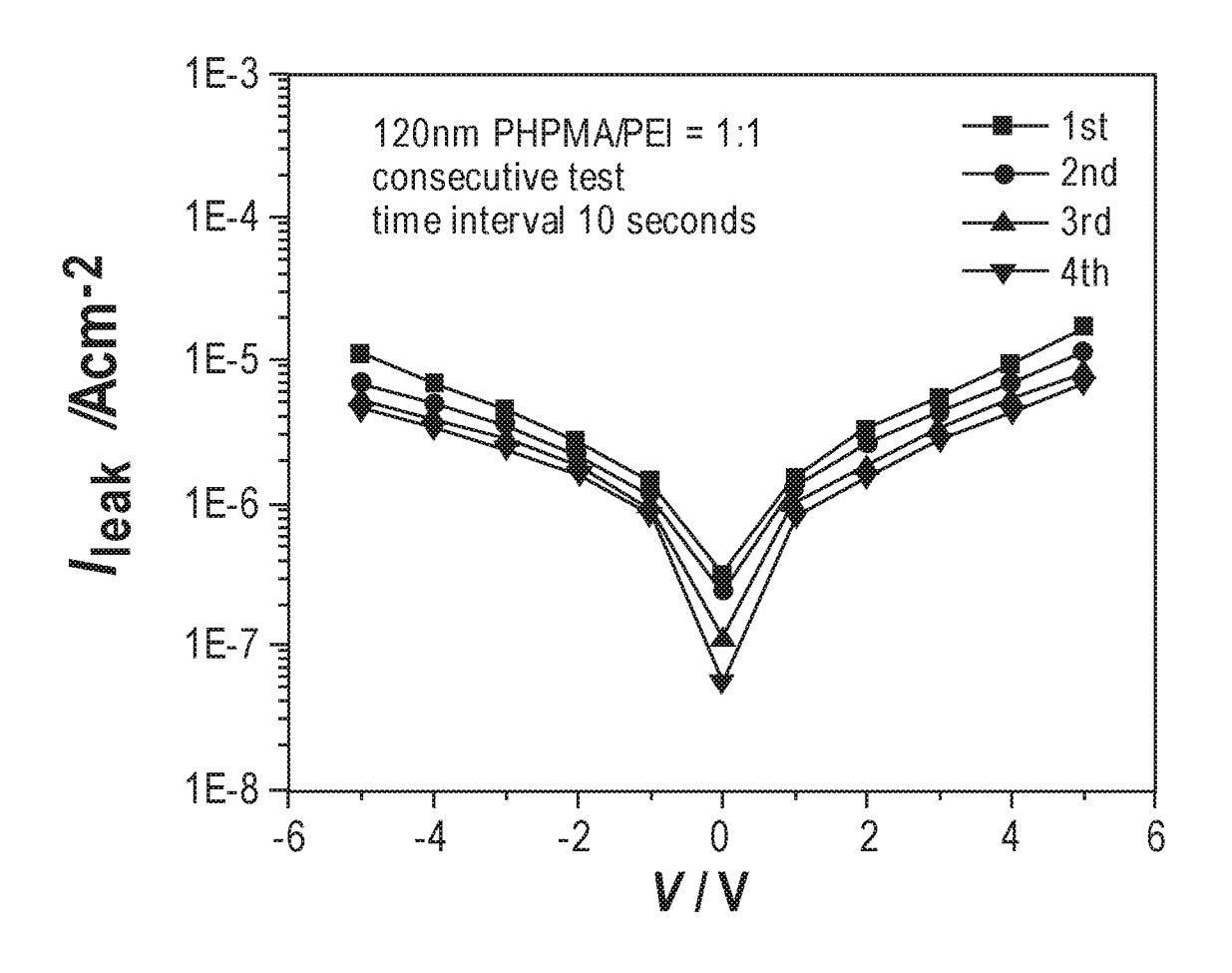
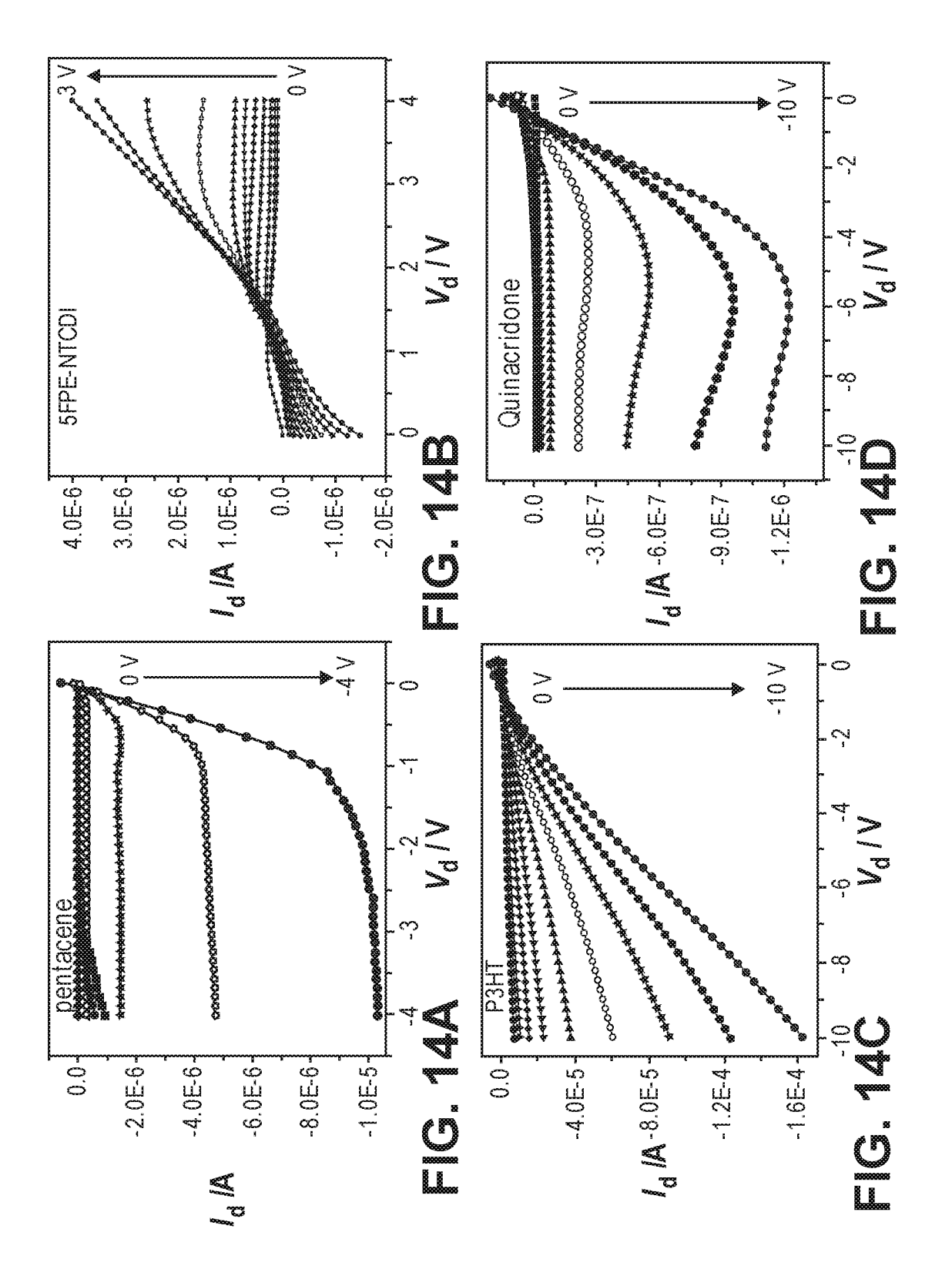
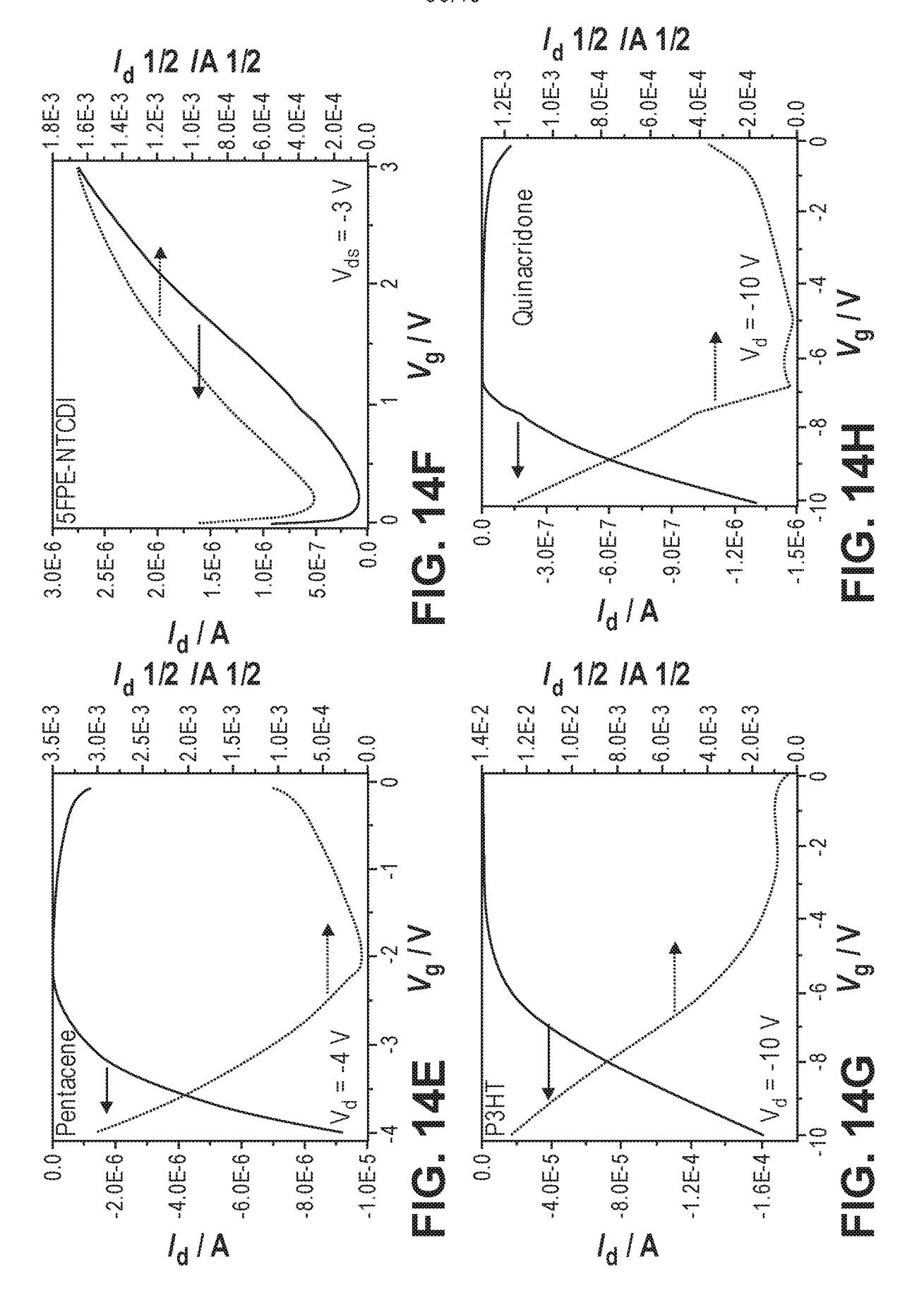
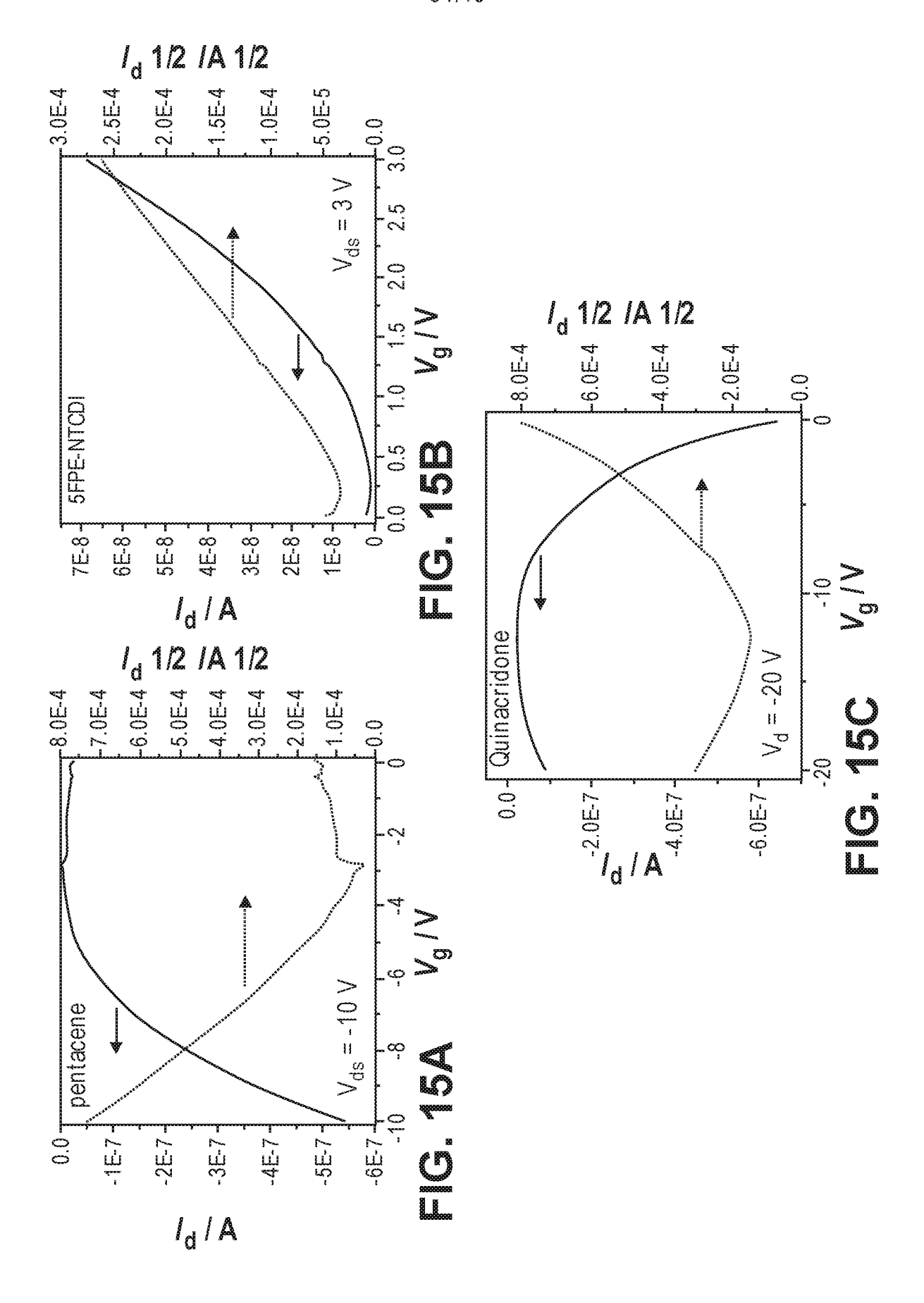


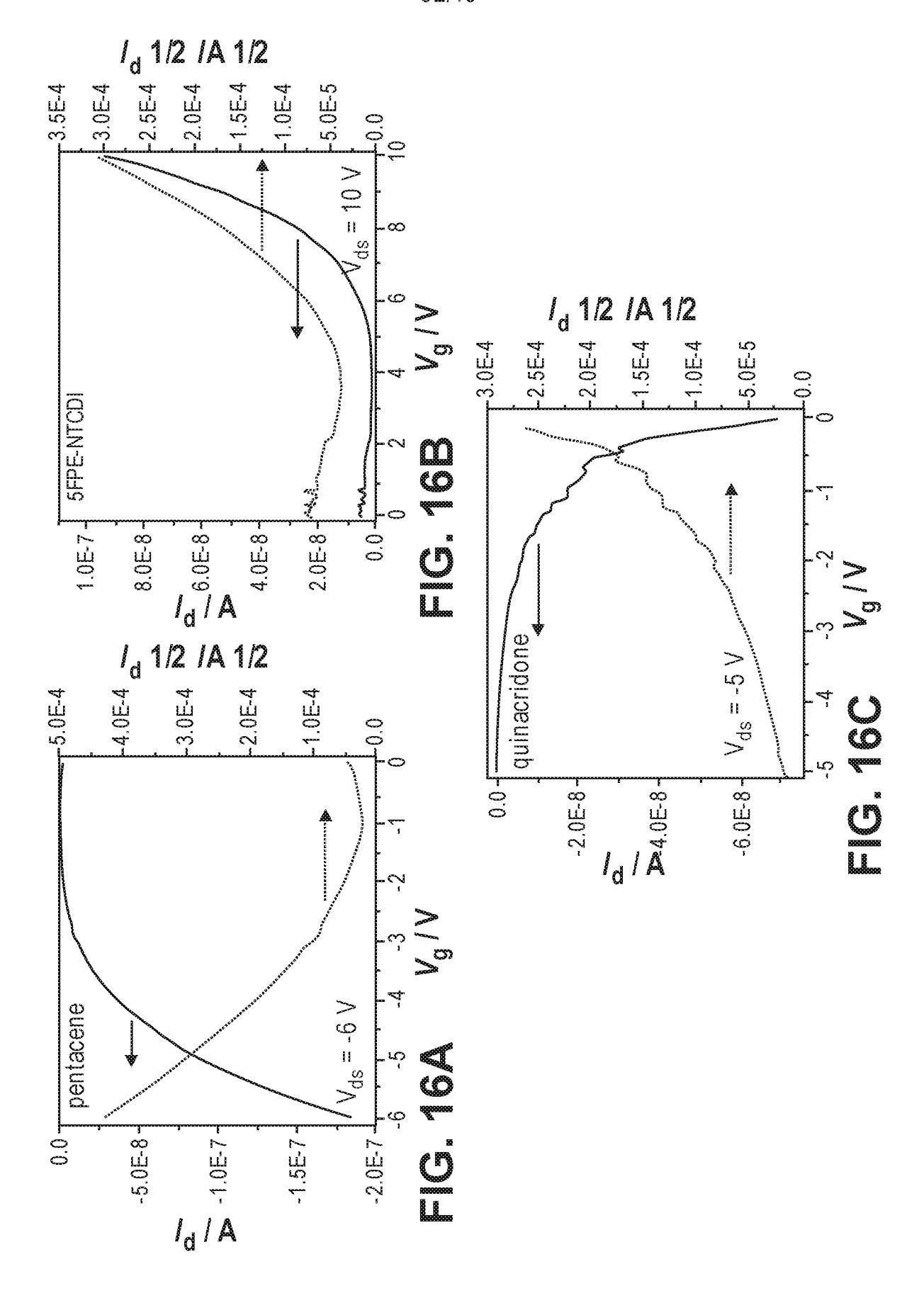
FIG. 131

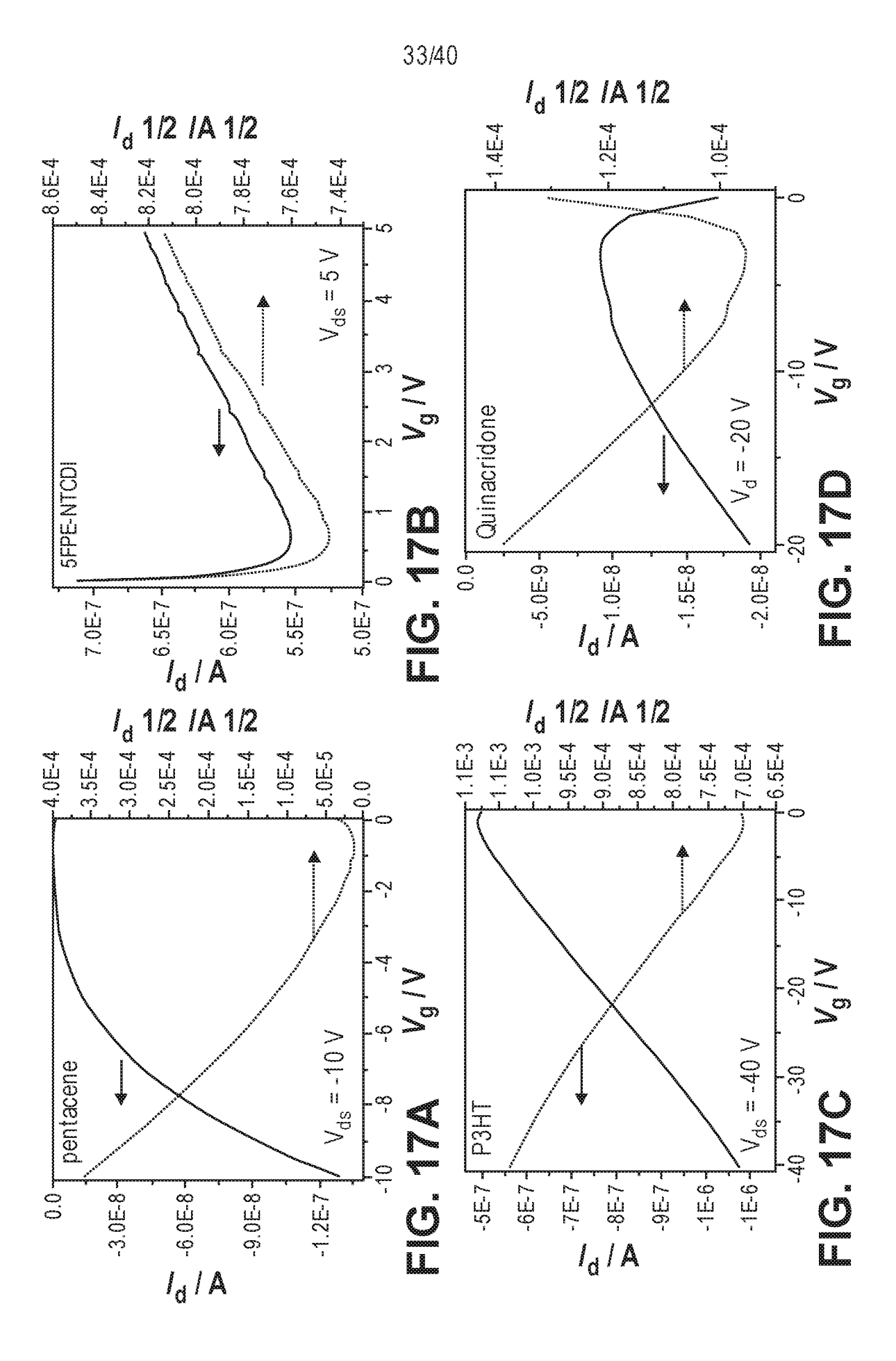


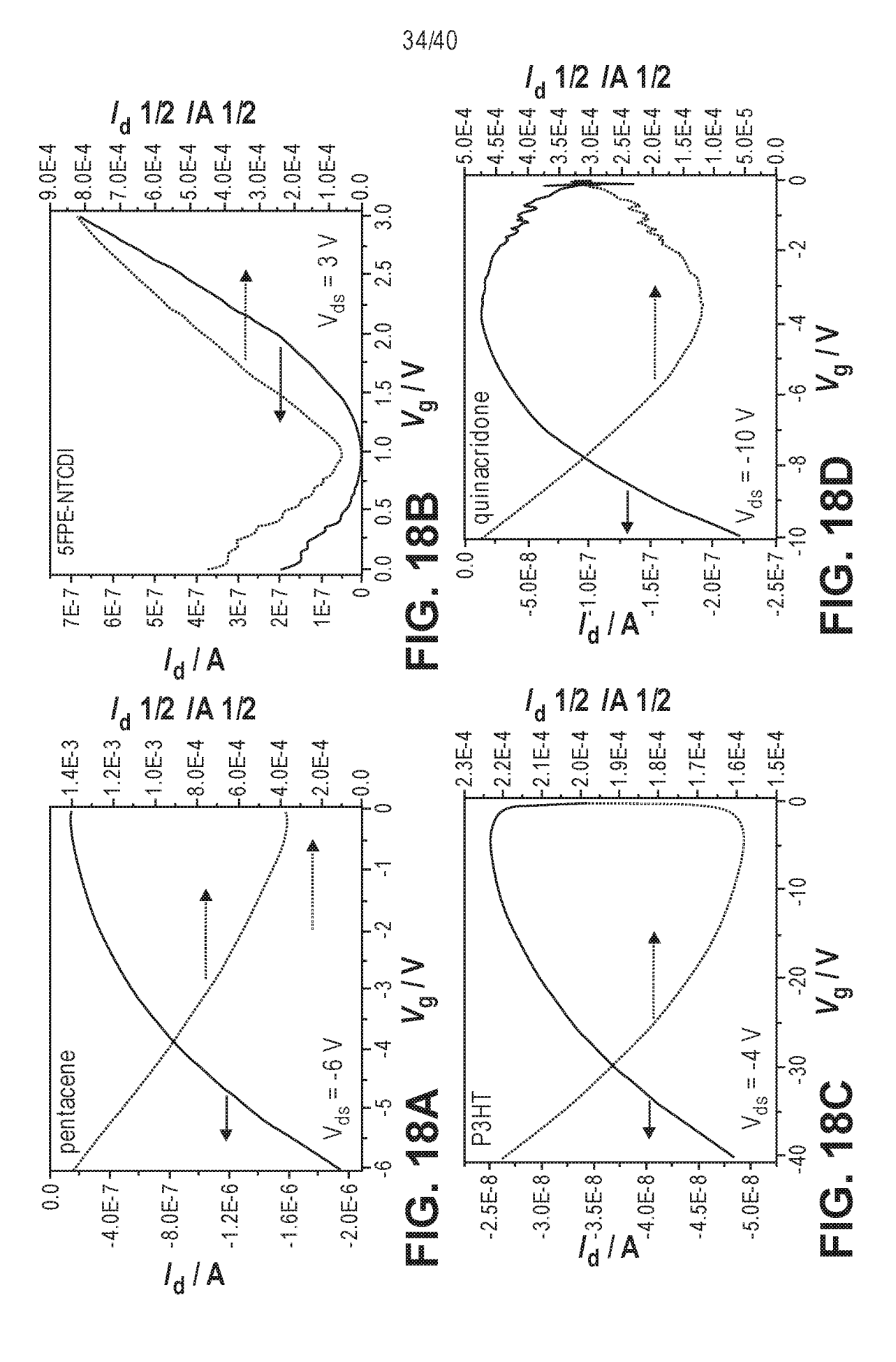
30/40











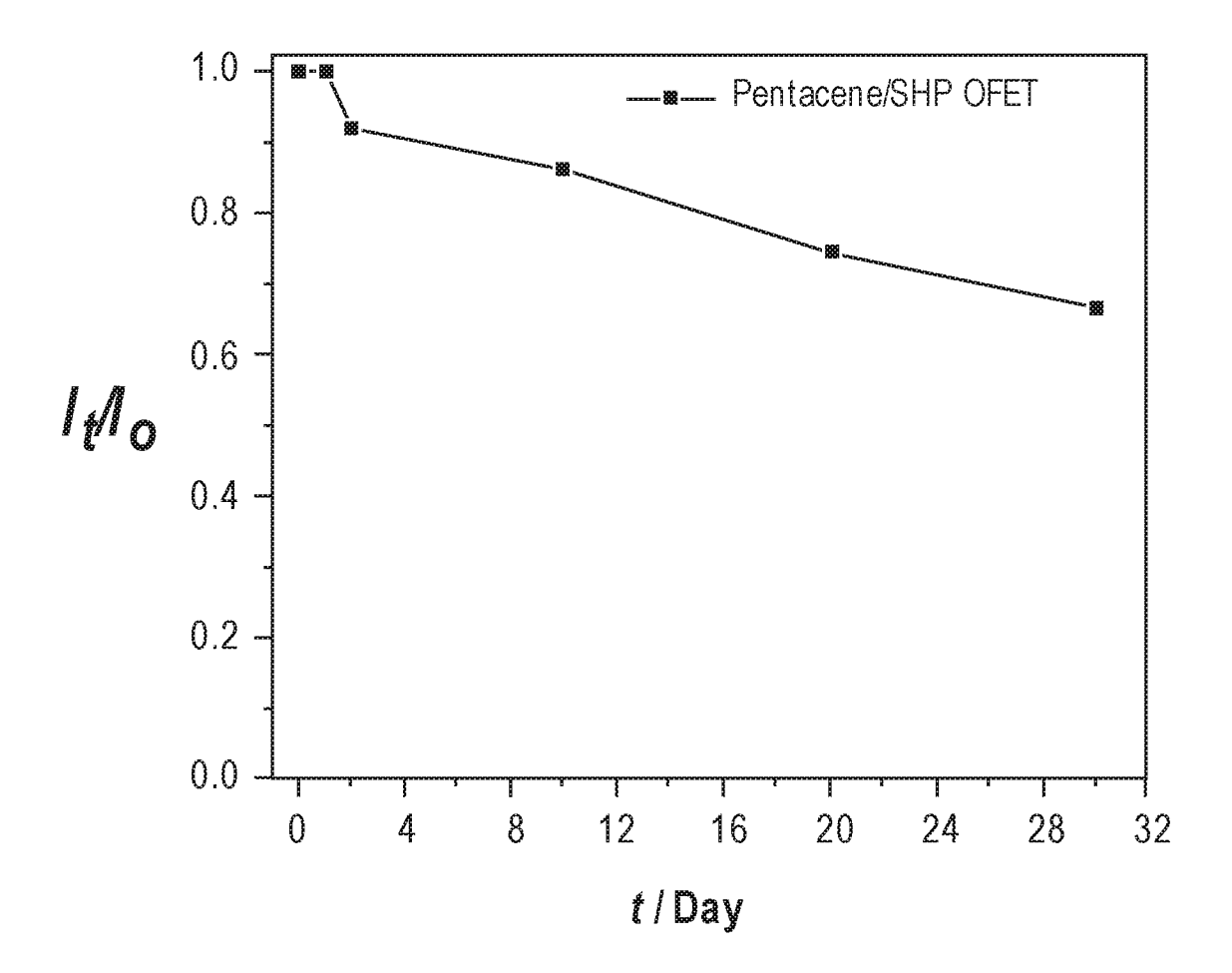
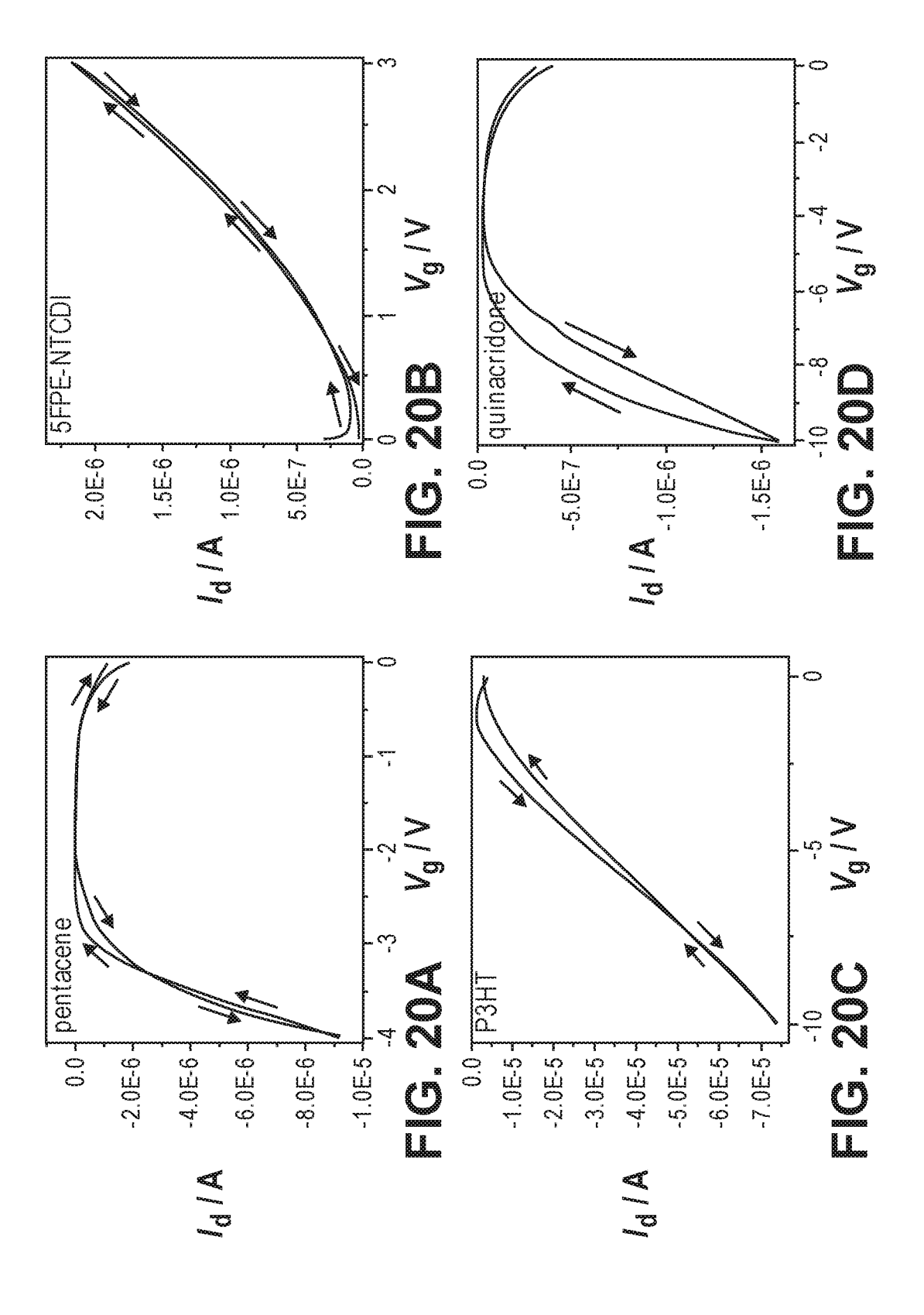


FIG. 19



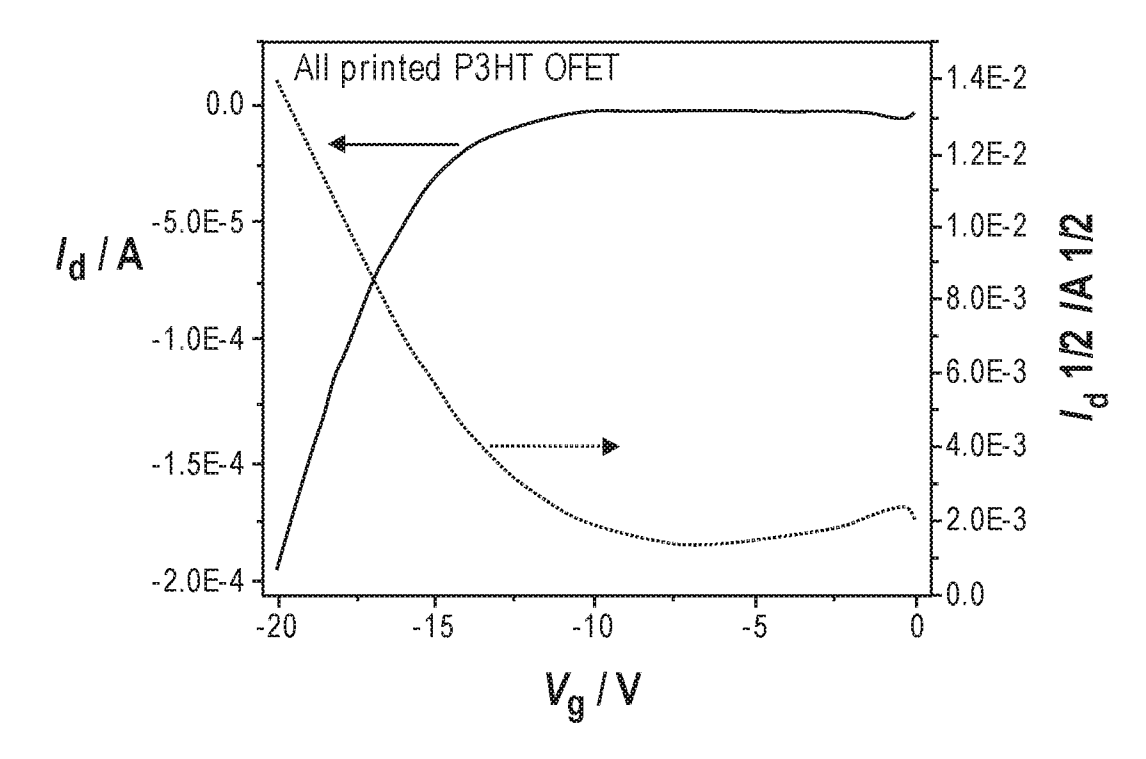


FIG. 21A

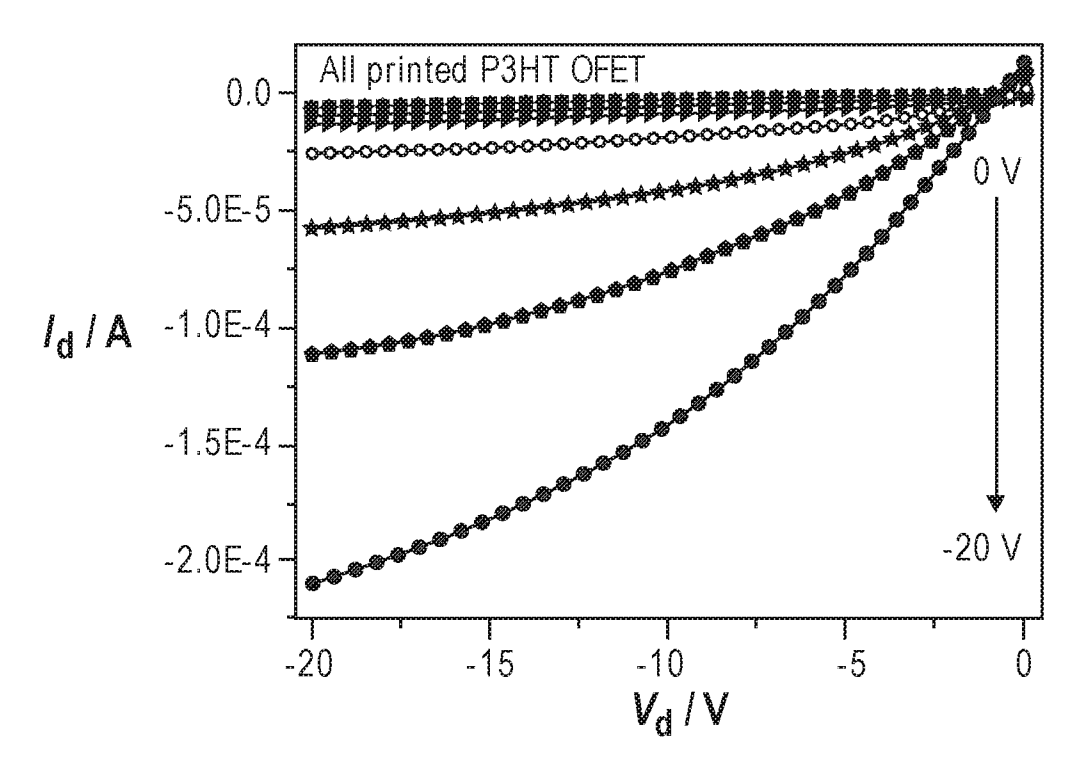


FIG. 21B

38/40



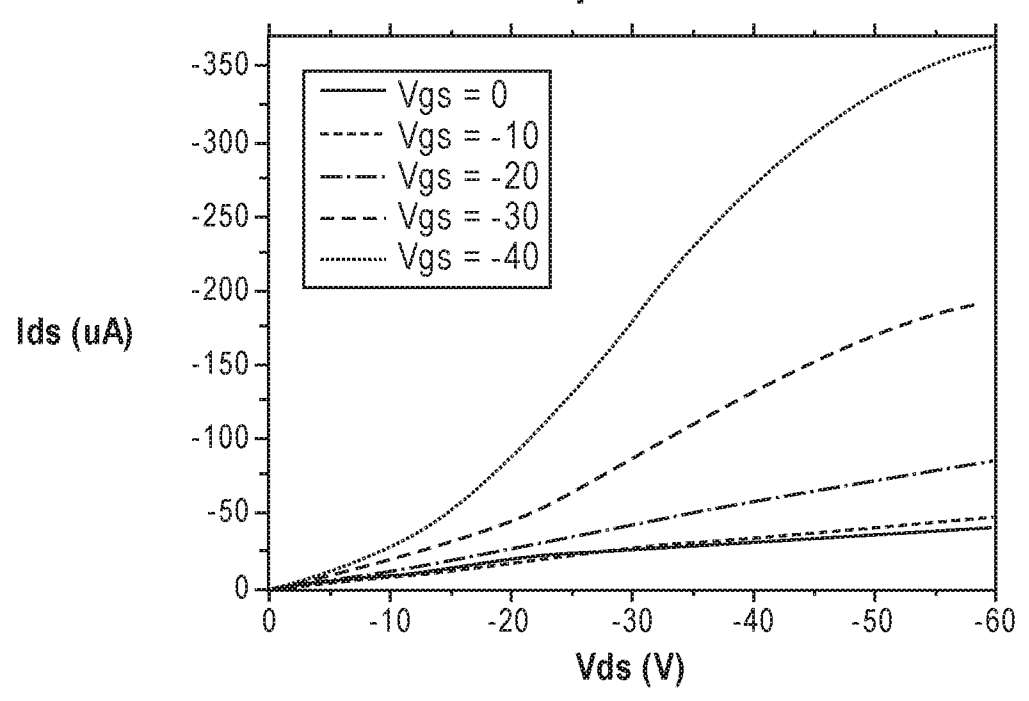


FIG. 21C

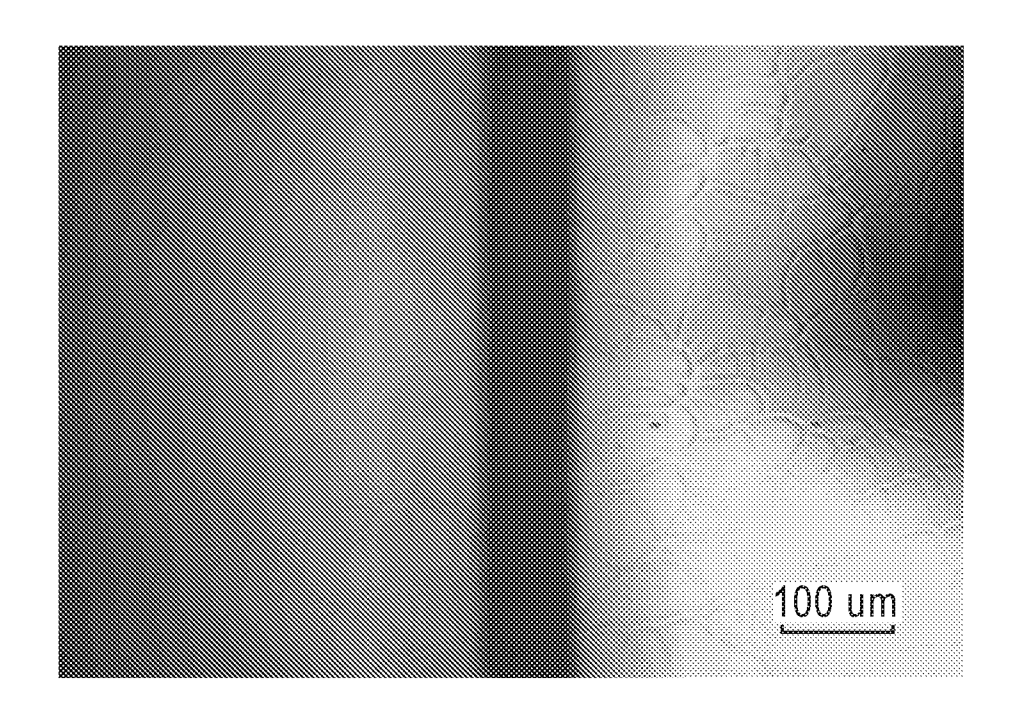


FIG. 21D

